Reviews in Computational Chemistry, Vol. 6, edited by K. B. Lipkowitz and D. B. Boyd, VCH Publishers, New York, 1995.

Contents

Reviews in Computational Chemistry, Vol. 6, edited by K. B. Lipkowitz and D. B. Boyd, VCH Publishers, New York, 1995.

CHAPTER 1

Continuum Solvation Models: Classical and Quantum Mechanical Implementations

Christopher J. Cramer and Donald G. Truhlar

Department of Chemistry and Supercomputer Institute, University of Minnesota, Minneapolis, MN 55455

INTRODUCTION

Theory and experiment often provide complementary information for a problem of interest. Given this relationship, a judicious combination of theory and experiment is often more powerful than using either approach alone. The explosive increase in the use of molecular modeling in modern chemical research is due in no small part to this kind of potential.

Early work in molecular modeling was primarily concerned with structural questions for molecular systems in a vacuum. Later work extended molecular theory to address issues of reactivity and dynamics. A long period of evolution, refinement, and calibration of various models has resulted in applications of theory that are increasingly successful in explaining and predicting molecular properties and reactivities in dilute gas-phase processes. However the bulk of practical chemistry and all of biological chemistry take place in condensed phases, typically liquid solutions, as opposed to the gas phase. It is primarily within the last decade that theoretical models capable of treating such systems accurately have emerged as working tools of the chemist.

Reviews in Computational Chemistry, Volume VI
Kenny B. Lipkowitz and Donald B. Boyd, Editors
VCH Publishers, Inc. New York, © 1995

In this chapter, we restrict ourselves to a discussion of models that treat molecules in dilute aqueous solutions. In general, the effect of aqueous solvation on chemical reactions is illustrated in the thermodynamic cycle of Figure 1. Depending on relative values of the free energies of solvation of the reactants, products, and transition state, both the equilibrium constant and the rate constant of the reaction may change in either direction, sometimes by very large factors.[1] Figure 2 illustrates the dramatic changes in the extensively studied S_N2 reaction of chloride anion with methyl chloride[2–7] on going from the gas phase to aqueous solution. The considerably more favorable solvation of the separated molecules relative to the transition state is sufficient to transform the low-barrier, double-well potential found in the gas phase into an aqueous phase potential of mean force[8–11] that involves no stable intermediates.

Biologically, the effect of aqueous solvation plays a critical role in determining the structure of biopolymers[12–15] and their interaction with other molecules.[16–18] In this context it is interesting to generalize our thermodynamic cycle to represent the interaction of an enzyme and substrate as illustrated in Figure 3. Here, the desolvation of the substrate prior to complexation in the enzyme active site may be a significant factor influencing the equilibrium constant for complex formation and thus the rate of enzymatic catalysis. The power of this simple analysis is made clear by the equation

$$\Delta G^\circ_{aq} = \Delta G^\circ_g + \Delta G^\circ_S(E{\cdot}S) - \Delta G^\circ_S(E) - \Delta G^\circ_S(S) \qquad [1]$$

which shows that if we know the solvation free energies, we can calculate the aqueous free energy change from the gas phase without directly simulating it.

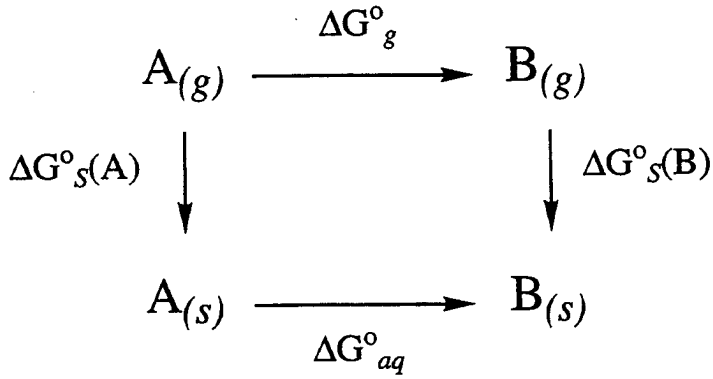

$$\Delta G^\circ_{aq} = \Delta G^\circ_g + \Delta G^\circ_S(B) - \Delta G^\circ_S(A)$$

Figure 1 The interrelationship of free energies in the gas and solution phases with free energies of solvation.

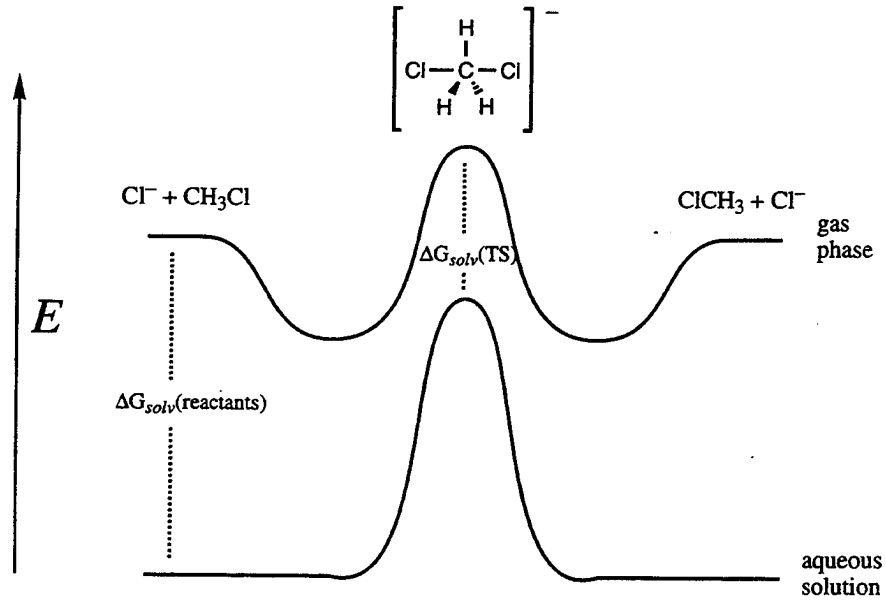

Figure 2 The effect of aqueous solvation on the reaction of chloride with chloromethane.

The direct simulation of the aqueous binding process is difficult because changes in solvation/desolvation that accompany association are slow and hard to sample, especially when hydrogen bonding patterns are coupled to conformational changes in the protein, or for recessed binding sites, where the associating substrate may hinder solvent escape. Another important kinetic factor is the differential stabilization (by enzyme vs. solvent) of the transition state of the

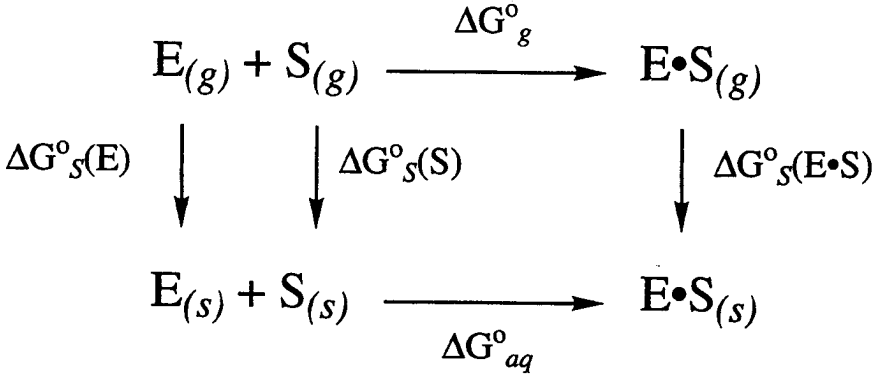

Figure 3 The effect of solvation on enzyme–substrate interactions.

reaction.[19] Similar differential solvation issues occur in the crossing of biological membranes.[20] The accurate modeling of these processes thus impacts on medicinal and pharmacological chemistry; as a result, there is widespread interest in applying solvation models to drug discovery and design.[21–25]

Aqueous Solvation Components

Aqueous solvation influences structure and reactivity via a combination of several distinct effects. One key property of a solvent is its ability to be electrically polarized,[1] a first measure of which is provided by the bulk dielectric constant, which is 78.3 for water at 298 K. Upon passing from the vacuum (or dilute gas phase) dielectric constant of unity into solution, the structure and charge distribution within a solute will generally relax to permit greater charge separation; these effects increase with increasing dielectric constant of the solvent and are referred to as solute polarization. Since solute polarization represents a distortion from the optimum gas phase structure, it necessarily increases the internal energy of the solute. Similarly it raises the free energy of the solvent. These effects partially cancel the gain in free energy due to more favorable interactions of the polarized solvent and solute. When the favorable solute–solvent consequences of further polarization are overcome by the intrasolute and intrasolvent costs of further distortion, relaxation is complete. These polarization interactions are often (especially for small systems), but certainly not always, governed to a large extent by the leading nonzero multipole moment of the solute, that is, its charge for an ion or, typically, its dipole moment for a neutral solute. Low-order multipole moments operate over a long range and, as a consequence these interactions, typically extend far beyond the first solvation shell.

We find it convenient to represent the combined contributions of the foregoing effects to the free energy of solvation by a term that we label ENP,[26,27] for electronic, nuclear, and polarization. In particular, this term includes (1) the change in the electronic and nuclear energies of the solute due to its electronic and geometric distortion in solution and (2) the free energy of electric polarization of the solvent, considered as a bulk dielectric medium. The electric polarization of water is dominated by the reorientation of individual water molecules throughout the volume of the dielectric. The seminal work on the molecular thermodynamics of the electric polarization of a continuum dielectric medium by a charged[28] or dipolar[29–31] solute was carried out by Born, Onsager, and Kirkwood more than fifty years ago. The fundamental concept involved in this work is the reaction field. This concept is explained as follows.[31] A charge, dipole, or higher multipole moment of a solute polarizes the surrounding medium, and the resulting electric polarization of that medium gives rise to a field at the solute, called the reaction field. We will see that the most complete treatments now available do include this effect in that molecular electronic wavefunctions and geometries of solutes are optimized self-consistently in the presence of this field.

In addition to bulk electric polarization of the volume surrounding the solute, there are other effects that are more specifically associated with the surface layer of solvent (i.e., with the first solvation shell). One example is the free energy required to make a fresh solvent surface around the solute. A certain part of this process is the same as increasing the surface area at a water–vacuum interface; the energy associated with this part may be called the cavitation energy. But there are additional components at a water–solute interface. For example, there are attractive dispersion forces between the solute and the nearby solvent molecules. Finally, there are local structural changes in the solvent as a result of the insertion of the solute: key examples in water are solute–solvent hydrogen bonding and the especially strong change in solvent–solvent hydrogen bonding in the first solvation shell. Whereas the electrostatic component of hydrogen bonding may be included to some degree in the dielectric polarization term, it also has short-range directional components that cannot be accounted for in a uniform dielectric. Especially for solutes that do not hydrogen-bond to the solvent, the solvent structural change may be unfavorable due to loss of entropy, and there is detailed experimental evidence[32,33] leading to the interpretation of the hydrophobic effect as due to loss of entropy in the solvent because of the introduction of chemical groups unable to participate in hydrogen bonding.

The difference between the electrostatic effect calculated using the bulk dielectric constant and that calculated taking account of local structural factors is sometimes called dielectric saturation, although it has been suggested[34] that a better phrase would be "inhomogeneous dielectric constant." We refer to the sum of these first-hydration-shell effects as the CDS term, representing structural rearrangements that entail cavitation, dispersion, and solvent disposition.

Available models consider or ignore these components of solvation in various ways, as discussed in detail in the sections that follow. One additional effect that should be mentioned is charge-transfer interactions between the solvent and the solute. Although most models do not treat these effects explicitly, they must be implicit to some extent in semiempirical models.

In discussing the various solvation models, we will use the term "molecular mechanics" to denote the modeling of solute–solvent forces (or any other forces) by a sum of terms corresponding to pair interactions (which may be Coulombic, multipolar, dispersion, repulsion, etc.) and angle distortion penalties (which may refer to bond angles or dihedrals). We will contrast this to quantum mechanical approaches, which explicitly address the quantal character of the electronic motions that are ultimately responsible for the balance of these forces.

Aqueous Solvation Modeling

Explicit-Solvent Approaches

Current efforts in solvation modeling in general follow one of two distinct approaches. The first involves the explicit consideration of hundreds or thousands of solvent molecules.[35–42] The supermolecular system consisting of these

molecules plus the solute, when statistically sampled as a canonical ensemble, serves as a basis for simulations from which thermodynamic data related to solvation may be extracted. A molecular mechanics force field is generally employed, since the significant size of the system makes the analysis of forces and energies at the quantum mechanical level difficult, although combinations of quantal treatments of the solute with molecular mechanical treatments of the explicit water molecules representing the bulk have begun to appear.[43–52]

This explicit solvent approach has certain inherent advantages and disadvantages. While a complete discussion is beyond the scope of this chapter, we will summarize those that are most relevant by comparison to continuum models. A key drawback of the molecular mechanics approach is that it almost always ignores the contribution of solute polarization to the ENP terms. (To compensate, the atom-centered partial charges from which the Coulomb interactions are calculated are often set to semiempirical values that exceed the best estimates of gas-phase partial charges.) A related issue is nonpairwise polarization of solvent molecules, which is missing when solvent interactions are treated by pair potentials. Although classically polarizable solvent models have been employed in specific simulations,[53–55] they are not yet general; therefore, electric polarization of the solvent does not include many-body effects on the solute electronic polarization in most simulations. Even simple electrostatic interactions pose difficulties in simulations. Because they operate over ranges so large that it is not computationally tractable to treat all pairwise interactions, a cutoff distance is generally employed, with some sort of correction applied when required.[56,57] Creative approaches addressing this difficulty have appeared.[58,59] Moreover, the choice of the atomic (or group) charges employed in the force field is not unambiguous,[60,61] although methods that use such charges, including continuum solvation models, suffer similarly, given the nonobservable nature of partial charges. In molecular mechanics, there is an ambiguity in empirical parameterizations as to whether dispersion and exchange repulsion are being partially modeled by the electrostatic terms or whether the electrostatic effects are being partially modeled by the van der Waals terms.

Another disadvantage of the explicit-water type of approach is that entropy-dependent properties (e.g., free energy) are notoriously difficult to determine accurately in simulations, since it is rarely clear to what extent all the important regions of phase space are sampled in the simulation.[35,42] This is partly a technical constraint, insofar as simulations are computationally demanding and can be run only for finite lengths of time (typically on the order of nanoseconds ± one order of magnitude). However, phase-space bottlenecks may prevent even very long simulations, which appear to have converged with respect to further sampling, from properly taking into account all accessible configurations of the system.[62] Several recent papers have discussed and addressed serious difficulties in reducing sampling errors.[58,59,63–65]

Finally, at least for the present, explicit-water simulations treat heavy-body motions by the laws of classical mechanics; this is not always valid,

especially for hydrogen bonds and transition states with a significant hydrogenic component in the reaction coordinate. A more rigorous treatment must take account of the possible consequences of quantum mechanical tunneling in these instances.

Probably the key advantages of explicit-water simulations are the great generality of the method and the extra level of molecular detail that simulations reveal. A recent example concerns the study of tightly bound water molecules near the surfaces of proteins.[66] Although typical experimental probes of protein structure give no information about these water molecules, because of the fluxional character of their binding, molecular dynamics simulations reveal both time-averaged and instantaneous views of protein hydration.

Furthermore, the explicit-water simulations do include the CDS terms to the extent that dispersion and hydrogen bonding are well represented by the force field. Finally, by virtue of the solvent being explicitly part of the system, it is possible to derive many useful non-entropy-based properties[35–42] (radial distribution functions, average numbers of hydrogen bonds, size and stability of the first solvation shell, time-dependent correlation functions, etc.). Since many of these properties are experimentally observable, it is often possible to identify and correct at least some deficiencies in the simulation. Simulation is thus an extremely powerful tool for studying solvation, especially when focused on the response of the solvent to the solute.

Continuum Solvent Approaches

An alternative simulation procedure is to replace the explicit solvent molecules with a continuous medium having the bulk dielectric constant.[67–74] Once the solvent has been simplified, it is much easier to employ quantum mechanical techniques for the ENP relaxation of electronic and molecular structure in solution; thus this approach is complementary to simulation insofar as it typically focuses on the response of the solute to the solvent. Since the properties of the continuum solvent must represent an average over solvent configurations, such approaches are most accurately described as quantum statistical models.

Although later in the chapter we develop these models in considerably more detail, it is worth noting that the complementarity of the continuum and explicit solvent approaches extends to their inherent advantages and disadvantages as well. With a continuum representation of the solvent, there is no cutoff distance beyond which electrostatic interactions are ignored. Moreover, the absence of explicit solvent eliminates the possibility of solvent configurational sampling errors, assuming that the continuum is developed so as to mimic the proper statistical average of solvation. Continuum models, like explicit-water models, are obviously limited by the size of the solute, but they do not suffer any limitations arising from a large number of (required) solvent molecules.

On the other hand, if the solvent is not represented, it is obviously impossible to arrive at many of the properties listed earlier as calculable by simulation

procedures. Furthermore, separation of free energies into enthalpic and entropic components is quite difficult in the absence of an explicit treatment of the solvent molecules.

Clearly, the two alternative methods are each of wide utility, and a choice of either or both can only be made after a careful consideration of the details and required answers unique to the modeling of a given system of interest.

Thermodynamics of Solvation

The central quantity in this chapter is the free energy of solvation, ΔG_S°. This quantity, with our choices (one molar ideal solution and one molar ideal gas) for standard states, is the free energy of transfer of a molecule X from an ideal gas at 1 mol/L concentration to an ideal solution at the same solute concentration [X] and temperature T. In practice, this is determined by[75]

$$\Delta G_S^\circ(\mathrm{X}) = -RT \lim_{[\mathrm{X}]_{aq},[\mathrm{X}]_g \to 0} \ln \left(\frac{[\mathrm{X}]_{aq}}{[\mathrm{X}]_g} \right)_{eq} \qquad [2]$$

where R is the universal gas constant, and the equilibrium constant, which is the argument of the natural logarithm, is unitless. This form of equilibrium constant is sometimes called the Ostwald convention (in contrast to Henry's law, discussed next). In Equation [2], the subscripts denote aqueous (aq), gas phase (g), and equilibrium (eq); the equilibrium constant must be measured for a dilute solution because the standard state, as usual, refers to an ideal solution. Thus, in particular, one cannot use solubilities and vapor pressures over saturated solutions.

We may derive the corresponding equation involving the logarithm of Henry's constant as

$$\Delta G_S^\circ(\mathrm{X}) = RT \ln \left[\lim_{p_X, x_X \to 0} \left(\frac{p_X}{x_X} \right)_{eq} \right] - RT \ln R^0 T \rho_w \qquad [3]$$

where p_X is the vapor pressure of X in atmospheres over an aqueous solution in which its mole fraction is x_X, ρ_w is the density of water in moles per liter, and R^0 is R expressed in units of atmospheres per degrees Kelvin per mole. Throughout this chapter, all results are given for a temperature of 298 K, and for this temperature the last term of Equation [3] is 4.26 kcal/mol. Note that the argument of the first logarithm in Equation [3] is the usual Henry's law constant. (Modern treatments express Henry's law in terms of mole fractions, although Henry used mass density.)

Some workers, while retaining the one-molar ideal solution standard state for the solution phase, use a one-atmosphere standard state in the gas

phase. If we denote the standard state free energy of solvation with the latter choice as $\Delta G_S^{\circ'}$, then it is related to the present choice by

$$G_S^{\circ'}(X) = G_S^{\circ}(X) + 1.89 \text{ kcal/mol} \quad [4]$$

at 298 K.

It is particularly unfortunate that many calculated free energies of solvation are published without explicit reference to the chosen standard state. By noting the particular value cited for an experimental free energy of solvation, it is sometimes possible to infer the choice of standard state (if one assumes the workers took care to be consistent), but this is dangerous. We have made every effort to convert all results presented in this chapter to the standard state used in Equation [2]: that is, one molar in both gaseous and solution phases. But some caution should be applied in accepting results where such conversion is necessary.

To relate these thermodynamic quantities to molecular properties and interactions, we need to consider the statistical thermodynamics of ideal gases and ideal solutions. A detailed discussion is beyond the scope of this review. We note for completeness, however, that a full treatment of the free energy of solvation should include the changes in the rotational and vibrational partition functions for the solute as it passes from the gas phase into solution, ΔG_{int}.[75]

In addition, corrections to the entropy of mixing arising from nonideality may be important. Sharp et al.[76] have advocated the approach of Huggins and Flory,[77–86] which establishes that long-chain molecules (e.g., polymers or very large n-alkanes) will have an excess entropy of solution proportional to the ratio of the volume of the solute to that of the solvent. This approach has been very successful for polymer solutions,[87,88] but for globular or small molecules it is not necessarily more valid than using the ideal solution entropy of mixing, ΔS_{is}.[89–94] Moreover, even for straight-chain alkanes, where the Flory–Huggins formula appears to work quite well,[76,95] the difference between ΔS_{FH} and ΔS_{is} scales (at least a rough approximation) with the solvent-accessible surface area.[76,93] Thus it is not clear whether an extra term is warranted in phenomenological or semiempirical treatments for general solutes or indeed whether such a term might diminish the success of such models. The replacement of the volume effect by a term proportional to solvent-accessible surface area seems even more intuitively reasonable for globular solutes. We repeat, however, that in this chapter we neglect both ΔG_{int} and any nonideal entropic corrections to ΔG_S° that are not potentially accounted for in a semiempirical fashion.

The explicit-solvent models discussed earlier attempt to directly evaluate thermodynamic averages by statistically sampling a large number of solvent configurations. The continuum solvation models, which are the main focus of this chapter, include this average implicitly; rather than considering the solvation free energy as the sum of contributions of individual solvent configurations, they consider it as a sum over contributions from one or more physical

effects and/or one or more parts of the solute. These partitionings are the subject of the next section.

CONTINUUM SOLVATION MODELS: THEORY AND APPLICABILITY

Classical Models

With any type of molecular modeling, there is generally a tradeoff between cost and reliability, and one typically shuns models that cost more without increasing reliability. In practice, this cost is usually expressed as computational effort, or computer time. In gas phase modeling, one typically finds molecular mechanics and semiempirical molecular orbital theory at the low-cost end and multireference configuration interaction or coupled-cluster theory at the other, with the choice dictated by the size of the system. System size also influences the choice of solvation model. We consider first the least expensive models, those that take no account of the quantum mechanical nature of the solute.

Solvent-Accessible Surface Area Models

One useful way to approximate the interactions of a solute with surrounding solvent is to partition the net solvation free energy into portions specific to distinct parts of the solute (e.g., atoms, functional groups, etc.). This partition is accomplished by assuming that the energetics for the interaction of any subgroup of the solute will be dominated by solvent–solute interactions that are *close* to that subgroup. The next step is to imagine partitioning the surrounding solvent shell into atom-specific or group-specific regions. One makes the further approximation that the size of these regions, and the corresponding magnitude of the interaction, is well represented by the size of the first solvation shell of the atom or group in question. And finally, one assumes a proportionality between the size of the first solvation shell and the exposed molecular surface area.[96] While the most efficient means for the calculation of molecular surface area remains a matter of active research, it is reasonably straightforward to accomplish either analytically[97–107] or numerically,[71,108–116] with varying degrees of accuracy and/or numerical precisions, depending on the algorithm and numerical parameters. Under the assumptions stated earlier, the free energy of solvation may be expressed as[107,117–122]

$$\Delta G_S^\circ = \sum_i \sigma_i A_i \qquad [5]$$

where the index of summation runs over the appropriate atoms or groups of the solute, A_i is the calculated surface area, and σ_i is the surface tension (units of energy per length squared) associated with atom or group i.

The choice of exactly what surface area to calculate is, however, not entirely unambiguous.[123] Although one might consider constructing a surface from standard[124] atomic van der Waals radii, the more typical approach is to use the so-called solvent-accessible surface area (SASA).[108,123,125] The solvent-accessible surface is defined as that generated by the center of a spherical solvent molecule rolling on the van der Waals surface of the solute. A moment's reflection shows that this is the same as the exposed surface obtained by placing spheres at each of the atomic centers, where each sphere has a radius equal to the van der Waals radius of the atom plus the radius of a solvent molecule. For water, which is reasonably well approximated as a spherical solvent, the radius is usually taken as 1.4 Å.[49]

Other definitions of molecular surface are discussed elsewhere,[93,114,115,123,125] but we will consider only the solvent-accessible surface area. This definition is preferred because it has a simple interpretation: namely, since the augmented sphere boundaries pass through the centers of the rolling solvent molecules, the exposed area of an augmented sphere centered at atom *i* is proportional to the number of solvent molecules in the first hydration shell of atom *i*. (The idea[32,96,126] that the solvation free energy is proportional to the number of solvent molecules in contact with the solute predates the definition of solvent-accessible surface area.) Since a surface through the first hydration shell defines the cavity, the term "cavity surface area,"[117] might be chosen, but we use "solvent-accessible surface area" because this term has received general acceptance.

Given the many simplifications inherent in the SASA model, it tends to find use primarily for very large molecules (e.g., biopolymers), where its great speed makes it attractive.[127,128] Also, there is some evidence that differential changes in the free energy associated with the solvent-accessible surface play an important role in the relative stabilization of one or another protein conformation. Ooi et al.[122] thus used experimental data from a series of small- to medium-sized organic molecules to parameterize seven surface tensions for distinct groups found in proteins: aliphatic, aromatic, and carbonyl CH_n groups, hydroxyl, amide, and amine groups, carboxyl oxygen, and sulfide and thiol groups. For example, $\sigma_{OH} = -172$ cal/Å^2 and σ for an aliphatic CH_n group is $+8$ cal/Å^2, corresponding well to one's intuitive feeling for the hydrophilic and hydrophobic character of the respective groups. These surface tensions were then used in a modified Empirical Conformational Energy Program for Peptides (ECEPP)[129] force field for the calculation of aqueous conformational preferences for all 20 *N*-acetyl-*N'*-methylamino acid carboxamides. The authors noted interesting effects of solvation on conformation; for example, the internally hydrogen-bonded C_7^{eq} conformation of the alanine derivative is favored by considerably less in aqueous solution than in the gas phase. Moreover, by examining the complete (ϕ, ψ) conformational energy surface, they calculated Boltzmann weighted net free energies of solvation (see later, Equation [44]), which are presented in Table 1. By applying this methodology to bovine pancreatic trypsin inhibitor, ribonuclease A, and elastase, the free energy of denaturation was found to be decreased by 93–441 kcal/mol relative to the gas

Table 1 Computed Aqueous ΔG_S° (kcal/mol) for the *N*-Acetyl-*N'*-Methylamides of the 20 Naturally Occurring Amino Acids Using the SASA Approximation of Equation [5][a]

Residue	ΔG_S°	Residue	ΔG_S°	Residue	ΔG_S°	Residue	ΔG_S°
Ala	−0.6	Gly	−1.2	Met	−1.1	Ser	−6.4
Asp	−8.0	His	−6.8	Asn	−7.9	Thr	−4.6
Cys	−2.5	Ile	0.3	Pro	−0.7	Val	−0.1
Glu	−8.2	Lys	−6.1	Gln	−7.9	Trp	−5.4
Phe	−2.1	Leu	0.2	Arg	−14.0	Tyr	−9.2

[a]From Reference 122.

phase, although in every case the fully extended, denatured protein remained significantly higher in energy than the native conformation.[129] A more detailed presentation of the small-molecule data of Scheraga and co-workers is found in a later section, in connection with Table 2.

The SASA approach makes no attempt to separate the free energy of solvation into distinct components, such as the ENP and CDS terms, but simply assumes the net solvation energy to be proportional to the SASA. In later sections we will consider models that separate these effects. Even there, though, by grouping cavity and solvent structural effects into the same term, one will not distinguish solvent structural effects that occur upon creating a cavity from those over and above the change at a solvent–vacuum interface.

Poisson–Boltzmann Models

The Poisson Equation From classical electrostatics, the free charge density $\rho(\mathbf{r})$—that is, the charge density due to the solute as opposed to the polarization charges in the solvent—in a continuous medium of homogeneous dielectric constant (relative permittivity) ε, where $\mathbf{r}$ denotes the position in space, is related to the electrostatic potential, $\phi(\mathbf{r})$, by Poisson's equation,[130–132] which takes the following form, in this case in Gaussian units:

$$\nabla^2\phi = -\frac{4\pi\rho(\mathbf{r})}{\varepsilon} \qquad [6]$$

Note that Equation [6] does not hold if ε depends on $\mathbf{r}$.[132] However, solutions to this equation can be obtained for multiple regions, each of which has constant ε, by enforcing continuity conditions at the boundaries between regions. Alternatively one can replace Equation [6] by[132]

$$\nabla\cdot\varepsilon(\mathbf{r})\nabla\phi = -4\pi\rho(\mathbf{r}) \qquad [7]$$

Either solution of Poisson's equation for $\phi(\mathbf{r})$ (i.e., Equation [6] or [7]) permits calculation of the free energy G as the maximum work extractable from the system by[132]

$$G = \frac{1}{2}\int d^3\mathbf{r}\ \rho\ \phi \qquad [8]$$

This equation takes account of the fact that to maintain T we have kept the dielectric medium in contact with a heat bath with which it can exchange heat to maintain thermal equilibrium. Equation [8] provides the simplest example of a reaction field effect. The electric field is in general given by[131,132]

$$\mathbf{E}(\mathbf{r}) = -\nabla\phi \qquad [9]$$

and thus it may be decomposed, at least mentally, into a contribution from the solute charges in vacuum and a contribution from the polarization induced in the solvent. The latter contribution within the solute cavity is called the reaction field. Then Equation [8], or the equivalent[131,132]

$$G = \frac{1}{2}\int d^3\mathbf{r}\ \mathbf{D}(\mathbf{r}) \cdot \mathbf{E}(\mathbf{r}) \qquad [10]$$

where $\mathbf{D}(\mathbf{r})$ is the dielectric displacement due to the free charges, shows that the solute interacts with its own reaction field, which has a significant effect on the energy of the system.

In practice, it is possible to solve Equation [6] or [7] analytically for ideal cases only. One such case is a charge q on a conducting sphere of radius α, which is a simple model of a monatomic ion. Recall that a charge on a metallic sphere is spread uniformly over its surface, but the effect of this outside the sphere is the same as for a point charge at the sphere center. The dielectric constant in a conductor is ∞, and the integral in Equation [8] becomes the integral of an analytically known central field in the homogeneous dielectric medium exterior to the sphere. Evaluating this integral both for the gas phase ($\varepsilon = 1$) and the dielectric medium ($\varepsilon > 1$) gives Born's formula[28] for the free energy of transfer from a dielectric of unity (vacuum or sufficiently dilute gas phase) to a solvent of dielectric ε:

$$\Delta G_S^\circ = -\frac{1}{2}\left(1 - \frac{1}{\varepsilon}\right)\frac{q^2}{\alpha} \qquad [11]$$

A continuing issue of discussion is the precise meaning of α in terms of atomic properties.[133–137] Obviously there is some ambiguity in the way that the radius of the sphere can be related to the various definitions of the radius of an atom or in whether[136] a shell of solvent should be included.

Note that Equations [8], [10], and [11] include not only the interaction energy of the ion with the solvent but also the change in solvent–solvent interactions when the ion is inserted. Under fairly mild assumptions, it can be shown that the latter increase in intrasolvent energy cancels half the favorable

ion–solvent interactions, which is one way to think about the factors of $1/2$ in these equations.[31,46,136,137,139–146]

A similar treatment for a point dipole of magnitude μ in a sphere of radius α yields the Kirkwood–Onsager result[29,30]

$$\Delta G_S^\circ = -\frac{(\varepsilon - 1)\mu^2}{(2\varepsilon + 1)\alpha^3} \qquad [12]$$

For a molecular charge distribution, such simple formulas are not applicable, but using either the finite difference method[147–158] or the boundary element method[135,156,159–165] one can convert the problem to a set of linear algebraic equations, which can be solved numerically. In the finite difference method, one solves directly for the electrostatic potential at a set of grid points. In the boundary element method, one solves for the distribution of induced polarization charge at the dielectric interface, taking advantage of the general result from electrostatic theory that permits one to replace the effect on the free charges of the polarization charges induced throughout the entire dielectric medium by the effect of a suitable distribution of surface charge on the interface with that medium.[132] One popular commercial software package to accomplish the solution of Poisson's equation is DelPhi.[155] Results for a selection of organic molecules are provided later. Since applications reported to date have treated the solvent as a homogeneous dielectric, these energies include only what we call the ENP component, and in fact only the unrelaxed-solute approximation to this component because polarization of the solvent is taken into account, not mutual, simultaneous polarization of both the solvent and the solute.

To account for solute polarization, still within the constraints of classical electrostatics, investigators have explored the equivalent approaches of employing an internal solute dielectric greater than one (typically 2 to 4,[156] reflecting the square of the index of refraction for most organic molecules) or placing point-inducible dipoles at some or all grid points.[74]

The Poisson–Boltzmann Equation Equation [7] may be modified to take account of mobile charge density within the surrounding continuum (e.g., the ions of a dissolved electrolyte). In the case of a 1:1 electrolyte, such as NaCl, this situation is treated by the nonlinear Poisson–Boltzmann equation[166]

$$\nabla\cdot\varepsilon(\mathbf{r})\nabla\phi - \varepsilon(\mathbf{r})\lambda\kappa^2 \frac{k_B T}{q} \sinh\left(\frac{q\phi}{k_B T}\right) = -4\pi\rho(\mathbf{r}) \qquad [13]$$

where k_B is Boltzmann's constant, T is temperature, q is the magnitude of the charge of the electrolyte ions, λ is a function that is zero in regions inaccessible to the electrolyte and one elsewhere, and κ^2 is the usual Debye–Hückel parameter

$$\kappa^2 = \frac{1}{r_D^2} = \frac{8\pi q^2 I}{\varepsilon k_B T} \qquad [14]$$

where r_D is the Debye length and I is the ionic strength of the bulk solution. Note that $\varepsilon(\mathbf{r})\nabla\phi(\mathbf{r})$ in Equation [13] is 4π times the electric displacement vector $\mathbf{D}(\mathbf{r})$.[131,132]

The three-dimensional, second-order, nonlinear, elliptic partial differential equation may be simplified in the limit of weak electrolyte solutions, where the hyperbolic sine of ϕ is well approximated by ϕ. This yields the linearized Poisson–Boltzmann equation

$$\nabla\cdot\varepsilon(\mathbf{r})\nabla\phi - \varepsilon(\mathbf{r})\lambda\kappa^2\phi(\mathbf{r}) = -4\pi\rho(\mathbf{r}) \qquad [15]$$

a special case of which is well known from Debye–Hückel theory.[8,9,166–170] Equations [13] and [15] are more complicated to solve than the Poisson equation, but numerical solutions by both the finite difference[153,156,163,165–184] and boundary element[163,164,177] methods are possible.

The ability to incorporate electrolyte effects is important because biological macromolecules like DNA, with its negatively charged phosphodiester backbone, are surrounded by multiple ions.[185] Moreover, the relaxation time of these ions is long enough to make explicit solvent simulations quite challenging.[186–188] By replacing the solvent by a continuum, the Poisson–Boltzmann approach affords an economical treatment of such effects for DNA, proteins, and so on.[183,189] Current efforts in this area include incorporation of solvation into molecular mechanics and dynamics force fields, either using the Poisson–Boltzmann equation to develop new force field parameters[190] or by incorporating approximate solutions of the Poisson–Boltzmann equation directly into the molecular model.[184,189]

The Generalized Born and Generalized Born/Surface Area Models in Molecular Mechanics

Most molecular mechanics programs incorporate a dielectric constant into their electrostatic interaction terms,[191] which may be thought of as a crude way to introduce a continuum model. This approach not only neglects solvent and solute polarization and first-hydration-shell effects, it also neglects the solvent's effect on the self-energy of an ion and its interaction with the solvent as incorporated in Equation [11]. Many workers use distance-dependent dielectric constants (e.g., tending to the free space value at small distances and the bulk value at large distances), but this usage, or using dielectric constants to account for reaction field effects in a cavity,[152,154,192] leads to severe conceptual difficulties. In fact, the concept of effective dielectric constant should be avoided wherever possible, especially for calculating forces.[156]

To include the effect of solvent polarization in molecular mechanics, Still and co-workers[193] turned to the generalized Born model.[5,71,142,194–203] In this model, the electric polarization free energy is written in atomic units as

$$G_P = -\frac{1}{2}\left(1 - \frac{1}{\varepsilon}\right)\sum_{k,k'} q_k q_{k'} \gamma_{kk'} \qquad [16]$$

where q_k is the net atomic partial charge, k and k' run over atomic centers, and $\gamma_{kk'}$ is a Coulomb integral. Still et al. approximated the Coulomb integrals as

$$\gamma_{kk'} = \{r_{kk'}^2 + \alpha_k \alpha_{k'} C_{kk'}(r_{kk'})\}^{-1/2} \qquad [17]$$

where α_k is the effective ionic radius of atom k, $r_{kk'}$ is the interatomic distance between atoms k and k', and $C_{kk'}$ is given by

$$C_{kk'} = \exp\left(\frac{-r_{kk'}^2}{d^{(0)}\alpha_k \alpha_{k'}}\right) \qquad [18]$$

where $d^{(0)}$ is an empirically optimized constant equal to 4. Equation [17] may be considered to be a generalization of older equations due to Ohno and Klopman.[204,205] Its analytic form is designed to ensure proper behavior in three important limits: infinite separation of atoms k and k' (where it yields a sum of Born formulas), coalescence of identical atoms (where it again yields a Born formula) and close approach of dissimilar atoms [where it yields the Kirkwood–Onsager result within 10% when $r_{kk'} < 0.1(\alpha_k \alpha_{k'})^{1/2}$].

For the monatomic case ($k = k' = 1$), α_k was defined[193] to be a parameter ρ_k, where the latter was taken to be the atomic radius from the Optimized Potentials for Liquid Simulations (OPLS)[206] force field less 0.09 Å, which is an empirical adjustment. In the multicenter case, α_k is defined numerically by a new procedure[193] that could be thought of as an approximation to the solutions of Equations [6]–[10]. In this procedure, α_k is chosen so that the G_P derived as in a monatomic case is equal to the G_P determined via numerical integration. Thus, one considers M spherical shells i around each atom k and calculates

$$\alpha_k^{-1} = \sum_{i=1}^{M} \frac{A_i(r_i;\{\rho k\})}{4\pi r_i^2}\left(\frac{1}{r_i - 0.5T_i} - \frac{1}{r_i + 0.5T_i}\right) + \frac{1}{r_{M+1} - 0.5T_{M+1}} \qquad [19]$$

where r_i and T_i are defined recursively by

$$r_i = \begin{cases} \rho_k + \frac{1}{2} T_1 & i = 1 \\ r_{i-1} + \frac{1}{2} (T_{i-1} + T_i) & i > 1 \end{cases} \quad [20]$$

and

$$T_i = \begin{cases} T_1 & i = 1 \\ (1 + F)T_{i-1} & i > 1 \end{cases} \quad [21]$$

and A_i $(r_i;\{\rho_k\})$ is the analytically determined[110] approximate exposed surface area of the sphere of radius r_i, that is, the area not included in any spheres centered around other atoms when those spheres have radii given by the set $\{\rho_k\}$. The summation limit M is reached when the sphere of radius $r_i - 0.5T_i$ encompasses the entire molecule (for the monatomic case, $M = 0$; in that case only the term outside the summation is used). The expansion factor F and the initial shell thickness T_1 are numerical parameters set to 0.5 and 0.1 Å, respectively. By virtue of the analytical approximation to A_i and by treating α as a periodically updated constant, analytical derivatives of Equation [16] may be included as forces within a molecular mechanics minimization.

This approach, then, accounts for the electrostatic and solvent polarization (but not the solute polarization) portions of the ENP term, using force field atomic partial charges. Still et al.[193] also included a part of the CDS energy term in their formalism by employing a SASA approach (i.e., Equation [5]), where the SASA is evaluated for the OPLS van der Waals surface plus solvent radius, and the surface tension σ is defined to be a constant of 7.2 cal mol^{-1} $Å^{-2}$. This positive surface tension term may be thought of as a cavity creation energy; clearly the atom-specific dispersion and hydrophilic contributions are not included.

This combination of Equations [5] and [16] is called the Generalized Born/Surface Area model (GB/SA), and it is currently available in the MacroModel[207] computer package. The speed of the molecular mechanics calculations is not significantly decreased by comparison to the gas phase situation, making this model well suited to large systems. Moreover, the model takes account of some first-hydration-shell effects through the positive surface tension as well as the volume polarization effects. A selection of data for aqueous solution is provided later (Table 2), and the model is compared to experiment and to other models. Nonaqueous solvents have been simulated by changing the dielectric constant in the appropriate equations,[208] but to take the surface tension to be independent of solvent does not seem well justified.

The choice of the partial charges requires some care when the GB/SA model is used. Still et al.[193] note that the model is very sensitive to the charge set (e.g., OPLS) chosen. This issue is particularly important when comparing

differences in the solvation energies of conformational isomers because force field studies usually assign atomic partial charges based only on atomic number, not molecular geometry, although the geometrical dependence of partial charges can have a significant effect on solvation energies.[60,61]

Quantum Mechanical Models

Since the models discussed up to this point do not take account of the quantum mechanical nature of a solute, they are incapable of a realistic self-consistent treatment of the mutual polarization of the solvent and the solute when the latter is placed in the former. Attempting to formulate such a treatment raises complex issues of time scales when one considers dynamics, especially of charge transfer reactions,[209–212] but in this chapter we consider only models that assume a simple Born–Oppenheimer treatment of the time scales. In this approach, for each nuclear geometry of the solute, one seeks a self-consistent equilibrium solution for the state in which the quantal electronic degrees of freedom of the solute are in equilibrium with the classical polarization modes of the solute. Then, in principle, the solute nuclear motion is treated using the resulting free energy surface as a potential of mean force.[8,9] In practice, one is usually satisfied to simply optimize the solute nuclear coordinates to minimize the free energy of the combined solute–solvent system with no solute nuclear kinetic energy.

In the following sections, we consider several different levels of approximation for the electronic structure of the solute and its interaction with the solvent.

Ab Initio Models

Born–Kirkwood–Onsager Reaction Field The result of the Onsager[30] reaction field model for a point dipole inside a spherical cavity is expressed in Equation [12]. Although the dipole moment and the electric field are vector quantities, in this simplification they are antiparallel, and thus their dot product involves simply the negative square of the dipole moment. Accounting for the reaction-field coupling tensor and the work of polarizing the solvent (half the polarization free energy) gives rise to the dielectric prefactor and the inverse cubic dependence on the cavity radius.[29,30,70]

The simplest quantum mechanical Hamiltonian operator that includes reaction field effects for neutral solutes is[71]

$$\left(H_0 - g\,\mu \cdot \langle \Psi|\mu|\Psi\rangle \right) |\Psi\rangle = E|\Psi\rangle \qquad [22]$$

where H_0 is the gas-phase Hamiltonian, $g = 2\,(\varepsilon - 1)(2\varepsilon + 1)^{-1}\alpha^{-3}$, and α is the solute cavity radius. For charged solutes, one should also include an ionic Born term derived from Equation [11]. The corresponding Hartree–Fock equations are then[70,71,144,213–224]

$$\left(F_0 - g\,\mu \cdot \langle \Psi|\mu|\Psi \rangle \right) |\phi_i\rangle = \varepsilon_i |\phi_i\rangle \qquad [23]$$

where F_0 is the usual gas-phase Fock operator,[225] and the ε_i are the one-electron orbital energies of the molecular orbitals ϕ_i. Note that in this approach the usual solutions of the self-consistent field equations are modified to include an additional level of self-consistency, since the Fock operator, the one-electron density matrix involved in the solution of the Hartree–Fock equations,[226] and the molecular dipole moment are all mutually interdependent. It is easily seen that the dipole moment calculated under the influence of solvation (i.e., from solving Equations [22] and [23] will be larger than the gas phase dipole moment. That is, increased charge separation is favored in solvents of increasing dielectric constant.[1] The electrostatic portion of the free energy of solvation, ΔG°_S, is then simply the energy calculated from Equation [12] minus the gas phase energy. This is the first level of theory we have considered that self-consistently takes account of the mutual polarization of the solvent and the solute. It is easily appreciated that the improvement in solvation energy from increased dipole moment is counterbalanced by an increase in the internal solute energy. The latter is clear because any deviation from the gas phase, optimized electronic structure necessarily involves an increase in internal energy. This is illustrated graphically in Figure 4, which shows the change in ΔG_{ENP} and its two components for a solute coordinate along which distortions lower the interaction energy with the solvent.

Several details with respect to implementation of Equations [22] and [23] deserve further discussion. Whereas the approximation of the solute residing in a spherical cavity is clearly of limited utility, since most molecules are not approximately spherical in shape, there is also the issue of the choice of the cavity radius, α. Obvious approaches include (1) recognizing that the spherical cavity approximation is arbitrary and thus treating α as a free parameter to be chosen by empirical rules, and (2) choosing α so that the cavity encompasses either the solvent-accessible van der Waals surface of the solute or the same volume. Wong et al.[227] have advocated a quantum mechanical approach like the last method wherein the van der Waals surface is replaced by an isodensity surface. Because g depends on the third power of α, the calculations are quite sensitive to the radius choice, and some nonphysical results have been reported in the literature when insufficient care was taken in assigning a value to α. Implementations that replace the cavity sphere with an ellipsoid have also appeared.[213]

As emphasized, the Born–Kirkwood–Onsager (BKO) approach includes only the solute's monopole and dipole interaction with the continuum. That is, the full classical multipolar expansion of the total solute charge distribution is truncated at the dipole term. This simplification of the electronic distribution fails most visibly for neutral molecules whose dipole moments vanish as a result of symmetry. A distributed monopole or distributed dipole model is more

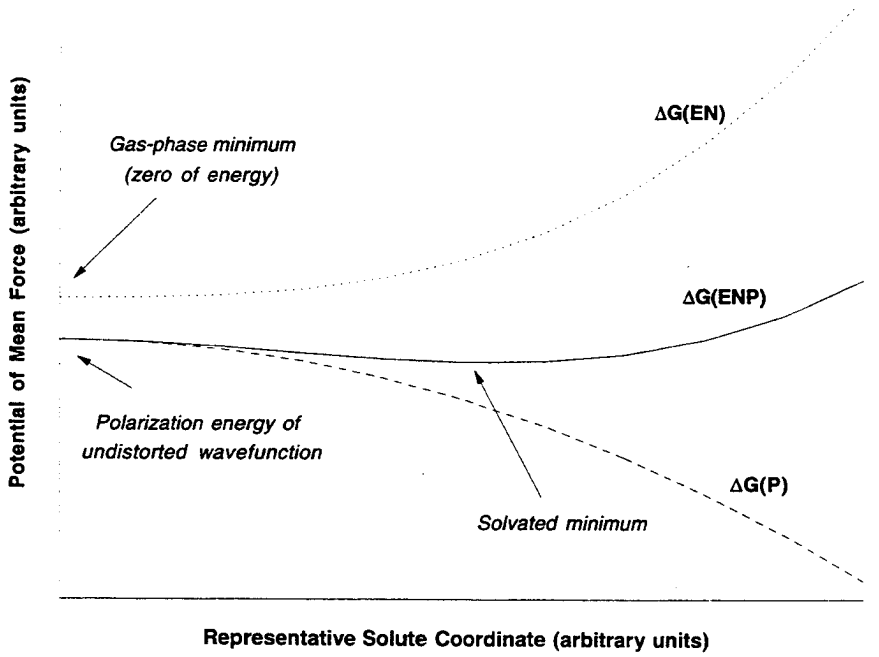

Figure 4 The ENP component of the potential of mean force is the sum of a positive distortion energy and a negative (but rapidly less steeply changing) polarization free energy. The solvated minimum occurs close to, but not precisely at, the minimum of ΔG_{ENP} because G°_{CDS} also has a (typically very small) dependence on geometry.

appropriate in such cases. To the extent that the full solute charge distribution is well modeled by a set of dipole distributions at various sites, the BKO approximation corresponds to replacing the sum of the interactions of the continuum with each of the individual site moments by a single interaction of the continuum with the sum of the site moments. This is inappropriate in certain cases; examples are dealt with in more detail in the final section. The generalized Born model does not have these deficiencies of the BKO model in representing realistic charge distributions.

The Born–Kirkwood–Onsager model, however, is particularly simple to implement; its advantages include the ability to use correlated wavefunctions[220,222] and to calculate analytic first and second derivatives.[214,219,220] As such, the BKO or Onsager model (the latter considers only the dipole—not the charge—and hence is appropriate only for neutral solutes) is available in many standard programs,[214,228,229] and it is widely employed.

It does not appear that any attempt has been made to couple this BKO model to a means by which to calculate the CDS components of solvation, and this limits the model's accuracy, especially for solvents like water, where the CDS terms are not expected to be trivial. For water as solvent, studies *have* appeared that surround the solute with some small to moderate number of explicit solvent molecules, with the resulting supermolecule treated as interacting with the surrounding continuum.[223,230] Although such a treatment has the virtue of probably making the calculation less sensitive to the now-large cavity radius, it suffers from the usual explicit-solvent drawbacks of the size of the system, the complexity of the hypersurface, and the need for statistical sampling.

Applications of the Born–Kirkwood–Onsager model at the ab initio level include investigations of solvation effects on sulfamic acid and its zwitterion,[231] an examination of the infrared spectra of formamide and formamidic acid,[227] and a number of studies focusing on heterocyclic tautomeric equilibria.[227,232,233] A more detailed comparison of some of the heterocyclic results is given later. The gas phase dipole moment depends on basis set, and systematic studies of this dependence are available. Furthermore, the effects of basis set choice and level of correlation analysis have been explored in solvation studies as well,[227,233] but studies to permit identification of particular trends in their impact on the solvation portion of the calculation are as yet insufficient.

Reaction Fields from Higher Order Multipolar Expansions Generalizations of the Born–Kirkwood–Onsager model have appeared which extend the multipole series to arbitrarily high order.[30,67,144,234–236] This approach yields

$$\Delta G_S^\circ = -\frac{1}{2}\sum_{l=0}^{\infty}\sum_{m=-l}^{+l}\sum_{l'=0}^{\infty}\sum_{m=-l'}^{+l'} M_l^m f_{ll'}^{mm'} M_{l'}^{m'} \qquad [24]$$

where each component m of every multipole M of order l interacts with all the reaction field multipole moments induced by the solute multipoles (e.g., the $M_{l'}^{m'}$ terms) via a coupling $f_{ll'}^{mm'}$, called the reaction field factor. The Born–Kirkwood–Onsager model is then seen as a special case involving only the charge ($l = 0$) and dipole moment ($l = 1$) terms; the spherical cavity eliminates any specific dependence on m (e.g., the Cartesian components of the dipole moment, although the orthogonality of these components for the dipole term causes them not to interact even in the absence of a spherical cavity), and $f_{ll'}$ is nonzero only for $l = l' = 0$ (the Born term) and $l = l' = 1$ (the g coupling).

More generally, the reaction field factors may either be determined numerically, since they appear in an overdetermined system of linear equations,[236] or they may be computed analytically for certain idealized cavities (e.g., sphere and ellipsoid).[30,66,213,214] Efficient optimization of solvated geometries motivates the latter approach,[213,235–237] but the formalism has also been ap-

plied with multipolar expansions fitted to completely arbitrary surfaces.[236] Ab initio implementation of the model using ellipsoidal cavities is available in SCRFPAC,[236,238] and the REFFAC numerical algorithms to find the reaction field factors are in the process of being incorporated into an ab initio code for distribution.[236] It also appears that the Gaussian program suite[228] will soon incorporate multipolar expansions in both ideal and general cavities.[239]

The multipole expansion model has seen use in the examination of solvation effects on both reaction coordinates and conformational equilibria, including the isomerization of push–pull ethylenes[240] (e.g., nitroenamines), the ketene-imine [2+2]-cycloaddition to form β-lactam,[241] and the Diels–Alder reaction.[242,243] Again, only the ENP terms are considered in general.

A critical point in the application of this model is the convergence of the solvation energy with respect to multipole order. Even for fairly simple molecules, this convergence can be quite slow. Thus, Pappalardo et al.[240] found a total electrostatic polarization free energy ($\varepsilon = 38.8$) for *Z*-3-aminoacrylonitrile of −13.2 kcal/mol, of which 66% was contained in the dipole term, 22% in the quadrupole, and the remaining 12% in the terms up through 2^6-pole, which was the highest multipole they considered. Moreover, this slow convergence becomes considerably more pronounced for the transition state for rotation about the double bond in this molecule, where the polarization free energy for the charge-separated structure is −44.8 kcal/mol, partitioned as 64% dipole, 18% quadrupole, and 19% in the higher order terms. These authors argue that as a result, the Born–Kirkwood–Onsager model, which is a truncation at the dipole term, should not in general be trusted for any but the most simple molecules.[239,240] This point is discussed in more detail in the survey section of this chapter.

The convergence of the multipole expansion is also apparently quite dependent on the shape (i.e., idealized or arbitrary) of the cavity employed.[236,239] In this regard, although the multipolar expansion of the electronic structure is typically performed for a single point—for example, the center of mass of the molecule (recall that only the first nonzero moment of the molecule is independent of the origin of the coordinate system)—this is not a requirement. Instead, an arbitrary number of distributed multipoles may be placed at any number of points (e.g., the atomic coordinates).[236,244–246] Fitting the multipoles and reaction field factors proceeds as before, although in this case even a neutral molecule usually has partial charge components at each point unless forbidden by symmetry—reminiscent of the generalized Born model (Equation [16]). As expected, the distributed approach leads to much more rapidly convergent calculations of electrostatic solvation free energies. In the modeling of formamide, using as a cavity the van der Waals contact surface, a one-center expansion still has 1% fluctuations by the 2^6-pole term. The distributed expansion, on the other hand, has a 1% contribution from the quadrupole and is essentially completely converged after this point.[236] It is generally more

efficient to describe molecular electronic structure as a set of n distributed monopoles rather than a single multipolar expansion of order n, although the method employed for determining the magnitude of the monopoles (partial charges) remains the subject of ongoing debate.[246–262] Including higher multipoles at every center obviously increases the flexibility of the approach, but at the cost of considerable computational effort.[236,246] A recent application of this approach, which includes electron correlation, has appeared for the NH_3/HCl complex.[263]

Generalized Reaction Fields from Surface Charge Densities Rather than centering attention on the charges or distributed multipoles, at various positions inside the solute cavity, that induce the reaction field, one can instead focus on the cavity surface. In particular, the effect of the reaction field may be modeled by an appropriately distributed set of induced polarization charges (virtual charges) on the surface S of the dielectric, as already mentioned. The virtual charge density, $\sigma(\mathbf{r})$, for each location $\mathbf{r}$ on S is

$$\sigma(\mathbf{r}) = \frac{1 - \varepsilon}{4\pi\varepsilon} \frac{\partial}{\partial n} [\phi_\rho(\mathbf{r}) + \phi_\sigma(\mathbf{r})]_{S_-} \qquad [25]$$

where $\phi_\rho(\mathbf{r})$ is the electrostatic potential due to the solute charge distribution and $\phi_\sigma(\mathbf{r})$ is a potential due to the virtual charges. The derivative is an outwardly normal one evaluated on the solute side (indicated by the S_- subscript) of the interface.[72,73,112,264–267] The potential created by the surface-distributed virtual charges is

$$\phi_\sigma(\mathbf{r}) = \int_S \frac{\sigma(\mathbf{r}')}{|\mathbf{r} - \mathbf{r}'|} d^2S \qquad [26]$$

where $\mathbf{r}'$ is a point on the surface S. This potential must be added to the potential due to the solute charges to obtain the total electrostatic potential ϕ at $\mathbf{r}$. The electrostatic portion of the free energy of solvation is then defined as

$$\Delta G_S^\circ = \langle \Psi | H_0 + \phi_\sigma | \Psi \rangle - \frac{1}{2} \int \phi(\mathbf{r}) [\rho_n(\mathbf{r}) + \rho_e(\mathbf{r})] d^3\mathbf{r} - G_g^\circ \qquad [27]$$

where ρ_n and ρ_e are the solute nuclear and electron density, respectively, the integral represents the cost of polarizing the solvent, and G_g° is the free energy of the solute in the gas phase. Available computer codes implementing this methodology include MONSTERGAUSS[268] and GAMESS-UK.[229,232]

This model, usually referred to as the Polarized Continuum Model (PCM) has a long history, and considerable effort has been spent in arriving at prescriptions for choosing the optimum cavity surface as a function of basis set,[269]

developing algorithms for efficient optimization of molecular geometries,[267,270] incorporating self-consistently the quantum mechanical effects of dispersion[271–274] and electron correlation,[274–276] and considering nonequilibrium solvation.[277] Cavitation effects are usually included in this model using the scaled-particle model of Pierotti,[278] which is not a necessary choice and is perhaps not the best choice. With this inclusion, the PCM model includes both ENP and, at least in part, CDS terms, but the directional components of hydrogen bonding in donor/acceptor solvents are not treated fully. At the correlated ab initio level of theory, with the additional overhead of the solvation portions of the calculation, implementation of these models is particularly demanding of computational resources. Thus one runs into the practical questions of precisely how accurate a continuum model may be expected to be, and how much added cost for a well correlated solute is a worthwhile expenditure. The answers are by no means clear, and certainly more work remains to be done to develop a better understanding of the tradeoffs.

Although the cost of the correlated models has limited their application to fairly small molecules,[272–277] implementations of the methodology at simply the Hartree–Fock level have been used to study the basicity of methylamines,[279] conformational equilibria in esters and amides,[280] the influence of solvation on the anomeric effect,[281] S_N2 reactions,[265,282] and even structural properties of biopolymers like DNA.[283–285] In addition, considerable attention has been paid to interfacial phenomena and the analysis of solvent transfer processes.[286–289] Finally, the influence of solvation on the reaction coordinate for the Menschutkin nucleophilic displacement reaction has been analyzed with the PCM formalism.[290]

The extremely general nature of the PCM technique makes it uniquely attractive, although the electrostatic solvation energies appear to be quite sensitive to choice of basis set.[232,274,279–281,291]

Semiempirical Models

The accounting of the quantum mechanical models for the mutual solvent–solute polarization in a self-consistent fashion is perhaps their greatest virtue. However, as already alluded to, the costs of ab initio formalisms may not be warranted—either because they cannot attain accuracies beyond the intrinsic limitations of the continuum solvation model or, alternatively, because they are simply not applicable to a prohibitively large system. In such instances, just as in the gas phase, semiempirical quantum mechanical models often provide an attractive alternative to the classical models discussed earlier.

Born–Kirkwood–Onsager Reaction Field The theory underlying the implementation of the BKO model at the semiempirical level is no different from that presented in Equations [22] and [23], although the approximations inherent to various levels of semiempirical theory make certain technicalities of the

calculation slightly different (e.g., the means by which dipole moment is calculated from the wavefunction).[292,293] Thus, the choice of semiempirical Hamiltonian is made for much the same reasons as in the gas phase.

The Neglect of Diatomic Differential Overlap (NDDO)[294] level of theory is the most general and successful,[292] and self-consistent reaction field (SCRF) studies employing the Modified Neglect of Diatomic Overlap (MNDO),[295] Austin Model 1 (AM1),[296] and Parametric Method 3 (PM3)[297,298] Hamiltonians have all appeared. Following implementation of the solvation model, one is afforded essentially free choice, since the majority of available semiempirical packages[228,299–302] incorporate all these NDDO Hamiltonians. Whereas the distributed version of GEOMOS[301] includes the SCRF model in the Born–Kirkwood–Onsager version, it appears that only locally modified versions of AMPAC and MOPAC do so as well.[214,303,304]

Other semiempirical Hamiltonians have also been used within the BKO model. A Complete Neglect of Differential Overlap (CNDO/2)[305] study of the effect of solvation on hydrogen bonds has appeared.[306] The Intermediate Neglect of Differential Overlap (INDO)[307] formalism has also been employed for this purpose.[308] Finally, the INDO/S model,[309] which is specifically parameterized to reproduce excited state spectroscopic data, has been used within the SCRF model to explain solvation effects on electronic spectra.[222,310–312] This last approach is a bit less intuitively straightforward, insofar as the INDO/S parameters themselves include solvation by virtue of being fit to many solution ultraviolet/visible spectroscopic data.[293]

With the NDDO methods, tautomeric equilibria,[230] especially in heterocycles,[216–219,223,224,227,232,233] have been a favorite topic for study using the BKO approach. The tautomeric equilibria of many heterocyclic systems are exquisitely sensitive to solvation,[1,313,314] making them interesting test cases for the validation of any solvation model. A detailed comparison is presented later in the section on relative free energies in heterocyclic equilibria. A comprehensive study of the stabilization of a wide variety of carbon radical and ionic centers has also been reported.[315]

As mentioned earlier, various workers have attempted to remove some of the strong dependence on the cavity radius by going to supermolecule systems incorporating explicit solvent molecules.[223,230,311,312] This approach has the additional benefit of including directional components of local solvation effects, which may be important in spectroscopy,[311,312] albeit at the expense of rapidly complicating the hypersurface.

In general, the BKO model as implemented at the semiempirical level suffers from the same drawbacks, and offers the same advantages, as those enumerated for the ab initio level. The chief difference is simply that larger systems may be addressed with the faster semiempirical models. A more complete discussion of cases where the model performs poorly is offered in the survey section.

Reaction Fields from Higher Order Multipolar Expansions Of the semiempirical programs already mentioned that include the Born–Kirkwood–Onsager model, it appears that only GEOMOS[301] allows inclusion of higher order multipoles and/or more generalized cavities. Using this generalized model with semiempirical molecular orbital theory, Terryn et al.[316] studied amine basicity at the CNDO/2 level with 8 multipole moments. Bertrán et al.[317] employed the same level of theory in a study of solvation effects on frontier molecular orbital energies. Ford and Wang,[318] who have discussed methodology for choosing optimal ellipsoidal cavities, have provided some results for a small number of neutral molecules and ions (see Table 2 later). They emphasize that the multipolar expansion model is significantly more sensitive to cavity variation than the simple BKO model. In addition, a study of the effect of solvation on the conformational equilibria of α-substituted carbonyl compounds has been undertaken at the PM3 level.[319] Again, the only distinctions between the ab initio and the semiempirical levels have to do with the means by which multipole moments are calculated within the NDDO approximation and the size of the systems that may be conveniently addressed —the virtues and failings of the model are largely unchanged.

Generalized Reaction Fields from Surface Charge Densities Ab initio formulations of the PCM model discussed earlier, undertaken primarily by Tomasi and co-workers (see, e.g., Refs. 72, 73, 266, 267), have very recently been implemented into four different semiempirical packages.[320–325] Available codes include MOPAC,[300,325] a locally modified[326] version of MOPAC,[300] and VAMP.[302] While the model used by Negre et al.[320] with NDDO Hamiltonians follows exactly the derivation of Equations [23] and [27], those of Wang and Ford,[321,322] Fox et al. (an INDO implementation),[323] Rauhut et al.,[324] and Klamt and Schüürmann[325] include the work of polarizing the solvent by a diferent derivation that yields the same result. Thus Equation [27] is reformulated as

$$\Delta G_S^\circ = \langle \Psi | H_0 + \frac{1}{2} V_\sigma | \Psi \rangle - G_g^\circ \qquad [28]$$

where V_σ is defined such that Equation [28] yields results equivalent to Equation [27]. Klamt and Schüürmann,[325] who extended the more general formulation of Hoshi et al.,[327] have presented an innovative Green's function approach, which they call COSMO, for determination of the surface virtual charge densities of Equation [25]. The cosmo method assumes conductorlike screening (i.e., $\epsilon = 00$) and empirically corrects for the effects of a finite dielectric constant. This approach, like other approaches discussed in this section, allows a more flexible description of the solute charge distribution than the distributed atom-centered monopoles of the generalized Born model in that COSMO includes single center dipoles, which are expected to be particularly important for centers with nonbonded electrons. In addition, the COSMO

approach potentially permits more rapid and efficient energy calculations and geometry optimizations for solutes described by general cavities. Other workers have also considered issues relevant to the optimization of solute geometry.[270,328–330]

Although few applications of these very recently implemented models have yet appeared, some calculations for free energies of transfer into aqueous solution are available.[320,321,331,332] Polarization of the solute has been analyzed by reference to the molecular dipole moment,[320] including comparison to a hybrid quantum mechanics/molecular mechanics approach,[50] and the effect of aqueous solvation on conformational equilibria and simple nucleophilic reactions has been examined.[322] No consideration of CDS solvation terms in conjunction with these models has appeared.

The SMx Approach: Generalized Born Electrostatics Augmented by First-Hydration-Shell Effects Each of the foregoing solvation models, when implemented at the semiempirical level, resembles closely its implementations employing ab initio molecular orbital theory—indeed, the ab initio versions often predate the semiempirical. On the other hand, the generalized Born model, discussed with respect to Equation [16] for the case of molecular mechanics,[193] has certain properties that make it particularly appropriate[71,142] to the semiempirical level.[26,27,202,203] Our own SM*x* models, where SM denotes "solvation model," take advantage of this, and we now review these models.

ΔG_S° is calculated from

$$\Delta G_S^\circ = G_S^\circ - E_{EN}(g) \qquad [29]$$

where $E_{EN}(g)$ is the gas-phase electronic kinetic and electronic and nuclear Coulombic energy, and G_S° is the part of the solute aqueous free energy given by

$$G_S^\circ = E_{EN}(aq) + G_P(aq) + G_{CDS}^\circ(aq), \qquad [30]$$

where $E_{EN}(aq)$ is the sum of the solute electronic kinetic and electronic–nuclear Coulombic energies in the presence of solvent (necessarily greater than or equal to the energy of the gas phase optimum, i.e., including any distortion energy), $G_P(aq)$ is the solution polarization free energy, and G_{CDS}° is the cavitation–dispersion–structural free energy. Other contributions to the "true" free energy (e.g., vibrational) are assumed to remain effectively constant and thus not to affect ΔG_S°, although they must be added to G_S° to obtain all the free energy in solution, as opposed to just the part defined in Equation [30].

We find it convenient to deal with the sum

$$G_{ENP}(aq) = E_{EN}(aq) + G_P(aq) \qquad [31]$$

where $G_P(aq)$ is defined as in Equations [16] and [17]. Equation [18] is modified, however, in this implementation,

$$C_{kk'} = C^{(0)}_{kk'}(r_{kk'}) + C^{(1)}_{kk'}(r_{kk'}) \qquad [32]$$

where

$$C^{(0)}_{kk'} = \exp\left(\frac{-r^2_{kk'}}{d^{(0)}\alpha_k\alpha_{k'}}\right) \qquad [33]$$

and $d^{(0)}$ remains an empirically optimized constant set equal to 4; the new $C^{(1)}_{kk'}$ is given by

$$C^{(1)}_{kk'} = \begin{cases} d^{(1)}_{kk'} \exp\left(\dfrac{-d^{(2)}_{kk'}}{\{1 - [(r_{kk'} - r^{(1)}_{kk'}/r^{(2)}_{kk'}]^2\}}\right), & |r_{kk'} - r^{(1)}_{kk'}| < r^{(2)}_{kk'} \\ 0 & \text{otherwise} \end{cases} \qquad [34]$$

where $d^{(1)}_{kk'}$ is nonzero only to correct for certain anomalous O—O and N—H interactions within the NDDO approximation.

For the monatomic case ($k = k' = 1$), α_k is set equal to the intrinsic Coulomb radius, ρ_k, where

$$\rho_k = \rho^{(0)}_k + \rho^{(1)}_k\left[-\frac{1}{\pi}\arctan\frac{q_k + q^{(0)}_k}{q^{(1)}_k} + \frac{1}{2}\right] \qquad [35]$$

where $\rho^{(0)}_k$, $\rho^{(1)}_k$, and $q^{(0)}_k$ are empirically optimized parameters, q_k is the calculated partial charge, and $q^{(1)}_k$ has been fixed at 0.1 for all atoms. Thus, unlike the molecular mechanics implementation, atomic radii are a function of the partial atomic charge, which is determined self-consistently in the semiempirical model. In the multicenter case, α_k is determined numerically as described in Equations [19]–[21].[193]

The E, N, and P terms at the semiempirical level are obtained from the density matrix **P** of the aqueous phase SCF calculation as

$$G_{ENP} = \frac{1}{2}\sum_{\mu\nu} P_{\mu\nu}(H_{\mu\nu} + F_{\mu\nu}) + \frac{1}{2}\sum_{k,k'\neq k}\frac{Z_k Z_{k'}}{r_{kk'}} - \frac{1}{2}\left(1 - \frac{1}{\varepsilon}\right)\sum_{k,k'} Z_k q_{k'}\gamma_{kk'} \qquad [36]$$

where **H** and **F** are, respectively, the one-electron and Fock matrices, μ and ν run over valence atomic orbitals, Z_k is the valence nuclear charge of atom k (equal to the nuclear change minus the number of core electrons), and q_k and $\gamma_{kk'}$ are defined as in Equation [16]. We point out here that two equations in

the literature (Equation [5] of Ref. 202 and Equation [19] of Ref. 203, both of which are analogs of Equation [36] above) are incorrect: the former is missing the last two terms of Equation [36] and the latter is missing the final term and has "=" in the summation index instead of "≠." These are typographical errors; the code has always been correct.

A key step in implementing the generalized Born model at the NDDO level is that the Fock matrix is related to the energy functional (Equation [31]) as its partial derivative with respect to the density matrix. The partial charges that appear in Equation [16] are easily derived from the density matrix. In our work we do this by computing the density matrix P neglecting overlap (as in approximate treatments of π systems by Coulson and Longuet-Higgins[247]), in which case

$$q_k = Z_k - \sum_{\mu \in k} P_{\mu\mu} \qquad [37]$$

(We note that under the assumption of zero overlap, the atomic charges computed this way are the same as the standard Mulliken[248,249] gross atomic charges.) Hence the differentiation of Equation [36] is straightforward, and, neglecting the dependence of ρ_k on q_k, it delivers a new Fock matrix that includes the effects of polarization self-consistently, just as for the other quantum reaction field formalisms, namely,

$$F_{\mu\nu} = F^{(0)}_{\mu\nu} + \delta_{\mu\nu}\left(1 - \frac{1}{\varepsilon}\right) \sum_{k',\mu' \in k'} (Z_{k'} - P_{\mu\mu'})\,\gamma_{kk'}, \qquad \mu \in k \qquad [38]$$

where $F^{(0)}_{\mu\nu}$ is the gas phase Fock matrix element and $\delta_{\mu\nu}$ is the Kronecker delta function. The density matrix is determined self-consistently in the presence of solvent. Thus, as for the other quantum models, there is a "triple" self-consistency in these calculations: the Fock matrix, the density matrix, and the interacting solvent field.

The remaining contribution to the free energy of solvation beyond $G_{ENP}(aq)$ is not ignored, but instead calculated using a formalism similar to the SASA models already discussed,

$$G^{\circ}_{CDS} = \sum_{k'} \{\sigma^{(0)}_{k'} + \sigma^{(1)}_{k'}[f(B_{k'H}) + g(B_{k'H})]\} A_{k'}(\beta_{k'}, \{\beta_k\}) \qquad [39]$$

where the $\sigma_{k'}$ are atomic surface tension parameters, and $A_{k'}(\beta_{k'},\{\beta_k\})$ is the solvent-accessible surface area for nonhydrogen atoms k'. The SASA is defined

as the exposed surface area of atom k', which equals the exposed surface area of the atom-centered sphere with radius $\beta_{k'}$. The latter is well described as

$$\beta_{k'} \approx R_{k'} + R_S \qquad [40]$$

where $R_{k'}$ is the van der Waals radius of atom k' and R_S is the solvent radius, taken for water as 1.4 Å. Exposed area is defined in this step as area that is not contained in any of the other atomic spheres when they also have radii given by Equation [33]; this is why $A_{k'}$ depends on the full set of $\{\beta_k\}$.

For the remaining portion of Equation [39], $B_{k\mathrm{H}}$ is the sum of the bond orders of atom k to all hydrogen atoms in the solute. Using the definition of bond order used by Armstrong et al.,[333] one obtains

$$B_{k\mathrm{H}} = \sum_{\mu \in k, \nu \in \mathrm{H}} P_{\mu\nu}^2 \qquad [41]$$

where μ runs over the valence orbitals of atom k, and ν runs over all hydrogen 1s orbitals. The hydrogen atom is defined (1) to have no solvent-accessible surface area and (2) not to block the solvent-accessible surface area of the underlying nonhydrogenic atom (i.e., $\beta_{\mathrm{H}} = 0$). Furthermore

$$f(B_{k\mathrm{H}}) = \tan^{-1}(\sqrt{3} B_{k\mathrm{H}}) \qquad [42]$$

$$g(B_{k\mathrm{H}}) = \begin{cases} a_k \exp\left\{ - \dfrac{b_k}{1 - [(B_{k\mathrm{H}} - c_k)/w_k]^2} \right\}, & |B_{k\mathrm{H}} - c_k| < w_k \\ 0 & \text{otherwise} \end{cases} \qquad [43]$$

where w_k defines the range of bond orders about c_k affected by g.

This more complicated version of Equation [5] is required to account for the ergonic effect of hydrogen atoms interacting with the local solvent in a fashion that is dictated by the heavy atom to which they are attached. That is, an alkane hydrogen is hydrophobic, whereas an alcohol hydrogen is hydrophilic. For the model to be maximally general, it is thus convenient to modify the heavy-atom surface tension as a function of the number of attached hydrogen atoms, rather than attempting to derive a single, unphysical surface tension for all hydrogen atoms. Although the motivation for parameterizing SM2 and SM3 in terms of united atoms was to achieve the best representation of the physics, not to minimize computation; it is efficient, and the united-atom approach has a potential added advantage if one considers large molecules in that the coordinates of the hydrogen atoms are rarely observed experimentally and hence are less certain than the coordinates of nonhydrogenic atoms. In SM2

and SM3, though, the coordinates of hydrogen atoms are needed for the ENP part of the calculation.

The various parameters have been fit to reproduce experimental[334–337] aqueous solvation data. Much like the earlier quantum models, the primary dependence of the ENP terms is on the solvent dielectric constant, which is taken from experiment. Cavity definition, regardless of shape, is parametric in every model, although many researchers avoid the term; nevertheless, van der Waals radii, isodensity surface values, and so on are parametric choices. The more important point is that the cavity parameters are not expected to show much sensitivity to solvent in any model.

The CDS parameters, on the other hand, are expected neither to be solvent-independent nor to be clearly related to any particular solvent bulk observable, especially insofar as they correct for errors in the NDDO wavefunction and its impact on the ENP terms. The CDS parameters also make up empirically for the errors that inevitably occur when a continuous charge distribution is modeled by a set of atom-centered nuclear charges and for the approximate nature of the generalized Born approach to solving the Poisson equation. Hence, the CDS parameters must be parameterized separately against available experimental data for every solvent. This requirement presents an initial barrier to developing new solvent parameter sets, and at present, published SM*x* models are available for water only (although a hexadecane parameter set[338] will be available soon).

As mentioned after Equation [24], atom-centered monopoles in principle generate the higher multipoles required to describe the electronic distribution (although, of course, a finite number n of charges can give at most n nonvanishing multipole moments), and as noted by Dillet et al.,[236] the distributed monopole term provides the vast majority of the polarization effect (albeit not all). We note this only for comparative purposes, though, since calculation of the ENP terms does not actually involve the multipole moments explicitly.

The SM*x* aqueous solvation models, of which the most successful are called AM1-SM2,[27] AM1-SM1a,[26] and PM3-SM3,[202] adopt this quantum statistical approach, which takes account of the ENP and CDS terms on a consistent footing. The NDDO models employed are specified as the first element (AM1 or PM3) of each identifier. It is worth emphasizing that the SM*x* models specifically calculate the absolute free energy of solvation—a quantity not easily obtained with other approaches. We have reviewed the development and performance of the models elsewhere.[203] We anticipate our further observations later in this chapter by noting that the mean unsigned error in predicted free energies of solvation is about 0.6–0.9 kcal/mol for the SM*x* models for a data set of 150 neutral solutes that spans a wide variety of functionalities. A number of examples are provided later in this chapter.

The models are all available in the semiempirical package AMSOL.[339] They have also been implemented in commercial software packages.[299,340] The

earliest versions of AMSOL were inefficient, but the computational speed was successively improved in versions 3.5 and later.

Comparison of Continuum Models

It is possible to imagine many ways to compare the various models. Moreover, every comparison will tend to illustrate the strengths of some models more than others. The choices of what data to present are driven, at least in part, by the requirement that calculated results be available from multiple models. Predictions for the influence of solvation on various heterocyclic equilibria are presented later (in connection, e.g., with Figure 5).

Theoretical models may be tested against more accurate theoretical treatments or against experiment. In this chapter, we concentrate on the latter. Because water is not only the solvent for which the most data appear to exist,[334–337] but is moreover the most important from a biological standpoint, it is the solvent on which we will focus.

Absolute Free Energies of Aqueous Solvation

Table 2 provides a large collection of data for aqueous solvation ($\varepsilon = 78.3$ at 25°C) from several of the methods we have discussed. Molecules have been chosen provided (1) they have been studied with two or more methods, and (2) an experimental free energy of solvation has been measured. For a few particularly interesting cases, comparisons are made even in the absence of experimental data.

Tables 3 and 4 are the cross-correlation matrices for the various methods and experiment, with a few positions missing because the number of molecules common to certain pairs of methods was not statistically significant. Finally, Table 5 lists the slopes and intercepts determined by linear regression of predicted values for each method against experiment for the neutral solutes. Because the experimental error is very high for the ions (at least ± 5 kcal/mol), the correlations in Table 4 should be analyzed with care.

It is important to emphasize that only the solvent-accessible surface area (SASA), the generalized Born/surface area (GB/SA), and the full AM1–SM2 models purport to address local, nonelectrostatic effects. There is no a priori reason to expect the remaining purely electrostatic models to correlate closely with experiment; nevertheless, it is worthwhile to examine the cross-correlations. We will highlight some of the most interesting trends.

The SASA model[121] enjoys the second-best correlation to experiment for the uncharged solutes, with slope and intercept values quite near the ideal unity and zero, respectively. This is particularly impressive given its great simplicity and extremely rapid application. On the other hand, the range of molecules to which it has been applied is fairly simple—a small handful of functionalities on simple alkyl chains of varying length. It is noteworthy that as functionality becomes more complex, performance appears to degrade, as for acetamide,

Table 2 Calculated Electrostatic Energies, Free Energies, and Experimental Free Energies (kcal/mol) of Solvation for Neutral and Ionic Solutes Using a Variety of Methods[a]

Solutes	SASA[b]	GB/SA[c]	FDPB (1)[d]	FDPB (2)[e]	AM1 ($l \leq 6$)[f]	AM1-PCM[g]	AM1-COSMO[h]	AM1-SM2 ENP[i]	AM1-SM2 Full[i]	Experimental[j] ΔG_S°
Hydrocarbons										
Methane	1.2					−0.1	−0.2	0.0[k]	1.0[k]	2.0
Ethane	1.5	1.3				−0.3	−0.3	0.0	1.2	1.8
Propane	1.7					−0.5	−0.3	0.0	1.4	2.0
Cyclopropane			−8.4			−1.1	−1.3	−0.1	1.1	0.8
Butane	2.0	1.9				−0.7	−0.3	0.1	1.7	2.1
2-Methylpropane	2.0				−0.2	−0.7	−0.3	0.1	1.6	2.3
Hexane	2.5	2.4				−1.0	−0.4	0.2	2.2	2.5
Cyclohexane		1.8				−1.0	−0.3	0.2	1.9	1.2
Octane	2.9	2.9				−1.3	−0.4	0.3	2.7	2.9
Ethene			−1.8			−1.0	−1.1	−0.3	0.8	1.3
Benzene	−1.8	−1.0	−4.9	−2.2		−6.1	−3.5	−2.0	−0.5	−0.9
Toluene	−0.7	−0.1	−5.2	−1.7		−6.8	−3.6	−1.9	−0.3	−0.9
Propyne						−4.5	−2.9	−2.1	−0.9	−0.3
H, C, and N Compounds										
Methylamine	−5.7					−1.2	−6.5	−1.6[k]	−6.2[k]	−4.5
Ethylamine	−4.9					−1.3		−1.3	−5.2	−4.5
1-Propylamine	−4.6					−1.4		−1.3	−5.0	−4.4
1-Butanamine	−4.4							−1.2	−4.7	−4.3
Aniline			−8.4			−8.2	−9.1	−2.6	−5.8	−4.9
Dimethylamine			−2.5			−1.7	−5.4	−2.6	−4.3	−4.3
Trimethylamine						−1.9	−4.8	−3.3	−2.6	−3.2
Pyridine		−4.4				−6.3	−7.8	−3.9	−4.4	−4.7
Acetonitrile		−4.8	−4.0		−5.4	−3.8	−6.5	−2.0	−4.3	−3.9

(continued)

Table 2 Calculated Electrostatic Energies, Free Energies, and Experimental Free Energies (kcal/mol) of Solvation for Neutral and Ionic Solutes Using a Variety of Methods[a] *(continued)*

Solutes	SASA[b]	GB/SA[c]	FDPB (1)[d]	FDPB (2)[e]	AM1 ($l \leq 6$)[f]	AM1-PCM[g]	AM1-COSMO[h]	AM1-SM2 ENP[i]	AM1-SM2 Full[i]	Experimental[i] ΔG_S°
H, C, and O Compounds										
Methanol	−5.8	−6.2		−8.1		−2.4	−6.9	−1.0	−5.8	−5.1
Ethanol	−5.0	−5.2	−2.2	−7.8		−2.7	−6.6	−1.0	−4.9	−5.0
Dimethyl ether		−2.0	−2.0			−3.5	−5.4	−1.1	−1.4	−1.9
Acetaldehyde						−5.3		−3.0	−4.5	−3.5
Acetic acid	−6.9	−6.5	−5.3	−10.1		−7.1		−2.1	−7.7	−6.7
1-Propanol	−4.8					−2.8	−6.5	−0.9	−4.6	−4.8
i-Propanol	−4.7	−4.3		−5.4	−4.7	−2.7	−5.9	−0.9	−4.1	−4.8
Propanone		−3.2		−3.9	−7.3	−5.6	−9.2	−3.2	−4.1	−3.9
Propanoic acid	−6.8							−1.6	−6.7	−6.5
Methyl acetate	−1.8	−2.2		−2.6		−7.6		−2.3	−4.0	−3.3
Butanoic acid	−6.6							−1.5	−6.3	−6.4
Tetrahydrofuran						−4.4	−5.9	−1.4	−1.5	−3.5
1,4-Dioxane						−6.5	−9.5	−2.0	−3.4	−5.1
Cyclopentanone						−5.2		−3.0	−3.8	
Phenol	−8.9	−6.3	−6.6	−8.8		−6.9	−7.9	−2.5	−5.8	−6.6
Anisole					−3.1	−8.4	−6.7	−2.8[k]	−2.3[k]	−2.4[l]
H, C, and S Compounds										
Methanethiol	−1.1	−3.3	−1.1				−6.5	−1.0	−0.8	−1.2
Ethanethiol	−0.7						−6.8	−0.6	−0.6	−1.3
Thiophenol	−3.2						−7.0	−3.9	−3.2	−2.6
H, C, and Cl Compounds										
Methyl chloride						−1.8	−3.1	−1.0	−0.7	−0.6
Chloroform			−3.9			−1.8	−3.8	−0.7	−1.2	−1.1
1,2-Dichloroethane			−2.8				−4.5	−1.0	−1.0	−1.7
Isopropyl chloride					−2.6	−2.4	−3.2	−1.1	−0.3	−0.3

Table 2 Calculated Electrostatic Energies, Free Energies, and Experimental Free Energies (kcal/mol) of Solvation for Neutral and Ionic Solutes Using a Variety of Methods[a] *(continued)*

Solutes	SASA[b]	GB/SA[c]	FDPB (1)[d]	FDPB (2)[e]	AM1 ($l \leq 6$)[f]	AM1-PCM[g]	AM1-COSMO[h]	AM1-SM2 ENP[i]	AM1-SM2 Full[i]	Experimental[j] ΔG_S°
H, C, N, and O Compounds										
Acetamide	−6.7	−10.6		−13.0	−11.2	−9.5	−16.1	−6.0[k]	−11.5[k]	−9.7
E-*N*-Methylacetamide		−7.7[k]		−6.2		−9.8		−7.5[k]	−10.4[k]	−10.0[m]
Z-*N*-Methylacetamide		−6.2[k]		−9.8		−9.4		−6.6[k]	−9.4[k]	−10.0[m]
N,*N*-Dimethylacetamide				−6.2		−9.8		−7.8[k]	−8.6[k]	
Cytosine						−18.6		−13.4[k]	−21.7[k]	
Guanine					−24.0	−22.2		−15.5[k]	−26.9[k]	
9-Methylguanine					−24.5	−22.6		−15.3[k]	−24.3[k]	
Compounds Without C										
Ammonia			−3.9			−1.0	−8.0	−0.3	−4.3	−4.3
Water			−3.0			−2.4	−9.2	−1.2	−6.3	−6.3
Ions										
OH^-			−112.3			−106.0	−123.	−99.9	−108.1	−106
CN^-			−79.9			−87.0	−95.	−80.8	−83.5	−77
O_2^-			−90.0				−101.	−84.3	−88.1	−87
HS^-			−86.3				−109.	−74.4	−76.3	−76
HC_2^-			−73.0			−86.1	−98.	−78.5	−77.8	−73
HO_2^-			−92.1			−101.9	−111.	−90.0	−97.0	−101
N_3^-			−72.1			−81.2	−87.	−69.5	−75.2	−74
NO_2^-			−78.7			−84.5	−90.	−73.0	−77.7	−72
CH_3O^-			−79.7			−85.6		−81.3	−83.5	−95
NO_3^-			−69.9			−74.9	−86.	−54.5	−59.0	−65
CH_2CN^-			−71.5			−79.4		−67.3	−69.7	−75
$CH_3CO_2^-$		−82.9	−72.2	−77.6		−83.3		−72.9	−75.9	−77
H_3O^+			−88.8			−91.5	−100.	−100.0	−103.8	−104

(continued)

Table 2 Calculated Electrostatic Energies, Free Energies, and Experimental Free Energies (kcal/mol) of Solvation for Neutral and Ionic Solutes Using a Variety of Methods[a] *(continued)*

Solutes	SASA[b]	GB/SA[c]	FDPB (1)[d]	FDPB (2)[e]	AM1 ($l \leq 6$)[f]	AM1-PCM[g]	AM1-COSMO[h]	AM1-SM2 ENP[i]	AM1-SM2 Full[i]	Experimental[j] ΔG_S°
NH_4^+		−90.8	−81.7	−95.2		−88.4	−90.	−77.3	−79.0	−79
$MeOH_2^+$			−70.8			−77.7		−79.0	−84.2	−85
$MeSH_2^+$			−70.5					−73.7	−73 6	−74
$MeNH_3^+$		−80.4	−68.5		−76.2	−75.6	−79.	−68.6	−71.9	−70
Me_2OH^+			−59.5		−69.1	−66.2		−60.9	−62.8	−70
$Me_2NH_2^+$			−59.2		−68.4	−66.9	−69.	−61.3	−63.3	−63
Me_3NH^+		−63.1	−52.6		−59.2	−59.8	−61.	−53.9	−53.7	−59
$CH_3C(O)CH_2^-$			−68.1			−79.0		−70.3[k]	−71.2[k]	−81
$CH_3C(OH)CH_3^+$			−56.6		−65.0	−63.6		−56.9[k]	−60.2[k]	−70
PhO^-			−60.7			−76.7		−65.0[k]	−65.6[k]	−72
Pyridine · H^+			−53.8			−60.6	−62.	−56.5[k]	−57.9[k]	−59
$PhCO_2^-$						−84.5		−68.9[k]	−70.9[k]	−76[n]

[a]The finite difference Poisson–Boltzmann methods (FDPB), classical multipole expansion, polarized continuum models (PCM and COSMO), and AM1-SM2 ENP terms all refer strictly to electrostatic solvation energies. The solvent-accessible surface area (SASA) model, generalized Born/surface area (GB/SA) model, and the full AM1-SM2 energies, are full free energies of solvation. See text for additional details on methodology.

[b]Reference 122.

[c]Reference 193.

[d]Reference 24.

[e]Reference 165.

[f]Reference 318 (AM1 Hamiltonian).

[g]References 322 and 322 (AM1 Hamiltonian).

[h]Reference 331 (AM1 Hamiltonian).

[i]Reference 203.

[j]Unless otherwise indicated, experimental data for the neutral solutes are from References 334 and 335; data for the ions from Reference 336.

[k]New data for this chapter.

[l]Reference 337.

[m]Reference 341.

[n]Estimation from Reference 318.

Table 3 Cross-Correlation Matrix for Neutral Solute Data in Table 2[a]

	SASA	GB/SA	FDPB1	FDPB2	Multiple	PCM	COSMO	SM2 DNP	SM2 Full	Experimental
SASA	1									
GB/SA	0.933	1								
FDPB1	0.480	0.166	1							
FDPB2	0.879	0.920	0.011	1						
Multipole					1					
PCM	0.530	0.713		0.190	0.967	1				
COSMO	0.834	0.942	0.026	0.826	0.971	0.708	1			
SM2 ENP	0.616	0.742	0.298	0.303	0.989	0.951	0.760	1		
SM2 full	0.939	0.960	0.151	0.801	0.993	0.894	0.918	0.923	1	
Experimental	0.967	0.955	0.128	0.813	0.950	0.664	0.935	0.736	0.977	1

[a]Correlations involving fewer than five data points have been left blank. See Table 2 for references.

Table 4 Cross-Correlation Matrix for Ionic Solute Data in Table 2[a]

	FDPB1	Multipole	PCM	COSMO	SM2 ENP	SM2 Full	Experimental
FDPB1	1						
Multipole	0.982	1					
PCM	0.958	0.979	1				
COSMO	0.957	0.994	0.983	1			
SM2 ENP	0.893	0.986	0.896	0.848	1		
SM2 full	0.915	0.994	0.905	0.864	0.990	1	
Experimental	0.847	0.679	0.851	0.845	0.924	0.934	1

[a]Correlations involving fewer than five data points do not appear. See Table 2 for references.

Table 5 Slopes and Intercepts from Linear Regression of Model Predictions Against Experimental Data in Table 2

Model	Slope	Intercept (kcal/mol)
SASA	0.98	0.07
GB/SA	1.04	−0.09
FDPB1[a]	0.15	−2.36
FDPB2[a]	0.72	−0.77
AM1 multipole expansion ($l \leq 6$)	1.00	1.70
AM1-PCM[a]	0.78	0.12
AM1-COSMO	0.81	1.96
AM1-SM2 ENP[a]	1.44	−0.41
AM1-SM2 full	0.95	−0.04

[a]Low correlation coefficients obtained in regression; see Table 3.

where SASA underestimates the solvation free energy by 3.0 kcal/mol. This underestimation probably is at least partly due to the failure of the model to account for the greater polarizability of the amide group than the simple carbonyl group; only a single surface tension is used to describe each.

The GB/SA model[193] also correlates quite well with experiment for the neutral solutes. As expected, the regression slope and intercept are also nearly ideal. Conversely, based on the four ions for which results have been reported, there seems to be a tendency to overestimate ionic solvation free energies, but definite conclusions cannot be drawn from so small a sampling. Whereas the available data span a larger range of functionality than do those from the SASA model, there is still a paucity of results for complex and polyfunctional solutes. It would be very interesting to see how robust the model is in such instances.

Two finite difference Poisson–Boltzmann data sets appear in Table 2. In FDPB1,[24] the atomic partial charges are taken from a best fit to the AM1 electrostatic potential,[257–259] and the atomic radii are set equal to their van der Waals radii.[122] In FDPB2,[165] the charges and radii are from the OPLS[204] force field. The internal dielectric constant in both cases is unity. The former set of atomic partial charges is almost certainly a better approximation to the proper quantum mechanical electronic distribution; nevertheless, the FDPB1 method is essentially uncorrelated with the neutral experimental data ($r = 0.128$). Although this purely electrostatic model might not be expected to correlate especially well with the experimental values, which include local effects, the FDPB2 model shows a moderate correlation with experiment (albeit with a very nonideal regression slope and intercept). Still more remarkable, there is no correlation between results from these two methods for the solutes studied! Indeed, neither of the FDPB models correlates significantly with any of the other electrostatic models. This result is surprising, even taking into account the failure of the FDPB to account for solute polarization. The strikingly large differences between the two implementations suggest that the FDPB formalism is very sensitive to charge modeling, since the radii are not much different. This

possibility is further supported by the FDPB1 study, where very different solvation free energies were observed when the AM1 ESP charges were replaced with AM1 Mulliken charges (e.g., aniline goes from −8.4 to −4.2 kcal/mol).[24]

Moreover, the FDPB2 results for acetamide, *E*- and *Z*-*N*-methylacetamide, and *N*,*N*-dimethylacetamide are decidedly odd. The unsubstituted amide is predicted to have a solvation free energy much larger than experiment, even in the absence of any accounting for local hydrogen bonding. Moreover, the experimental values for the solvation free energies of the two monomethylated congeners are identical at −10.0 kcal/mol.[341] FDPB2 predicts them to differ by 3.6 kcal/mol, with the parent acetamide experiencing a decrease of almost 7 kcal/mol in solvation free energy upon methylation at the *Z* position! Continuing in this vein, although methylation of the parent acetamide in the *E* position decreases the solvation free energy a full 3.2 kcal/mol, methylation of *Z*-*N*-methylacetamide at this same position to form the dimethylamide does not change the free energy of solvation at all. This is quite different from the full AM1-SM2 results (which are in better agreement with experiment), where the effect of each methyl group is approximately additive. Despite possible expectations to the contrary, the AM1-SM2 ENP results yield an inverse correlation with the experimental solvation free energies, thanks to the greater polarizability of the methylated amide compared to the parent.

The FDPB results are more consistent for the ionic data, as might be hoped given the dominance of electrostatic interactions for these charged species. Nevertheless, the correlation is not particularly high. Our conclusions about the relative merits of the SM*x* and Poisson–Boltzmann approaches are consistent with the study of Alkorta et al.,[24] who found that both methods work well for ions, but the SM*x* approach is more successful for neutrals, with the differences being more pronounced for systems with smaller free energies of solvation. Thus, while the FDPB formalism has certain particular strengths, as discussed earlier, work remains to be done in the selection of optimal charges and molecular surfaces.

Calculations employing the single-center, classical multipolar expansion,[318] complete to sixth order ($l \leq 6$) to fit the AM1 electronic density in an ellipsoid, show a very high correlation with the other three quantum mechanical electrostatics-only models for neutral solutes. Rather surprisingly, it does so as well with full AM1-SM2 and experiment. Focusing on the regression against experiment, it appears that there is a nearly uniform 2.0 kcal/mol overestimation of solvation free energy for each neutral solute, with isopropanol and acetone being the only two significant exceptions. Given the small number of data, and the great difference in say, anisole and methane, this finding must be regarded as coincidental, although it is noteworthy that there is fairly close agreement between this model and full AM1-SM2 for guanine and 9-methylguanine, where no experimental values are available. The same trend in correlations appears for the ions, although the correlation with experiment is not particularly meaningful in this instance, because three of the five points have an

identical experimental free energy of solvation. Further work on this approach would thus be quite interesting, although clearly the requirement for more and more multipoles as molecules become larger and larger presents an obstacle, and multicenter approaches will perhaps prove more successful.

The AM1 polarized continuum model of Wang and Ford,[322] on the other hand, exhibits a very poor correlation with experiment, although it correlates moderately well with the other quantum mechanical electrostatic models. Whereas the correlation with experiment will clearly be improved in many cases by inclusion of such effects as cavitation and hydrogen bonding, there remain very unusual outliers (e.g., propyne, the aromatic hydrocarbons, anisole), in which these effects will either be much too small or in the wrong direction to correct the error. Given the still limited data available from this method, the origins of these problems are not entirely clear, although Ford and Wang[347] have suggested a means for improving the AM1 electrostatic potential that may be helpful. Correlation with experiment for the ions, though only moderate, improves as expected. Further development of this method too would be of great interest.

The other surface charge density method is the AM1-COSMO formalism of Klamt and Schüürmann.[325] This method, based on a combination of atomic partial charges and atom-centered dipoles, is particularly efficient for deriving the surface virtual charges. Because AM1-COSMO results correlate well with experiment (albeit with a sizable positive intercept and a slope significantly less than unity), it is perhaps surprising that they do not correlate particularly well with either the AM1-PCM or the AM1-SM2 ENP models. Inasmuch as each of these three models addresses only the electrostatic component of the solvation free energy, one would expect them to be much better mutually correlated. Whereas the electrostatic energies from AM1-COSMO and the AM1 multipole expansion models are well correlated, it must be recognized that that comparison involves only seven data points, compared to 39 for AM1-PCM and AM1-SM2 ENP.

It appears that much of the deviation between AM1-COSMO and the AM1-PCM and AM1-SM2 ENP results may be traced to heteroatoms, which make much larger negative contributions to the electrostatic solvation free energy in AM1-COSMO than in the other two models. Water and ammonia, for instance, are predicted to be 7–8 kcal/mol better solvated by AM1-COSMO than by AM1-PCM or AM1-SM2 ENP. Moreover, the AM1-COSMO solvation energies for these molecules are much more negative than the experimental free energies of solvation; it is unlikely that the nonelectrostatic components of solvation can be positive enough (if positive at all) to bring these COSMO energies into reasonable agreement with experiment. Other amines show very similar behavior, as do alcohols, ethers, esters, and carboxylic acids. AM1-PCM values are unavailable for thiols, but AM1-COSMO predicts these compounds to be much better solvated electrostatically than does the AM1-SM2 ENP model. In ionic cases as well as for neutrals, AM1-COSMO predicts the

most negative electrostatic solvation free energy in every instance. Interestingly, the AM1-PCM and AM1-COSMO results are in good agreement for aromatic systems with heteroatom substituents; this appears to be because the larger AM1-COSMO heteroatom contribution is balanced by the anomalously large AM1-PCM aromatic hydrocarbon contribution. AM1-COSMO does not appear to exhibit the latter behavior. It must be emphasized, of course, that the cavity parameters in the AM1-COSMO formalism have not been optimized,[325,331] and it is quite possible that considerable improvement will be observed with better atomic radii.

The AM1-SM2 ENP values[203] have been provided primarily to compare to the other quantal models, which address only the electrostatic component of the solvation free energies. As expected, this component correlates closely with each ΔG°_{S}. Interestingly, however, by comparing the slopes for the regressions against experiment of the multipole expansion in the AM1-PCM, AM1-COSMO, and AM1-SM2 ENP models, it is apparent that the degree of solute polarization is greatest for the AM1-COSMO and AM1-PCM models (a slope of less than 1 and/or a large positive intercept implies that the electrostatic energies must be "scaled back" to bring them into agreement with experiment), less for the multipole expansion model, and least for the AM1-SM2 ENP model. This is not an indication of which, if any, has higher accuracy, since the magnitudes and corrections of both local effects and inadequacies in the solute wavefunctions are not obvious. It does, however, suggest overpolarization as a possible cause for the problems of the AM1-PCM model with molecules such as propyne, the aromatic hydrocarbons, and anisole, and the large values predicted by AM1-COSMO for heteroatom-containing systems.

The full AM1-SM2 model is discussed in more detail in the final section. Within the context of Tables 2–5, however, it is worth noting that the model enjoys the largest correlation to experimental data for the neutral solutes. All but a few of the molecules listed comprise a subset of a larger data set of 147 neutral solutes spanning many functionalities (e.g., nitro groups, phosphorus compounds, sulfides, bromides, fluoroalkanes, iodides, polyfunctional compounds), not shown because they have not been studied by other methods, for which the AM1-SM2 model has a mean absolute error of 0.6 kcal/mol.[203] One apparent flaw illustrated here is that AM1-SM2 consistently underestimates the free energies of solvation for aliphatic and alicyclic ethers.

Finally, it is apparent that the reported solvation free energy for methoxide, −95 kcal/mol,[336] is much larger than the predictions of FDPB1, AM1-PCM, or AM1-SM2. Because the calculated values from these diverse methods are all in fairly close agreement with each other, it is tempting to believe that the experimental number may be in error in this instance.

Relative Free Energies in Heterocyclic Equilibria

Solvation may have a dramatic effect on tautomeric equilibria, especially in heterocyclic systems.[1,313,314] For instance, the equilibrium constant for the

4-hydroxypyridine/4-pyridone tautomerization is changed more than a millionfold upon transfer from the gas phase to aqueous solution.[314] Not only is the differential absolute free energy of solvation large, but the calculated electronic structures are greatly perturbed by the solvent. For example, in the gas phase the AM1 Mulliken partial charges on the nitrogen H and the O in 4-pyridone are 0.25 and −0.34, respectively, whereas in solution (AM1-SM2 model) these partial charges become 0.35 and −0.52, respectively,[203] with a concomitant increase in the dipole moment from 6.3 D to 10.8 D. Similar effects are found in thymine,[343] as discussed later in the biochemistry section.

The significant changes in solvation energy upon tautomerization as well as the importance of aqueous heterocyclic equilibria in biochemistry make such systems particularly interesting test cases for theoretical models of solvation. We focus on two specific test cases for which data from a number of different models are available: the tautomeric equilibrium between 2-hydroxypyridine and 2-pyridone and the aqueous population of tautomers in the 5-(2*H*)-isoxazolone system (Figure 5). The first case is somewhat simpler to focus upon, because the tautomeric equilibrium in the gas phase is known.[314] Solution measurements thus provide directly the differential free energies of solvation for the two tautomers, relieving the models of the burden of accurately accounting for the relative gas-phase free energies as discussed later. The size and complexity of this system has limited the application of theoretical models to a number of different Born–Kirkwood–Onsager approaches and the generalized Born formalism. Results are summarized in Table 6, where the cavity radius is α of Equation [12].

Wong, Wiberg, and Frisch,[227] at the correlated ab initio level, obtained excellent agreement with experiment for $\varepsilon = 2$, and reasonable agreement for $\varepsilon = 36$. They explicitly assign the greater error in the latter dielectric as arising from specific interactions not accounted for in the BKO model, and as a result

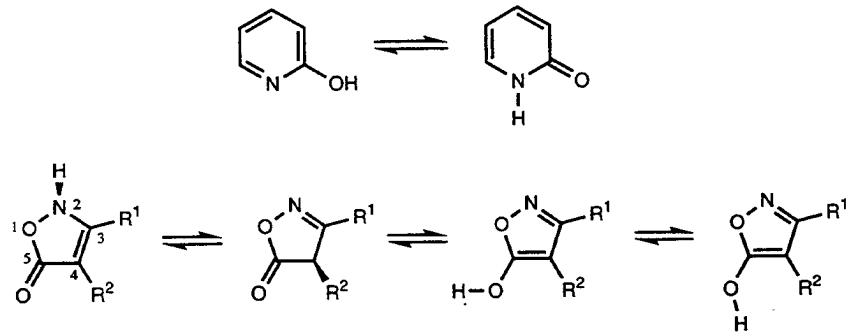

Figure 5 Two heterocycles that have tautomeric equilibria and are sensitive to solvation: the equilibrium between 2-hydroxypyridine and 2-pyridone (*top*) and equilibrium between the NH, CH, OH_Z, and OH_E tautomers of 5-isoxazolone (*bottom*).

Table 6 Differential Free Energies of Solvation (kcal/mol) for 2-Hydroxypyridine and 2-Pyridone in Different Dielectrics with Different Solvation Models[a]

ε	BKO1[b]	BKO2[c]	BKO3[d]	AM1-PCM[e]	AM1-SM1[f]	AM1-SM2[g]	PM3-SM3[f]	Experimental[b]
2	1.0	0.9		1.6				1.1
5		1.5		3.3				1.8
36	3.0	2.1		4.8				3.8
78		2.2	4.8	5.0	4.4	2.6	4.3	4.3
Cavity radius, Å	3.80	3.88	3.00	vdw[i]				

[a]In all cases, 2-pyridone is the better solvated tautomer by the magnitude indicated.
[b]Reference 227.
[c]Reference 224.
[d]Reference 223.
[e]Reference 332.
[f]Reference 344.
[g]Reference 203.
[h]Reference 314.
[i]van der Waals.

they do not attempt an aqueous ($\varepsilon = 78$) calculation. Their choice of cavity radius is intuitively reasonable and derives from calculation of the volume enclosed by the 0.001 atomic unit isodensity surface, to which is added a constant of 0.5 Å. This prescription gives reasonably close agreement with volumes obtained from simple van der Waals surfaces. It is by means of this latter approach that Szafran et al.[224] arrive at a cavity radius of 3.88 Å. Here again, agreement with experiment falls off rapidly at higher dielectrics. In this instance, Szafran et al. observed improved results upon inclusion of one specific water molecule.[224]

The BKO study of Freitas, Longo, and Simas,[223] on the other hand, ignored the specific interactions in water and instead adopted an unrealistically small cavity radius of 3.0 Å to obtain agreement with experiment. Such a cavity cannot be justified in a physical sense. An earlier study of Karelson et al.[216] employed a similarly small cavity radius of 3.15 Å and thereby also obtained reasonable agreement with experiment for water.

The AM1-PCM model does surprisingly well, even without including specific solvent interactions, suggesting that this effect may account for only a portion of the BKO discrepancies in more polar solvents. Evidently, higher multipole moments may also be important.

The generalized Born solvation models[203,344] take account of specific water interactions explicitly and give excellent agreement in the AM1-SM1 and PM3-SM3 cases; AM1-SM2 is less successful, albeit still improved over the most reasonable BKO treatment. Cavity radii are not an issue for these models.

The aqueous solvation free energies of the four tautomers available to the 5-(2*H*)-isoxazolone system have also been studied using a variety of continuum models (Table 7). Hillier and co-workers[232,345] have provided data at the ab initio level using the Born–Kirkwood–Onsager model, the classical multipolar expansion model (up to $l = 7$), and an ab initio polarized continuum model. We examined the same BKO model with a different cavity radius and the AM1-SM2 and AM1-SM1a[26,203] models,[346] and Wang and Ford have performed calculations with the AM1-PCM model.[332]

Table 7 illustrates the tremendous sensitivity of the BKO model to decreasing cavity radius. The 3.6 Å cavity radius was arrived at by following the Wiberg, Wong, and Frisch prescription[227] and is in reasonable agreement with what one would expect from the volume enclosed by a van der Waals surface. Ab initio BKO/6-31G** calculations with this cavity are in remarkably close agreement with the AM1-SM2 ENP values (i.e., comparing to the electrostatic portion of the AM1-SM2 results) with the exception of the OH_Z tautomer, where the very small dipole moment of this structure causes the BKO model to be inappropriate.

The 2.5 Å radius, on the other hand, gives drastically different results, both in absolute and relative magnitudes. With this cavity radius, the solvation free energy for the NH tautomer is in the range for a medium-sized ion! The ab initio PCM model also gives surprisingly large absolute free energies of solva-

Table 7 Comparison of Calculated Free Energies of Solvation (kcal/mol) for 5-(2*H*)-Isoxazolone Tautomers

	NH	CH	OH_Z	OH_E	Ref.
Absolute					
BKO/6-31G**, 2.5 Å cavity	−38.0	−22.4	−3.0	−18.5	232
BKO/6-31G**, 3.6 Å cavity	−6.2	−5.0	−0.7	−4.3	346
SCRF ($l \leq 7$)/6-31G**, ellipsoid	−10.9	−9.7	−6.4	−8.1	345
PCM/6-31G**, van der Waals cavity	−17.2	−16.3	−12.3	NA[a]	232
PCM/AM1, van der Waals cavity	−10.8	−9.2	−5.9	−6.4	332
Explicit water, AMBER	NA[a]	NA[a]	NA[a]	NA[a]	232
AM1-SM2, ENP only	−6.2	−4.5	−3.2	−3.6	346
AM1-SM2, full	−11.0	−8.2	−9.5	−9.9	346
AM1-SM1a, full	−14.0	−10.0	−11.6	−12.1	346
Relative to CH tautomer					
BKO/6-31G**, 2.5 Å cavity	−15.6	0.0	19.4	5.9	232
BKO/6-31G**, 3.6 Å cavity	−1.2	0.0	4.3	0.7	346
SCRF ($l \leq 7$)/6-31G**, ellipsoid	−1.2	0.0	3.3	1.6	345
PCM/6-31G**, van der Waals cavity	−0.9	0.0	4.0	NA[a]	232
PCM/AM1, van der Waals cavity	−1.2	0.0	3.3	2.8	332
Explicit water, AMBER	−2.1	0.0	1.8	0.3	232
AM1-SM2, ENP only	−1.7	0.0	1.3	0.9	346
AM1-SM2, full	−2.8	0.0	−1.3	−1.7	346
AM1-SM1a, full	−4.0	0.0	−1.6	−2.2	346

[a]Not available.

tion, given that only the electrostatics are being considered. However, the relative free energies for this model are in very reasonable agreement with the AM1-SM2 ENP, the SCRF ($l \leq 7$), and BKO/6-31G** (3.6 Å cavity radius) results. The AM1-PCM model is in similarly good agreement for both absolute and relative energies.[332] It is interesting to note that all these models also agree closely with explicit-water calculations employing the AMBER force field.[347] This last result is a bit surprising considering that the latter approach does not account for solute polarization but does account for local solvent interactions —it may be that these two effects fortuitously cancel.

In their original work, Hillier and co-workers[232] invoked the BKO model with a 2.5 Å cavity radius as being the most trustworthy, even though this cavity excluded sizable portions of the heterocycle itself. Their analysis suffered from two critical problems. First, the authors were victims of an error propagated through the theoretical literature,[217] namely, that in aqueous systems the NH tautomer was the only observed species in solution. In fact, no experimental details support this statement; analysis of methylated analogs suggests that the NH and CH tautomers should be present to a similar degree with no detectable amounts of the OH tautomers.[313,346] Second, unlike the earlier example of 2-pyridone, no gas-phase experimental data are available for this

heterocycle. Hence, meaningful comparisons of differential free energies of solvation cannot be made. Instead, these differential free energies of solvation must be added to relative gas-phase free energies. Because of a faulty geometry optimization and a poorly converged gas-phase level of theory, Hillier and coworkers believed that to "correctly" predict the predominance of the NH tautomer in aqueous solution, they had to overcome a 13 kcal/mol difference in relative gas phase energies favoring the CH tautomer. Gould and Hillier[345] later corrected these errors.

In fact, very large basis set, correlated calculations suggest that the CH tautomer is favored over the NH in the gas phase by only 6.2 kcal/mol.[346] Assuming an approximately equal mixture of the two tautomers in aqueous solution,[313] the AM1-SM1a model is within about 1 kcal/mol of correctly predicting the relative free energies of solvation. The more general AM1-SM2 model is not quite as accurate in its consideration of heteroatom-bound protons, and it thus provides a somewhat poorer prediction in this instance, although it remains closer than any of the other models.

The last example illustrates the difficulties involved in studying the effects of solvation on conformational equilibria and chemical reactions. Whereas it is important to have a solvation model that performs reasonably accurately (e.g., the 0.6 kcal/mol mean error for neutral solutes observed with AM1-SM2) such accuracy is of little use when the gas phase surface of the same system contains significantly larger errors.

SURVEY OF SELECTED SM*x* RESULTS

This section provides further information on the SM*x* parameterizations and discusses examples of special results to illustrate the kinds of problem that can be considered.

Four SM*x* parameterizations have been published to date.[26,27,202] Three (SM1, SM1a, and SM2) are based on the AM1 model for the solute, and one (SM3) is based on PM3. In the most general terms, we consider SM1 to be replaced by SM2. The choice between SM2 and SM3 is probably best made in terms of whether AM1 or PM3 gives a better description of the solute properties of interest; see, however the following subsection in regard to PM3 for compounds with nitrogen. The SM1a model requires the user to assign nitrogen centers as sp^3, amide, sp^2, or sp and oxygen centers as sp^2 or sp^3. Furthermore, hydrogens must be characterized in terms of the atoms to which they are bonded. This requirement limits or prevents the applicability to many ions and strained or nonclassical compounds and to transition states for proton, hydrogen, or hydride transfer. The SM1a model is the most accurate model on the average, though, when it is applicable.

Organic Chemistry

Average Performance on a Test Set

The SM1a, SM2, and SM3 models have been applied to the same representative test set of 147 molecules, consisting of 143 organics plus ammonia, phosphine, hydrogen sulfide, and water itself. Here we overview the results discussed in detail elsewhere.[203]

The mean unsigned errors are 0.6, 0.6, and 0.9 kcal/mol, respectively, for SM1a, SM2, and SM3. It is interesting to divide the 147 test molecules into two sets, 27 nitrogen-containing compounds and 120 without nitrogen. The respective mean unsigned errors of the SM1a, SM2, and SM3 models for the nitrogen-containing set are 0.6, 1.0, and 1.6 kcal/mol, while for the set without nitrogen they are 0.6, 0.6, and 0.8 kcal/mol. Thus the differences in overall performance are primarily attributable to nitrogen. Examination shows that the poor results of the SM3 model for nitrogen-containing compounds are due to the unrealistic partial charges on nitrogen produced by PM3.

Another way to partition the test set is into 27 compounds with $\Delta G_S^\circ \geq 0.1$ kcal/mol, 3 with $\Delta G_S^\circ = 0.0$ kcal/mol, and 117 with $\Delta G_S^\circ \leq -0.1$ kcal/mol. The first two groups (30 compounds) will be called the hydrophobic subset, and the other 117, the hydrophilic subset. The respective mean unsigned errors of the SM1a, SM2, and SM3 models for the hydrophobic subset are 0.7, 0.5, and 0.6 kcal/mol, whereas for the hydrophilic subset they are 0.6, 0.7, and 1.0 kcal/mol. This breakdown confirms the success of the major performance enhancement specifically designed into the SM2 parameterization, namely, to improve the accuracy for the hydrophobic effect. We believe that the high accuracy attained for the hydrophobic subset of molecules also gives confidence that hydrophobic side chains are treated accurately in hydrophilic molecules.

Nearly symmetrical molecules deserve special mention. Benzene and piperazine are uncharged and have no dipole moment, so the Born–Kirkwood–Onsager model predicts $\Delta G_S^\circ = 0$. However, AM1-SM2 predicts -0.5 and -7.8 kcal/mol, respectively, in good agreement with the experimental -0.9 and -7.4 kcal/mol. In benzene the result comes as the sum of a hydrophobic $\Delta G_{CDS}^\circ = 1.4$ kcal/mol and a hydrophilic $\Delta G_{ENP} = -2.0$ kcal/mol; whereas in piperazine both terms are hydrophilic ($\Delta G_{CDS}^\circ = -4.1$ kcal/mol, $\Delta G_{ENP}^\circ = -3.7$ kcal/mol), and they reinforce each other. Similar reinforcement occurs in many other compounds [e.g., *p*-bromophenol ($\Delta G_S^\circ = -4.4$ kcal/mol, $\Delta G_{ENP}^\circ = -2.7$ kcal/mol)], in which case AM1-SM2 predicts $\Delta G_S^\circ = -7.0$ kcal/mol versus an experimental value of -7.1 kcal/mol.

These models were also applied to a test set of 28 ions, consisting of 13 organic ions and 15 inorganics. The average unsigned errors in the SM1, SM2, and SM3 models for this set are about 3–4%, which may well lie within the experimental uncertainty because the errors in assigning absolute free energies of solvation to charged species are large. In the SM2 model, 9 of the 28 ions

have errors of 5% or more. For illustration purposes, we mention $(CH_3)_3PH^+$, NO_3^-, $CH_3SH_2^+$, HS^-, and $CH_3OH_2^+$, with experimental solvation free energies of −53, −65, −74, −76, and −83, respectively. The SM3 model yields −47.9, −59, −74, −76, and −84 kcal/mol for unsigned errors of 10, 9, 0, 0, and 1%, respectively, an average of 4%.

Illustrative Applications

Equilibria Solvation has important quantitative effects on many kinds of organic equilibria.[1] We use the acid–base equilibria of $CH_3NH_3^+$ as an example. Consider

$$CH_3NH_3^+(g) + B(g) \rightleftharpoons CH_3NH_2 + BH^+(g) \qquad \Delta G = \Delta G_1$$

$$CH_3NH_3^+(aq) + B(aq) \rightleftharpoons CH_2NH_2 + BH^+(aq) \qquad \Delta G = \Delta G_2$$

where $\Delta\Delta G = \Delta G_2 - \Delta G_1$. Table 8 gives $\Delta\Delta G$ values for five neutral and four anionic bases as computed by the AM1-SM2 model[344] and from experiment. The main trends are well reproduced. Good results are also obtained for tautomeric equilibria as detailed for several examples in the earlier section on heterocyclic equilibria.

Dynamics In light of the encouraging results for absolute solvation energies and equilibria, applications of continuum solvation models to the dynamics of organic reactions also are expected to be very fruitful. Ionic reactions (e.g., the classical S_N2 mechanism) may proceed in qualitatively different ways in solution and in the gas phase, and continuum solvation models provide a convenient and economical way to map out solvation energy changes as a function of the reaction coordinate.

Solvation can also have large quantitative effects on reactions of uncharged species. For example, these effects have been considered in detail re-

Table 8 Solvation Effects on the Acid-Base Equilibria of Methylamine

Base B	ΔΔG (kcal/mol)	
	SM2	Experiment
NH_3	−9	−10
Aniline	8	3
$(CH_3)_2NH$	7	8
$(CH_3)_3N$	15	14
Pyridine	12	15
Cyclopentadienyl anion	124	128
Benzoate	130	128
Phenoxide	125	132
Acetate	134	127

cently for sigmatropic rearrangements. Such reactions, especially the Claisen rearrangement and its variations, are among the most synthetically useful methods for creating new asymmetric centers.[348] Solvent effects on the reaction rates and the stereochemical outcome are therefore of great interest.

There has been considerable interest in the effect of solvation on the Claisen reaction and other pericyclic reactions. Both continuum solvation models and explicit solvent treatments have been applied. Interpretation of these results in terms of the efficacy of the solvation treatments is clouded by uncertainties in the underlying treatment of the electronic structures of the solute. These issues have been discussed extensively in recent literature on the Claisen reaction,[349–356] and there is an even larger literature for the Diels–Alder cycloaddition reaction. Transition states for pericyclic reactions may be roughly categorized in terms of varying amounts of biradicaloid (diyl), zwitterionic, and aromatic character; these qualitative distinctions have a considerable effect on the partial charges and electronic and geometric polarizability, and hence on the solvation effects. The character of the transition states in these terms as well as chair versus boat energy differences of the six-membered ring transition states are sensitive to the size of the basis set in ab initio calculations. In semiempirical molecular orbital theory, the charge character at a given geometry is similar to minimum basis set Hartree–Fock results, which are less polar than double-zeta-basis structures, but the geometric character is more biradicaloid as a tendency. Proper assessment of the biradicaloid character at the ab initio level requires some treatment of internal correlation (e.g., multiconfiguration SCF), and the calculation of accurate energetics for transition states often requires inclusion of external correlation and extended basis sets. We believe that these issues must be resolved satisfactorily for the gas phase before definitive statements can be made about solvation, but when this has been accomplished, continuum solvation models should be very useful for exploring the effect of solvent.[356]

Biochemistry

Even the simplest level of understanding of most reactions of interest in biochemistry requires taking some account of the effects of aqueous solvation on both structure and dynamics. In this section, we consider examples of solvation studies on three biomolecules: dopamine, glucose, and thymine.

Dopamine

Dopamine is a neurotransmitter, and the understanding of its conformational preferences may advance our understanding of its biological functions. The critical dihedral angles ϕ_1 and ϕ_2 for the protonated form of dopamine, which is the prevalent species at biological pH, are illustrated in Figure 6. Free energy of solvation maps as functions of ϕ_1 and ϕ_2 were generated by AM1-SM1 calculations for the neutral, N-protonated, and OH-deprotonated forms

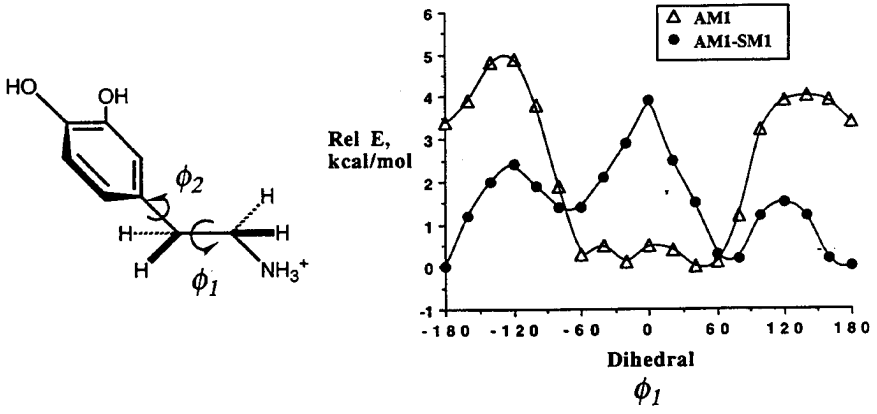

Figure 6 The effect of aqueous solvation on the conformation of dopamine. For all points in the graph, $\phi_2 = 90°$, which is the value illustrated in the structure.

of dopamine.[357] For both latter forms, the solvation energy has a significant effect on the conformational preferences. Qualitatively, the AM1-SM1 calculations reflect what one would expect for solvation effects, and quantitatively they lead to markedly improved agreement with experiment. Thus, the anti conformation ($\phi_1 = 180°$) illustrated in Figure 6 is predicted to be preferred in aqueous solution, even though the most favorable gas-phase conformation finds the ammonium moiety gauche to the aromatic ring ($\phi_1 \approx 60°$). The magnitude of this effect is on the order of 7 kcal/mol for the differential free energy of solvation of these rotamers. The ratio of gauche to anti about ϕ_1 is determined by NMR spectroscopy to be 58:42; AM1 (gas phase) calculations predict a 99:1 ratio, whereas AM1-SM1 predicts 37:63 (representing an error of 0.5 kcal/mol). Aqueous solvation is also found to lower the rotational barrier about ϕ_2, consistent with the rapid rotation observed experimentally by NMR techniques.

Glucose

Glucose is a system in which the conformational average of multiple low energy isomers cannot be ignored.[358] That is, the free energy of solvation is a Boltzmann probability-weighted average over conformations[75]

$$\exp\left[-\frac{\Delta G_S^\circ}{RT}\right] = \sum_C P_C \exp\left[-\frac{\Delta G_S^\circ(C)}{RT}\right] \qquad [44]$$

where P_C is the equilibrium mole fraction of conformation C in the gas phase. If there is only one important conformation in both gas phase and solution, only a single term need be retained in Equation [44], which becomes a tautology.

Background on glucose conformations and the glucose solvation problem may be found in four recent references.[359–362] Here we summarize some of the main results of our own studies[358] with the SM1a, SM2, and SM3 models as examples of the kinds of information available from continuum solvation studies. We concentrated entirely on the dominant pyranose ring form of D-glucose. The first issue studied was the relative stability in solution of the three hydroxymethyl conformers G, $\bar{G}$, and T of both the α and β anomers, as illustrated in Figure 7. For both anomers, we found the G conformer to be better solvated than the other two, in agreement with explicit-water molecule dynamics simulations.[360,361] In our calculations, we found that solvation stabilizes the G form by 0.5–0.7 kcal/mol compared to the other conformers for both the α and β anomers. Furthermore, the difference in solvation energies between the various hydroxymethyl conformers was dominated by CDS terms, and in particular by contributions to this term from the C-6 hydroxyl group, in good agreement with the conclusions of Kroon-Batenburg and Kroon[360] based on their explicit-water molecular dynamics simulations. This is very encouraging.

Next we turn to the torsional nightmare of the ring hydroxyls. The computational convenience of the continuum solvation model allowed us to examine all 81 ring hydroxyl rotamers of the G hydroxymethyl conformer of the α-D anomer with both the AM1-SM2 and PM3-SM3 parameter sets, fully optimizing the geometry in both the gas phase and solution for every case. We found 33 stationary structures in the former case and 40 in the latter. There are many low energy rotamers in the gas phase, and solvation somewhat flattens the landscape, but not by a large amount. Strikingly, though, the most favorable

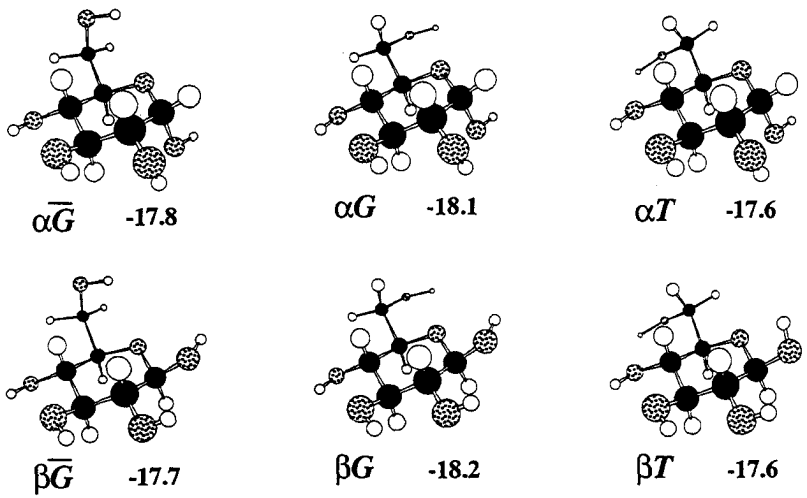

Figure 7 $\bar{G}$, G, and T hydroxymethyl conformers of both anomers of D-glucose. Under each structure is the anomer designation, the conformer label, and the AM1-SM2 value of ΔG_S° (kcal/mol).

gas phase rotamer is the least well solvated. Our calculations indicated that cooperative hydrogen bonding may occur for several rotamers likely to be present in aqueous solution in nonnegligible amounts. When the nonanomeric hydroxyls are engaged in a clockwise hydrogen bonding array, which is common, the anomeric hydroxyl prefers to engage in intramolecular hydrogen bonding in preference to taking advantage of exoanomeric[363] stabilization.

The solvation effect on the α/β anomeric equilibrium was calculated to be essentially zero. This interesting result awaits further study at higher levels.

Finally we compared the AM1-SM2 ENP values to those calculated by the Onsager model (Equation [12]). The Onsager model yields solvation energies from -0.004 kcal/mol to -2.1 kcal/mol. In addition to being uncorrelated with the AM1-SM2 ENP results, the Onsager values were about 18–19 kcal/mol less negative than the full AM1-SM2 values. This illustrates just how dangerous it is to ignore specific first-shell effects and focus only on the dipole moment for electrostatic effects in large molecules.

Thymine

As discussed earlier in the section on heterocyclic equilibria, heterocycles show large changes in electronic structure between the gas phase and solution, and thus the effects of aqueous solvation on nucleic acid bases is very interesting.

Consider, for example, thymine.[344] Figure 8 shows the free energy contributions by groups (where a group is C, CH, CH_3, NH, or O) from the ENP and CDS terms. The procedure for partitioning the ENP terms into group contributions is explained elsewhere.[343] Partitioning of the CDS contributions is obvious.

The major changes in the partial charges due to solvation are toward more positive at N(1)H and C(6)H and more negative at both oxygens, increasing the dipole moment, which points from C(5) to C(2), from 4.2 D in the gas phase to 6.7 D in solution. Especially noteworthy is the different behavior of

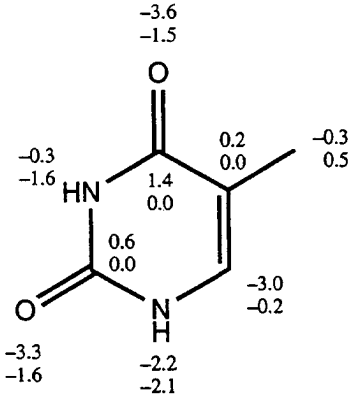

Figure 8 Free energy of solvation contributions (kcal/mol) by groups for thymine. The upper number for each group is the ENP contribution, and the lower number is the CDS contribution.

the two nitrogens, with N(1) contributing much more to the ENP term and polarizing much more in solution than N(3). This situation might be hard to model classically. The increase in ΔG_S° of thymine due to aqueous solvation is 29%, which is typical of the nucleic acid bases. The average increase for the other four is 31%.

The net ENP and CDS contributions to the solvation energy of thymine are −10.4 and −6.1 kcal/mol, respectively, for a net ΔG_S° of −16.5 kcal/mol. Similar calculations for 1-methylthymine yield −13.3 kcal/mol; this solute has also been studied by explicit-water calculations in which the solute is classical, where a value of only −7.7 kcal/mol was predicted.[364] Even the value calculated without relaxation in solution by AM1-SM2 model is −10.8 kcal/mol, predicting that thymine is solvated significantly more favorably than was indicated by the earlier calculations.

No experimental results are available for the nucleic acids, with or without methyl substitution, to test the theories, but we can compare the results for thymine to three theoretical estimates[157] based on the linearized Poisson–Boltzmann equation. The AM1-SM2 and PM3-SM3 values are −16.5 and −20.1 kcal/mol, respectively. Using charges and force field parameters from the AMBER,[347] CHARMM,[365] and OPLS[366] molecular mechanics force fields and a solute dielectric constant of 1, Mohan et al.[157] calculated solvation energies of −19.1, −10.4, and −8.4 kcal/mol. The wide variation is disconcerting. In light of such wide variations with "off-the-shelf" parameters, the SM*x* approach based on parameters specifically adjusted to solvation energies appears to be more reliable.

FUTURE DIRECTIONS AND CONCLUDING REMARKS

Selection of an optimum solvation model must always be based on the issues requiring resolution. For instance, continuum models are obviously not appropriate when the specific structure of the first solvation shell is of interest. Often, however, they are appropriate, offering great speed and the option of employing quantal treatments of the solute. Continuum models are particularly useful in that they generally calculate absolute free energies of solvation, although not necessarily for more than a few components of the total free energy of solvation—thus, as detailed earlier, if one is interested in first-solvation-shell effects, one should not choose a continuum model that is limited to electrostatic polarization effects. Depending on the rigor with which the solute is treated, continuum models range in speed from extremely fast molecular mechanics implementations to much more cumbersome (but potentially more accurate) ab initio implementations. Judiciously balancing these considerations is, of course, the daily task of the computational chemist.

Continuum models like the SM*x* approaches allow for a myriad of additional higher order refinements that have not been included yet. We give only one example here. Urry[367] has argued that water molecules involved in hydrophobic hydration cannot, in general, simultaneously perform the function of polar hydration. Thus the dielectric constant may be lower near hydrophobic sites. It would be straightforward to include a region-dependent dielectric constant in the generalized Born models employing Equation [19], but this has not been done yet.

In addition to methodological refinements, a number of general issues deserve more focus. Accurate modeling of the electronic structure of solutes with efficient formalisms (e.g., partial atomic charges) continues to be an active area of study. More work remains to be done for the quantal models on identifying the point at which improving the solute wavefunction fails to be worthwhile, given the limitations implicit in the continuum approximation. Moreover, it seems clear that combined quantal/molecular mechanics treatments will be worthwhile when significant changes in electronic and nuclear structure are expected for only a small portion of a solute (e.g., a quantum substrate interacting with a classical enzyme). Physically meaningful models for changes in the solute rotational and vibrational partition functions following solvation remain to be proposed. Nonequilibrium solvation models are required for processes that occur rapidly relative to solvent structure relaxation. Finally, whereas the dielectric constant of a solvent is one bulk property that has been useful in developing continuum models for the electrostatic components of solvation free energy, little work has been done on identifying how other bulk properties (e.g., cohesive energy density, internal pressure, viscosity) may be used to develop models for local effects occurring in the first (and perhaps second) solvation shell. Addressing some of these questions will enhance the utility of these already extremely powerful models.[368]

ACKNOWLEDGMENTS

This work was supported in part by the National Science Foundation under grant CHE89-22048 and by the In-House Laboratories Independent Research program of the United States Army. We thank Drs. G. Ford, I. Hillier, A. Klamt, M. Newton, J. Urban, and A. Warshel for their gracious assistance in providing thoughtful criticism and suggesting improvements.

REFERENCES

1. C. Reichardt, *Solvents and Solvent Effects in Organic Chemistry*, VCH Publishers, New York, 1990.
2. W. N. Olmstead and J. I. Brauman, *J. Am. Chem. Soc.*, 99, 4219 (1977). Gas-Phase Nucleophilic Displacement Reactions.

3. D. J. McLennan, *Aust. J. Chem.*, **31**, 1897 (1978). Semi-Empirical Calculation of Rates of S_N2 Finkelstein Reactions in Solution by a Quasi-Thermodynamic Cycle.
4. J. Chandrasekhar and W. L. Jorgensen, *J. Am. Chem. Soc.*, **107**, 2974 (1985). Energy Profile for a Nonconcerted S_N2 Reaction in Solution.
5. S. C. Tucker and D. G. Truhlar, *Chem. Phys. Lett.*, **157**, 164 (1989). Generalized Born Fragment Charge Model for Solvation Effects as a Function of Reaction Coordinate.
6. R. M. Whitnell and K. R. Wilson, in *Reviews in Computational Chemistry*, Vol. 4, K. B. Lipkowitz and D. B. Boyd, Eds., VCH Publishers, New York, 1993, pp. 67–148. Computational Molecular Dynamics of Chemical Reactions in Solution.
7. S. S. Shaik, H. B. Schlegel, and S. Wolfe, *Theoretical Aspects of Physical Organic Chemistry. the S_N2 Reaction*, Wiley, New York, 1992, Chapter 5.
8. T. L. Hill, *An Introduction to Statistical Thermodynamics*, Addison-Wesley, Reading, MA, 1960, pp. 75–76, 312–314, 323–325.
9. D. A. McQuarrie, *Statistical Mechanics*, Harper & Row, New York, 1976, pp. 83, 331–332.
10. H. L. Friedman, *A Course in Statistical Mechanics*, Prentice-Hall, Englewood Cliffs, NJ, 1985, pp. 86–89.
11. J. T. Hynes, in *Theory of Chemical Reaction Dynamics*, Vol. 4, M. Baer, Ed., CRC Press, Boca Raton, FL, 1985, p. 171. The Theory of Reactions in Solution.
12. J. T. Kellis, Jr., K. Nyberg, D. Sali, and A. R. Fersht, *Nature*, **333**, 788 (1988). Contribution of Hydrophobic Interaction to Protein Stability.
13. K. A. Dill, *Biochemistry*, **29**, 7133 (1990). Dominant Forces in Protein Folding.
14. A. Nicholls, K. A. Sharp, and B. Honig, *Proteins*, **11**, 281 (1991). Protein Folding and Association: Insights from the Interfacial and Thermodynamic Properties of Hydrocarbons.
15. P. S. Subramanian and D. L. Beveridge, *Theor. Chim. Acta*, **85**, 3 (1993). A Monte Carlo Simulation Study of the Aqueous Hydration of *d*(CGCGCG) in Z Form.
16. G. Neméthy, W. J. Peer, and H. A. Scheraga, *Annu. Rev. Biophys. Bioeng.* **10**, 459 (1981). Effect of Protein–Solvent Interactions on Protein Conformation.
17. A. Fersht, *Enzyme Structure and Mechanism*, 2nd ed., Freeman, New York, 1985, pp. 65, 300–301.
18. R. Wolfenden and W. M. Kati, *Acc. Chem. Res.*, **24**, 209 (1991). Testing the Limits of Protein–Ligand Binding Discrimination with Transition-State Analogue Inhibitors.
19. A. Warshel, J. Åqvist, and S. Creighton, *Proc. Natl. Acad. Sci., U.S.A.*, **86**, 5820 (1989). Enzymes Work by Solvation Substitution Rather than by Desolvation.
20. C. Hansch, in *QSAR: Rational Approaches to the Design of Bioactive Compounds*, C. Silipo and A. Vittoria, Eds., Elsevier, Amsterdam, 1991, pp. 3–10. New Perspectives in QSAR.
21. R. C. Wade, *J. Comput.-Aided Mol. Design*, **4**, 199 (1990). Solvation of the Active Site of Cytochrome P450-cam.
22. I. N. Demetropolous and N. Gresh, *J. Comput.-Aided Mol. Design*, **5**, 81 (1991). A Supermolecule Study of the Effects of Hydration on the Conformational Behavior of Leucine-Enkephalin.
23. A. Goldblum and G. H. Loew, *Eur. J. Pharmacol., Mol. Pharm. Sect.*, **206**, 119 (1991). A Molecular Model for an Anionic Opiate μ-Receptor—Affinity and Activation of Morphine Conformers.
24. I. Alkorta, H. O. Villar, and J. J. Perez, *J. Comput. Chem.*, **14**, 620 (1993). Comparison of Methods to Estimate the Free Energy of Solvation: Importance in the Modulation of the Affinity of 3-Benzazepines for the D_1 Receptor.
25. C. J. Cramer, G. R. Famini, and A. H. Lowrey, *Acc. Chem. Res.*, **26**, 599 (1993). Use of Calculated Quantum Chemical Properties as Surrogates for Solvatochromic Parameters in Structure–Activity Relationships.

26. C. J. Cramer and D. G. Truhlar, *J. Am. Chem. Soc.*, 113, 8305, 9901(Erratum) (1991). General Parameterized SCF Model for Free Energies of Solvation in Aqueous Solution.
27. C. J. Cramer and D. G. Truhlar, *Science*, 256, 213 (1992). An SCF Solvation Model for the Hydrophobic Effect and Absolute Free Energies of Aqueous Solvation.
28. M. Born, *Z. Physik*, 1, 45 (1920). Volumes and Heats of Hydration of Ions.
29. J. G. Kirkwood, *J. Chem. Phys.*, 2, 351 (1934). Solutions of Molecules Containing Widely Separated Charges—Amphoteric Ions.
30. L. Onsager, *J. Am. Chem. Soc.*, 58, 1486 (1936). Electric Moments of Molecules in Liquids.
31. C. J. F. Böttcher, O. C. van Belle, P. Bordewicijk, and A. Rip, *Theory of Electric Polarization*, 2nd ed., Elsevier, Amsterdam, 1973, Chapter IV and pp. 94–143.
32. A. J. Hopfinger, *Conformational Properties of Macromolecules*, Academic Press, New York, 1973, pp. 64–65, 70–73.
33. E. M. Huque, *J. Chem. Educ.* 66, 581 (1989). The Hydrophobic Effect.
34. G. R. Fleming, *Faraday Discuss. Chem. Soc.*, 85, 231 (1988). General Discussion.
35. M. P. Allen and D. J. Tildesley, *Computer Simulations of Liquids*, Oxford University Press, London, 1987.
36. J. A. McCammon and S. C. Harvey, *Dynamics of Proteins and Nucleic Acids*, Cambridge University Press, Cambridge, 1987.
37. D. L. Beveridge and F. M. DiCapua, *Annu. Rev. Biophys. Chem.*, 18, 431 (1989). Free Energy via Molecular Simulation—Applications to Chemical and Biomolecular Systems.
38. W. L. Jorgensen, *Acc. Chem. Res.*, 22, 184 (1989). Free Energy Calculations: A Breakthrough for Modeling Organic Chemistry in Solution.
39. C. L. Brooks III, M. Karplus, and B. M. Pettitt, *Adv. Chem. Phys.*, 71, 1 (1989). Proteins: A Theoretical Perspective of Dynamics, Structure, and Thermodynamics.
40. P. A. Kollman and K. M. Merz Jr., *Acc. Chem. Res.*, 23, 246 (1990). Computer Modeling of the Interactions of Complex Molecules.
41. A. Warshel, *Computer Modeling of Chemical Reactions in Enzymes and Solutions*, Wiley-Interscience, New York, 1991.
42. J. M. Haile, *Molecular Dynamics Simulation*, Wiley-Interscience, New York, 1992.
43. A. Warshel and M. Levitt, *J. Mol. Biol.*, 103, 227 (1976). Theoretical Studies of Enzymic Reactions: Dielectric, Electrostatic and Steric Stabilization of the Carbonium Ion in the Reaction of Lysozyme.
44. A. Warshel, *J. Phys. Chem.*, 83, 1640 (1979). Calculations of Chemical Processes in Solutions.
45. M. J. Field, P. A. Bash, and M. Karplus, *J. Comput. Chem.*, 11, 700 (1990). A Combined Quantum Mechanical and Molecular Mechanical Potential for Molecular Dynamics Simulations.
46. O. Tapia, F. Colonna, and J. G. Ángyán, *J. Chim. Phys.*, 87, 875 (1990). Generalized Self-Consistent Reaction Field Theory in a Multicenter–Multipole *Ab Initio* LCGO Framework. I. Electronic Properties of the Water Molecule in a Monte Carlo Sample of Liquid Water Molecules Studied with Standard Basis Sets.
47. O. Tapia, *J. Mol. Struct. (THEOCHEM)*, 226, 59 (1991). On the Theory of Solvent–Effect Representation. I. A Generalized Self-Consistent Reaction Field Theory.
48. V. Luzhkov and A. Warshel, *J. Comput. Chem.*, 13, 199 (1992). Microscopic Models for Quantum Mechanical Calculations of Chemical Processes in Solutions: LD/AMPAC and SCAAS/AMPAC Calculations of Solvation Energies.
49. J. Gao, *J. Phys. Chem.*, 96, 537 (1992). Absolute Free Energy of Solvation from Monte Carlo Simulations Using Combined Quantum and Molecular Mechanical Potentials. J. Gao, in *Reviews in Computational Chemistry*, Vol. 7, in press.

50. J. Gao, F. J. Luque, and M. Orozco, *J. Chem. Phys.*, **98**, 2975 (1993). Induced Dipole Moment and Atomic Charges Based on Average Electrostatic Potentials in Aqueous Solution.

51. J.-K. Hwang and A. Warshel, *J. Phys. Chem.*, **97**, 10053 (1993). A Quantized Classical Path Approach for Calculations of Quantum Mechanical Rate Constants.

52. J. Åqvist and A. Warshel, *Chem. Rev.*, **93**, 2523 (1993). Simulation of Enzyme Reactions Using Valence Bond Force Fields and Other Hybrid Quantum/Classical Approaches.

53. G. King and A. Warshel, *J. Chem. Phys.*, **91**, 3647 (1989). A Surface Constrained All-Atom Solvent Model for Effective Simulations of Polar Solutions.

54. L. X. Dang, J. E. Rice, J. Caldwell, and P. A. Kollman, *J. Am. Chem. Soc.*, **113**, 2481 (1991). Ion Solvation in Polarizable Water: Molecular Dynamics Simulations.

55. Y. W. Xu, C. X. Wang, and Y. Y. Shi, *J. Comput. Chem.*, **13**, 1109 (1992). Improvements on the Protein–Dipole/Langevin–Dipole Model.

56. K. Tasaki, S. McDonald, and J. W. Brady, *J. Comput. Chem.* **14**, 278 (1993). Observations Concerning the Treatment of Long-Range Interactions in Molecular Dynamics Simulations.

57. J. Guenot and P. A. Kollman, *J. Comput. Chem.*, **14**, 295 (1993). Conformational and Energetic Effects of Truncating Nonbonded Interactions in an Aqueous Protein Dynamics Simulation.

58. F. S. Lee and A. Warshel, *J. Chem. Phys.*, **97**, 3100 (1992). A Local Reaction Field Method for Fast Evaluation of Long-Range Electrostatic Interactions in Molecular Simulations.

59. F. S. Lee, Z.–T. Chu, and A. Warshel, *J. Comput. Chem.*, **14**, 161 (1993). Microscopic and Semimicroscopic Calculations of Electrostatic Energies in Proteins by the POLARIS and ENZYMIX Programs.

60. C. A. Reynolds, J. W. Essex, and W. G. Richards, *Chem. Phys. Lett.*, **199**, 257 (1992). Errors in Free-Energy Perturbation Calculations Due to Neglecting the Conformational Variation of Atomic Charges.

61. J. J. Urban and G. R. Famini, *J. Comput. Chem.*, **14**, 353 (1993). Conformational Dependence of the Electrostatic Potential–Derived Charges of Dopamine: Ramifications in Molecular Mechanics Force Field Calculations in the Gas Phase and in Aqueous Solution.

62. C. B. Post, C. M. Dobson, and M. K. Karplus, *Proteins*, **5**, 337 (1989). A Molecular Dynamics Analysis of Protein Structural Elements.

63. D. A. Pearlman and P. A. Kollman, *J. Chem. Phys.*, **94**, 4532 (1991). The Overlooked Bond-Stretching Contribution in Free Energy Perturbation Calculations.

64. M. H. Mazor and B. M. Pettitt, *Mol. Simulation*, **6**, 1 (1991). Convergence of the Chemical Potential in Aqueous Simulation.

65. M. J. Mitchell and J. A. McCammon, *J. Comput. Chem.*, **12**, 271 (1991). Free Energy Difference Calculations by Thermodynamic Integration. Difficulties in Obtaining a Precise Value.

66. V. Lounnas, B. M. Pettitt, L. Findsen, and S. Subramanian, *J. Phys. Chem.*, **96**, 7157 (1992). A Microscopic View of Protein Solvation.

67. J.-L. Rivail and D. Rinaldi, *Chem. Phys.*, **18**, 233 (1976). Quantum Chemical Approach to Dielectric Solvent Effects in Molecular Liquids.

68. J. Hylton, R. E. Christofferson, and G. G. Hall, *Chem. Phys. Lett.*, **26**, 501 (1974). Model for Ab-Initio Calculation of Some Solvent Effects.

69. J. H. McCreery, R. E. Christofferson, and G. G. Hall, *J. Am. Chem. Soc.*, **98**, 7191 (1976). Development of Quantum Mechanical Solvent Effect Models—Microscopic Electrostatic Contributions.

70. O. Tapia and O. Goscinski, *Mol. Phys.*, **29**, 1653 (1975). Self-Consistent Reaction Field Theory of Solvent Effects.

71. O. Tapia, in *Quantum Theory of Chemical Reactions*, Vol. 2, R. Daudel, A. Pullman, L. Salem, and A. Veillard, Eds., Reidel, Dordrecht, 1980, p. 25. Local Field Representation of Surrounding Medium Effects. From Liquid Solvent to Protein Core Effects.

72. S. Miertuš, E. Scrocco, and J. Tomasi, *Chem. Phys.*, 55, 117 (1981). Electrostatic Interaction of a Solute with a Continuum. A Direct Utilization of Ab Initio Molecular Potentials for the Provision of Solvent Effects.

73. J. Tomasi, G. Alagona, R. Bonaccorsi, and C. Ghio, in *Modelling of Structure and Properties of Molecules*, Z. B. Maksic, Ed., Horwood, Chichester, 1987, p. 330. A Theoretical Model for Solvation—Some Applications to Biological Systems.

74. J.-L. Rivail, D. Rinaldi, and M. F. Ruiz-López, in *Theoretical and Computational Models for Organic Chemistry*, S. J. Formosinho, I. G. Czismadia, and L. G. Arnaut, Eds., Kluwer, Dordrecht 1991, p. 79.

75. A. Ben-Naim, *Solvation Thermodynamics*, Plenum, New York, 1987, pp. 4–6, 11–12, 125–126; *Statistical Thermodynamics for Chemists and Biochemists*, Plenum, New York, 1992, pp. 5, 38, 321, 372, 410, 422–423, 434, 443.

76. K. Sharp, A. Nicholls, R. Friedman, and B. Honig, *Biochemistry*, 30, 9686 (1991). Extracting Hydrophobic Free Energies from Experimental Data: Relationship to Protein Folding and Theoretical Models.

77. M. L. Huggins, *J. Chem. Phys.*, 9, 440 (1941). Solutions of Long Chain Compounds.

78. M. L. Huggins, *J. Phys. Chem.*, 46, 151 (1942). Some Properties of Solutions of Long-Chain Compounds.

79. M. L. Huggins, *Ann. N.Y. Acad. Sci.*, 43, 1 (1942). Thermodynamic Properties of Solutions of Long-Chain Molecules.

80. P. J. Flory, *J. Chem. Phys.*, 9, 660 (1941). Thermodynamics of High-Polymer Solutions, Part I.

81. P. J. Flory, *J. Chem. Phys.*, 10, 51 (1942). Thermodynamics of High Polymer Solutions, Part II.

82. P. J. Flory, *J. Chem. Phys.*, 13, 453 (1945). Thermodynamics of Dilute Solutions of High Polymers.

83. J. H. Hildebrand, *J. Chem. Phys.*, 15, 225 (1947). The Entropy of Molecules of Different Sizes.

84. M. L. Huggins, *J. Phys. Colloids*, 52, 248 (1948). The Effects of Size, Shape, and Flexibility of the Solute Molecules on the Properties of Colloidal Systems.

85. H. C. Longuet-Higgins, *Faraday Soc. Discuss.*, 15, 73 (1953). Solutions of Chain Molecules—A New Statistical Theory.

86. P. J. Flory, *J. Am. Chem. Soc.*, 87, 1833 (1965). Statistical Thermodynamics of Liquid Mixtures.

87. P. J. Flory, *Discuss. Faraday Soc.*, 49, 7 (1970). Thermodynamics of Polymer Solutions.

88. P. J. Flory, *Ber. Bunsenges. Phys. Chem.*, 81, 855 (1977). Statistical Thermodynamics of Macromolecular Liquids and Solutions.

89. A. Abe and P. J. Flory, *J. Am. Chem. Soc.*, 87, 1838 (1965). The Thermodynamic Properties of Mixtures of Small, Nonpolar Molecules.

90. A. Abe and P. J. Flory, *J. Am. Chem. Soc.*, 88, 2887 (1966). Treatment of Liquid–Liquid Phase Equlibria. Hydrocarbon–Perfluorocarbon Mixtures.

91. A. Holtzer, *Biopolymers*, 32, 711 (1992). The Use of Flory–Huggins Theory in Interpreting Partitioning of Solutes Between Organic Liquids and Water.

92. A. Ben-Naim and R. M. Mazo, *J. Phys. Chem.*, 97, 10829 (1993). Size Dependence of the Solvation Free Energies of Large Solutes.

93. D. J. Giesen, C. J. Cramer, and D. G. Truhlar, *J. Phys. Chem.*, 98, 4141 (1994). Entropic Contributions to Free Energies of Solvation.

94. M. H. Abraham and P. Sakellariou, *J. Chem. Soc., Perkin Trans. 2*, 405 (1994). The Honig–Flory–Huggins Combinatorial Entropy Correction—Is It Valid for Aqueous Solutions?

95. L. R. DeYoung and K. A. Dill, *J. Phys. Chem.*, 94, 801 (1990). Partitioning of Nonpolar Solutes into Bilayers and Amorphous *n*-Alkanes. *J. Phys. Chem.*, 94, 4756 (1990). Correction.

96. G. Némethy and H. A. Scheraga, *J. Chem. Phys.*, **36**, 3401 (1962). Structure of Water and Hydrophobic Binding in Proteins. 2. Model for Thermodynamic Properties of Aqueous Solutions of Hydrocarbons.

97. M. L. Connolly, *J. Appl. Crystallogr.*, **16**, 548 (1983). Analytical Molecular Surface Calculation.

98. M. L. Connolly, *Science*, **221**, 709 (1983). Solvent-Accessible Surfaces of Proteins and Nucleic Acids.

99. M. L. Connolly, *J. Am. Chem. Soc.*, **107**, 1118 (1985). Computation of Molecular Volume.

100. T. J. Richmond, *J. Mol. Biol.*, **178**, 63 (1984). Solvent Accessible Surface Area and Excluded Volume in Proteins—Analytical Equations for Overlapping Spheres and Implications for the Hydrophobic Effect.

101. A. Y. Meyer, *J. Chem. Soc., Perkin Trans. 2*, 1161 (1985). Molecular Mechanics and Molecular Shape. 1. Van der Waals Descriptors of Simple Molecules.

102. A. Y. Meyer, *J. Comput. Chem.*, **7**, 144 (1986). Molecular Mechanics and Molecular Shape. 3. Surface Area and Cross-Sectional Areas of Organic Molecules.

103. M. L. J. Drummond, *J. Chem. Phys.*, **88**, 5021 (1988) A Supertensor Formalism for Solute Continuum Solvent Interactions with an Arbitrarily Shaped Cavity. 2. Preliminary Applications to Model Systems.

104. H. R. Karfunkel and V. E. Eyraud, *J. Comput. Chem.*, **10**, 628 (1989). An Algorithm for the Representation and Computation of Supermolecular Surfaces and Volumes.

105. R. Voorinthold, M. T. Kosters, G. Vegter, G. Vriend, and W. G. J. Hol, *J. Mol. Graphics*, **7**, 243 (1989). A Very Fast Program for Visualizing Protein Surfaces, Channels, and Cavities.

106. G. Perrot, B. Cheng, K. D. Gibson, J. Vila, K. A. Palmer, A. Nayeem, B. Maigret, and H. A. Scheraga, *J. Comput. Chem.*, **13**, 1 (1992). MSEED: A Program for the Rapid Analytical Determination of Accessible Surface Areas and Their Derivatives.

107. B. von Freyberg and W. Braun, *J. Comput. Chem.*, **14**, 510 (1933). Minimization of Empirical Energy Functions in Proteins Including Hydrophobic Surface Area Effects.

108. B. Lee and F. M. Richards, *J. Mol. Biol.*, **55**, 379 (1971). The Interrelation of Protein Structures: Estimation of Static Accessibility.

109. A. Shrake and J. A. Rupley, *J. Mol. Biol.*, **79**, 351 (1973). Environment and Exposure to Solvent of Protein Atoms—Lysozyme and Insulin.

110. W. Hasel, T. F. Hendrickson, and W. C. Still, *Tetrahedron Comput. Methodol.*, **1**, 103 (1988). A Rapid Approximation to the Solvent Accessible Surface Area of Atoms.

111. W. Heiden, M. Schlendrich, and J. Brinkmann, *J. Comput.-Aided Mol. Design*, **4**, 255 (1990). Triangulation Algorithms for the Representation of Molecular Surface Properties.

112. J. L. Pascual-Ahuir, E. Silla, J. Tomasi, and R. Bonaccorsi, *J. Comput. Chem.*, **8**, 778 (1987). Electrostatic Interaction of a Solute with a Continuum. Improved Description of the Cavity and of the Surface Cavity Bound Charge Distribution.

113. J. L. Pascual-Ahuir and E. Silla, in *Quantum Chemistry-Basic Aspects, Actual Trends*, R. Carbó, Ed., Elsevier, New York, 1989, p. 587 or 597.

114. J. L. Pascal-Ahuir and E. Silla, *J. Comput. Chem.*, **11**, 1047 (1990). GEPOL: An Improved Description of Molecular Surfaces. I. Building the Spherical Surface Set.

115. E. Silla, I. Tuñón, and J. L. Pascual-Ahuir, *J. Comput. Chem.*, **12**, 1077 (1991). GEPOL: An Improved Description of Molecular Surfaces. II. Computing the Molecular Area and Volume.

116. S. M. Le Grand and K. M. Merz Jr., *J. Comput. Chem.*, **14**, 349 (1993). Rapid Approximation to Molecular Surface Area via the Use of Boolean Logic and Look-Up Tables.

117. R. B. Hermann, *J. Phys. Chem.*, **76**, 2754 (1972). Theory of Hydrophobic Bonding. 2. Correlation of Hydrocarbon Solubility in Water with Solvent Cavity Surface Area.

118. G. L. Amidon, S. H. Yalkowsky, S. T. Anik, and S. C. Valvani, *J. Phys. Chem.*, **79**, 2239 (1975). Solubility of Nonelectrolytes in Polar Solvents. 5. Estimation of Solubility of Aliphatic Monofunctional Compounds in Water Using a Molecular Surface Area Approach.

119. S. C. Valvani, S. H. Yalkowsky, and G. L. Amidon, *J. Phys. Chem.*, **80**, 829 (1976). Solubility of Nonelectrolytes in Polar Solvents. VI. Refinements in Molecular Surface Area Computations.

120. G. D. Rose, A. R. Geselowitz, G. J. Lesser, R. H. Lee, and M. H. Zehfus, *Science*, **229**, 834 (1985). Hydrophobicity of Amino-Acid Residues in Globular Proteins.

121. D. Eisenberg and A. D. McLachlan, *Nature*, **319**, 199 (1986). Solvation Energy in Protein Folding and Binding.

122. T. Ooi, M. Oobatake, G. Némethy, and H. A. Scheraga, *Proc. Natl. Acad. Sci. U.S.A.*, **84**, 3086 (1987). Accessible Surface Areas as a Measure of the Thermodynamic Parameters of Hydration of Peptides.

123. F. M. Richards, *Annu. Rev. Biophys. Bioeng.*, **6**, 151 (1977). Areas, Volumes, Packing and Protein Structure.

124. A. Bondi, *J. Phys. Chem.*, **68**, 441 (1964). Van der Waals Volumes and Radii.

125. I. Tuñón, E. Silla, and J. L. Pascual-Ahuir, *Protein Eng.*, **5**, 715 (1992). Molecular-Surface Area and Hydrophobic Effect.

126. J. A. Reynolds, D. B. Gilbert, and C. Tanford, *Proc. Natl. Acad. Sci. U.S.A.*, **71**, 2925 (1974). Empirical Correlation between Hydrophobic Free Energy and Aqueous Cavity Surface Area.

127. J. Vila, R. L. Williams, M. Vásquez, and H. A. Scheraga, *Proteins*, **10**, 199 (1991). Empirical Solvation Models Can be Used to Differentiate Native from Near-Native Conformations of Bovine Pancreatic Trypsin Inhibitor.

128. R. L. Williams, J. Vila, G. Perrot, and H. A. Scheraga, *Proteins*, **14**, 110 (1992). Empirical Solvation Models in the Context of Conformation Energy Searches: Application to Bovine Pancreatic Trypsin Inhibitor.

129. F. A. Momany, R. F. McGuire, A. W. Burgess, and H. A. Scheraga, *J. Phys. Chem.*, **79**, 2361 (1975). Energy Parameters in Polypeptides. VII. Geometric Parameters, Partial Atomic Charges, Nonbonded Interactions, Hydrogen Bond Interactions, and Intrinsic Torsional Potentials for the Naturally Occurring Amino Acids.

130. N. H. Frank and W. Tobocman, in *Fundamental Formulas of Physics*, D. H. Menzel, Ed., Dover, New York, 1960, pp. 307–349. Electromagnetic Theory.

131. D. R. Corson and P. Lorrain, *Introduction to Electromagnetic Fields and Waves*, Freeman, San Francisco, 1992, pp. 31, 96–115,

132. R. K. Wangsness, *Electromagnetic Fields*, Wiley, New York, 1979, pp. 78, 163–167, 178–185.

133. W. M. Latimer, K. S. Pitzer, and C. M. Slansky, *J. Chem. Phys.*, **7**, 108 (1939). Free Energy of Hydration of Gaseous Ions and the Absolute Potential of the Normal Calomel Electrode.

134. A. A. Rashin and B. Honig, *J. Phys. Chem.*, **89**, 5588 (1985). Reevaluation of the Born Model of Ion Hydration.

135. A. A. Rashin and K. Namboodiri, *J. Phys. Chem.*, **91**, 6003 (1987). A Simple Method for the Calculation of Hydration Enthalpies of Polar Molecules with Arbitrary Shapes.

136. F. Hirata, P. Refern, and R. M. Levy, *Int. Quantum Chem., Symp.*, **15**, 179 (1988). Viewing the Born Model for Ion Hydration Through a Microscope.

137. B. Jayaram, R. Fine, K. Sharp, and B. Honig, *J. Phys. Chem.*, **93**, 4320 (1989). Free Energy Calculations of Ion Hydration: An Analysis of the Born Model in Terms of Microscopic Simulations.

138. P. T. van Duijnen, *J. Chem. Soc., Faraday Trans.*, **90**, 1611 (1994). General Discussion.

139. H. L. Friedman, *Mol. Phys.*, **29**, 1533 (1975). Image Approximation to the Reaction Field.

140. O. Tapia and B. Silvi, *J. Phys. Chem.*, **84**, 2646 (1980). Solvent Effects on the Structure and the Electronic Properties of Simple Molecules—A MINDO/3-SCRF-MO Study.

141. P. Claverie, in *Quantum Theory of Chemical Reactions*, Vol. 3, R. Daudel, A. Pullman, L. Salem, and A. Veillard, Eds., Reidel, Dordrecht, 1982, p. 151.

142. R. Costanciel and R. Contreras, *Theor. Chim. Acta*, **65**, 1 (1984), Self-Consistent Field

Theory of Solvent Effects. Representation by Continuum Models—Introduction of Desolvation Contribution.

143. H.-A. Yu and M. Karplus, *J. Chem. Phys.*, **89**, 2366 (1988). A Thermodynamic Analysis of Solvation.

144. J.-L. Rivail, in *New Theoretical Concepts for Understanding Organic Reactions*, J. Bertrán and I. G. Czismadia, Eds., Kluwer, Dordrecht, 1989, p. 219.

145. B. Roux, H.-A. Yu, and M. Karplus, *J. Phys. Chem.*, **94**, 4683 (1990). Molecular Basis for the Born Model of Ion Solvation.

146. F. S. Lee, Z.-T. Chu, M. B. Bolger, and A. Warshel, *Protein Eng.*, **5**, 215 (1992). Calculations of Antibody–Antigen Interactions: Microscopic and Semimicroscopic Evaluation of the Free Energies of Binding of Phosphorylcholine Analogs to McP603.

147. J. Warwicker and H. C. Watson, *J. Mol. Biol.*, **157**, 671 (1982). Calculation of the Electric Potential in the Active Site Cleft Due to α-Helix Dipoles.

148. N. K. Rogers and M. J. E. Sternberg, *J. Mol. Biol.*, **174**, 527 (1984). Electrostatic Interactions in Globular Proteins. Different Dielectric Models Applied to the Packing of α-Helices.

149. D. T. Edmonds, N. K. Rogers, and M. J. E. Sternberg, *Mol. Phys.*, **52**, 1487 (1984). Regular Representation of Irregular Charge Distributions. Application to Electrostatic Potentials of Globular Proteins.

150. N. K. Rogers, G. M. Moore, and M. J. E. Sternberg, *J. Mol. Biol.*, **182**, 613 (1985). Electrostatic Interactions in Globular Proteins: Calculation of the pH Dependence of the Redox Potential of Cytochrome *c*551.

151. J. Warwicker, D. Ollis, F. M. Richards, and T. A. Sietz, *J. Mol. Biol.*, **186**, 645 (1985). Electrostatic Fields of the Large Fragment of *Escherichia coli* DNA Polymerase I.

152. N. K. Rogers, *Progr. Biophys. Mol. Biol.*, **48**, 37 (1986). The Modeling of Electrostatic Interactions in the Function of Globular Proteins.

153. H. Nakamura, *J. Phys. Soc. Japan*, **57**, 3702 (1988). Numerical Calculations of Reaction Fields of Protein–Solvent Systems.

154. D. Bashford, M. Karplus, and G. W. Canters, *J. Mol. Biol.*, **203**, 507 (1988). Electrostatic Effects of Charge Perturbations Introduced by Metal Oxidation in Proteins. A Theoretical Analysis.

155. M. Gilson, K. Sharp, and B. Honig, *J. Comput. Chem.*, **9**, 327 (1988). Calculating Electrostatic Interactions in Bio-Molecules: Method and Error Assessment.

156. S. C. Harvey, *Proteins*, **5**, 78 (1989). Treatment of Electrostatic Effects in Macromolecular Modelling.

157. V. Mohan, M. E. Davis, J. A. McCammon, and B. M. Pettitt, *J. Phys. Chem.*, **96**, 6428 (1992). Continuum Model Calculations of Solvation Free Energies: Accurate Evaluation of Electrostatic Contributions.

158. K. Sharp, A. Jean-Charles, and B. Honig, *J. Phys. Chem.*, **96**, 3822 (1992). A Local Dielectric Constant Model for Solvation Free Energies Which Accounts for Solute Polarizability.

159. R. J. Zauhar and R. S. Morgan, *J. Mol. Biol.*, **186**, 815 (1985). A New Method for Computing the Macromolecular Electric Potential.

160. R. J. Zauhar and R. S. Morgan, *J. Comput. Chem.*, **9**, 171 (1988). The Rigorous Computation of the Molecular Electric Potential.

161. A. A. Rashin, *Int. J. Quantum Chem., Quantum Biol. Symp.*, **15**, 103 (1988). Continuum Electrostatics and Hydration Phenomena.

162. A. A. Rashin, *J. Phys. Chem.*, **94**, 1725 (1990). Hydration Phenomena, Classical Electrostatics, and Boundary Element Method.

163. A. H. Juffer, E. F. F. Botta, B. A. M. van Keulen, A. van der Ploeg, and H. J. C. Berendsen, *J. Comput. Phys.*, **97**, 144 (1991). The Electric Potential of a Macromolecule in a Solvent—A Fundamental Approach.

164. B. J. Yoon and A. M. Lenhoff, *J. Comput. Chem.*, **11**, 1080 (1990). A Boundary Element Method for Molecular Electrostatics with Electrolyte Effects.

165. A. Jean-Charles, A. Nicholls, K. Sharp, B. Honig, A. Tempczyk, T. F. Hendrickson, and W. C. Still, *J. Am. Chem. Soc.*, 113, 1454 (1991). Electrostatic Contributions to Solvation Energies: Comparison of Free Energy Perturbation and Continuum Calculations.

166. R. Fowler and E. A. Guggenheim, *Statistical Thermodynamics*, Cambridge University Press, London, 1956, pp. 385–408.

167. L. Onsager, *Chem. Rev.*, 13, 73 (1933). Theories of Concentrated Electrolytes.

168. N. K. Adam, *Physical Chemistry*, Oxford University Press, London, 1956, pp. 391–393.

169. F. T. Wall, *Chemical Thermodynamics*, Freeman, San Francisco, 1958, pp. 374–376.

170. H. Eyring, D. Henderson, D. J. Stover, and E. M. Eyring, *Statistical Mechanics and Dynamics*, 2nd ed., Wiley, New York, 1982, pp. 640–643.

171. I. Klapper, R. Hagstrom, R. Fine, K. Sharp, and B. Honig, *Proteins*, **1**, 47 (1986). Focusing of Electric Fields in the Active Size of Cu-Zn Superoxide Dismutase: Effects of Ionic Strengths and Amino-Acid Modification.

172. J. Warwicker, *J. Theor. Biol.*, 121, 199 (1986). Continuum Dielectric Modeling of the Protein–Solvent System and Calculation of the Long-Range Electrostatic Field of the Enzyme Phosphoglycerate Mutase.

173. M. K. Gilson and B. Honig, *Proteins*, 3, 32 (1988). Energetics of Charge–Charge Interactions in Proteins.

174. M. K. Gilson and B. Honig, *Proteins*, 4, 7 (1988). Calculation of Total Electrostatic Energy of a Macromolecular System: Solvation Energies, Binding Energies, and Conformational Analysis.

175. B. Jayaram and K. A. Sharp, *Biopolymers*, 28, 975 (1989). The Electrostatic Potential of B-DNA.

176. M. E. Davis and J. A. McCammon, *J. Comput. Chem.*, **10**, 386 (1989). Solving the Finite Difference Linearized Poisson–Boltzmann Equation: A Comparison of Relaxation and Conjugate Gradient Algorithms.

177. M. E. Davis and J. A. McCammon, *Chem. Rev.*, **90**, 509 (1990). Electrostatics in Biomolecular Structure and Dynamics.

178. K. A. Sharp and B. Honig, *Annu. Rev. Biophys. Biophys. Chem.*, **19**, 301 (1990). Electrostatic Interactions in Macromolecules—Theory and Applications.

179. A. Nicholls and B. Honig, *J. Comput. Chem.*, **12**, 435 (1991). A Rapid Finite Difference Algorithm, Utilizing Successive Over-Relaxation to Solve the Poisson–Boltzmann Equation.

180. B. A. Luty, M. E. Davis, and J. A. McCammon, *J. Comput. Chem.*,**13**, 768 (1992). Electrostatic Energy Calculations by a Finite-Difference Method: Rapid Calculation of Charge–Solvent Interaction Energies.

181. B. A. Luty, M. E. Davis, and J. A. McCammon, *J. Comput. Chem.*, 13, 1114 (1992). Solving the Finite-Difference Non-Linear Poisson—Boltzmann Equation.

182. M. Holst and F. Saied, *J. Comput. Chem.*, 14, 105 (1993). Multigrid Solution of the Poisson–Boltzmann Equation.

183. B. Honig, K. Sharp, and A.-S. Yang, *J. Phys. Chem.*, 97, 1101 (1993). Macroscopic Models of Aqueous Solutions: Biological and Chemical Applications.

184. M. K. Gilson, M. E. Davis, B. A. Luty, and J. A. McCammon, *J. Phys. Chem.*, 97, 3591 (1993). Computation of Electrostatic Forces on Solvated Molecules Using the Poisson–Boltzmann Equation.

185. G. S. Manning, *Biophys. Chem.*, 7, 95 (1977). Limiting Laws and Counterion Condensation in Polyelectrolyte Solutions. 4. Approach to Limit and Extraordinary Stability of Charge Fraction.

186. G. L. Seibel, U. C. Singh, and P. A. Kollman, *Proc. Natl. Acad. Sci. U.S.A.*, 82, 6537 (1985). A Molecular Dynamics Simulation of Double Helical B-DNA Including Counterions and Water.

187. A. Laaksonen, L. Nilsson, B. Jönsson, and O. Teleman, *Chem. Phys.*, **129**, 175 (1989). Molecular Dynamics Simulation of Double Helix Z-DNA in Solution.

188. A. Pohorille, W. S. Ross, and I. Tinoco, Jr., *Int. J. Supercomput. Appl.*, **4**, 81 (1990). DNA Dynamics in Aqueous Solution: Opening the Double Helix.

189. K. Sharp, *J. Comput. Chem.*, **12**, 454 (1991). Incorporating Solvent and Ion Screening into Molecular Dynamics Using the Finite-Difference Poisson–Boltzmann Method.

190. M. K. Gilson and B. Honig, *J. Comput.-Aided Mol. Design*, **5**, 5 (1991). The Inclusion of Electrostatic Hydration Energies in Molecular Mechanics Calculations.

191. J. P. Bowen and N. L. Allinger, in *Reviews in Computational Chemistry*, Vol. 2, K. B. Lipkowitz and D. B. Boyd, Eds., VCH Publishers, New York, 1991, pp. 81–97. Molecular Mechanics. The Art and Science of Parameterization.

192. A. Warshel, S. T. Russell, and A. K. Churg, *Proc. Natl. Acad. Sci. U.S.A.*, **81**, 4785 (1984). Macroscopic Models for Studies of Electrostatic Interactions in Proteins: Limitations and Applicability.

193. W. C. Still, A. Tempczyk, R. C. Hawley, and T. Hendrickson, *J. Am. Chem. Soc.*, **112**, 6127 (1990). Semianalytical Treatment of Solvation for Molecular Mechanics and Dynamics.

194. G. J. Hoijtink, E. de Boer, P. H. van der Meij, and W. P. Weijland, *Recl. Trav. Pays-Bas*, **75**, 487 (1956). Potentials of Various Aromatic Hydrocarbons and Their Univalent Anions.

195. F. Paradejordi, *Cahiers Phys.*, **17**, 393 (1963). On the Pariser and Parr Semiempirical Method for Computing Molecular Wave Functions. The Basic Strength of N-Heteroatomic Compounds and Their Monoamines.

196. I. Jano, *C. R. Acad. Sci. (Paris)*, **261**, 103 (1965). Sur l'Énergie de Solvation.

197. G. Klopman, *Chem. Phys. Lett.*, **1**, 200 (1967). Solvatons: A Semi-Empirical Procedure for Including Solvation in Quantum Mechanical Calculations of Large Molecules.

198. I. Fischer-Hjalmars, I. Hendriksson-Entlo, and C. Hermann, *Chem. Phys.*, **24**, 167 (1977). Theoretical Study of Shifts of Electronic Spectra from Solute–Solvent Interactions.

199. G. Klopman and P. Andreozzi, *Theor. Chim. Acta*, **55**, 77 (1980). Solvatons. II. Aqueous Dissociation of Hydrides in the MINDO/S Approximation.

200. R. Contreras and J. S. Gomez-Jeria, *J. Phys. Chem.*, **88**, 1905 (1984). Proton Transfer in Water Polymers as a Model for In-Time- and Solvent-Separated Ion Pairs.

201. T. Kozaki, M. Morihasi, and O. Kikuchi, *J. Am. Chem. Soc.*, **111**, 1547 (1989). MNDO-Effective Charge Model Study of Solvent Effect on the Potential Energy Surface of the S_N2 Reaction.

202. C. J. Cramer and D. G. Truhlar, *J. Comput. Chem.*, **13**, 1089 (1992). PM3-SM3: A General Parameterization for Including Aqueous Solvation Effects in the PM3 Molecular Orbital Model.

203. C. J. Cramer and D. G. Truhlar, *J. Comput.-Aided Mol. Design*, **6**, 629 (1992). AM1-SM2 and PM3-SM3 Parameterized SCF Solvation Models for Free Energies in Aqueous Solution. See also erratum to be published.

204. K. Ohno, *Theor. Chim. Acta*, **2**, 219 (1964). Some Remarks on the Pariser–Parr–Pople Method.

205. G. Klopman, *J. Am. Chem. Soc.*, **86**, 4550 (1964). Semiempirical Treatment of Molecular Structures. 2. Molecular Terms and Application to Diatomic Molecules.

206. W. L. Jorgensen and J. Tirado-Rives, *J. Am. Chem. Soc.*, **110**, 1657 (1988). The OPLS Potential Functions for Proteins. Energy Minimizations for Crystals of Cyclic Peptides and Crambin.

207. F. Mohamadi, N. G. J. Richards, W. C. Guida, R. Liskamp, M. Lipton, C. Caufield, G. Chang, T. Hendrickson, and W. C. Still, *J. Comput. Chem.*, **11**, 440 (1990). MacroModel—An Integrated Software System for Modeling Organic and Bioorganic Molecules Using Molecular Mechanics.

208. D. A. Smith and S. Vijayakumar, *Tetrahedron Lett.*, 32, 3617 (1991). Molecular Modeling of Intramolecular Hydrogen Bonding in Simple Oligoamides. 2. GB/SA CH_2Cl_2.

209. J. Jortner, *Mol. Phys.*, 5, 257 (1962). Dielectric Medium Effects on Loosely Bound Electrons.

210. R. A. Marcus, *J. Chem. Phys.*, 24, 966 (1956). On the Theory of Oxidation–Reduction Reactions Involving Electron Transfer I.

211. J. Gehlen, D. Chandler, H. J. Kim, and J. T. Hynes, *J. Chem. Phys.*, 96, 1748 (1992). Free Energies of Electron Transfer.

212. M. V. Basilevsky, G. E. Chudinov, and M. D. Newton, *Chem. Phys.*, 179, 263 (1994). The Multiconfigurational Adiabatic Electron Transfer Theory and Its Invariance Under Transformations of Charge Density Basis Functions.

213. J. L. Rivail, B. Terryn, and M. F. Ruiz-López, *J. Mol. Struct. (THEOHEM)*, 120, 387 (1985). Liquid State Quantum Chemistry—A Cavity Model.

214. M. M. Karelson, A. R. Katritzky, and M. C. Zerner, *Int. J. Quantum Chem., Symp.*, 20, 521 (1986). Reaction Field Effects on the Electronic Distribution and Chemical Reactivity of Molecules.

215. K. V. Mikkelson, H. Agren, H. J. A. Jensen, and T. Helgaker, *J. Chem. Phys.*, 89, 3086 (1988). Multiconfigurational Self-Consistent Reaction Field Method.

216. M. M. Karelson, A. R. Katritzky, M. Szafran, and M. C. Zerner, *J. Org. Chem.*, 54, 6030 (1989). Quantitative Predictions of Tautomeric Equilibria for 2-, 3-, and 4-Substituted Pyridines in Both the Gas Phase and Aqueous Solution: Combination of AM1 with Reaction Field Theory.

217. M. M. Karelson, A. R. Katritzky, M. Szafran, and M. C. Zerner, *J. Chem. Soc., Perkin Trans. 2*, 195 (1990). A Theoretical Treatment of Solvent Effects on the Tautomeric Equilibria of Five-Membered Rings with Two Heteroatoms.

218. A. R. Katritzky and M. Karelson, *J. Am. Chem. Soc.*, 113, 1561 (1991). AM1 Calculations of Reaction Field Effects on the Tautomeric Equilibria of Nucleic Acid Pyrimidine and Purine Bases and Their 1-Methyl Analogues.

219. H. S. Rzepa, M. Y. Yi, M. M. Karelson, and M. C. Zerner, *J. Chem. Soc., Perkin Trans. 2*, 635 (1991). Geometry Optimisation at the Semiempirical Self-Consistent-Reaction-Field Level Using the AMPAC and MOPAC Programs.

220. M. W. Wong, M. J. Frisch, and K. B. Wiberg, *J. Am. Chem. Soc.*, 113, 4776 (1991). Solvent Effects. 1. The Mediation of Electrostatic Effects by Solvents.

221. M. W. Wong, K. B. Wiberg, and M. J. Frisch, *J. Chem. Phys.*, 95, 8991 (1991). Hartree–Fock Second Derivatives and Electric Field Properties in a Solvent Reaction Field: Theory and Application.

222. M. M. Karelson and M. C. Zerner, *J. Phys. Chem.*, 96, 6949 (1992). Theoretical Treatment of Solvent Effects on Electronic Spectroscopy.

223. L. C. G. Freitas, R. L. Longo, and A. M. Simas, *J. Chem. Soc., Faraday Trans.*, 88, 189 (1992). Reaction-Field–Supermolecule Approach to Calculation of Solvent Effects.

224. M. Szafran, M. M. Karelson, A. R. Katritzky, J. Koput, and M. C. Zerner, *J. Comput. Chem.*, 14, 371 (1993). Reconsideration of Solvent Effects Calculated by Semiempirical Quantum Chemical Methods.

225. W. J. Hehre, L. Radom, P. v. R. Schleyer, and J. A. Pople, *Ab Initio Molecular Orbital Theory*, Wiley, New York, 1986, pp. 324–336.

226. A. Szabo and N. Ostlund, *Modern Quantum Chemistry*, Macmillan, New York, 1982.

227. M. W. Wong, K. B. Wiberg, and M. J. Frisch, *J. Am. Chem. Soc.*, 114, 1645 (1992). Solvent Effects. 3. Tautomeric Equilibria of Formamide and 2-Pyridone in the Gas Phase and Solution. An Ab Initio SCRF Study.

228. M. J. Frisch, G. W. Trucks, M. Head-Gordon, P. M. W. Gill, M. W. Wong, J. B. Foresman, B. G. Johnson, H. B. Schlegel, M. A. Robb, E. S. Replogle, R. Gomperts, J. L. Andres, K. Raghavachari, J. S. Binkley, C. Gonzales, R. L. Martin, D. J. Fox, D. J. Defrees, J. Baker,

J. J. P. Stewart, and J. A. Pople, Gaussian 92, Revision B, Gaussian, Inc., Pittsburgh, PA 1992.

229. M. F. Guest and J. Kendrick, GAMESS-UK, Daresbury Laboratory, Warrington, U.K., 1986.

230. H. S. Rzepa and M. Y. Yi, *J. Chem. Soc. Perkin Trans. 2*, 531 (1991). An AM1 and PM3 Molecular Orbital and Self-Consistent Reaction-Field Study of the Aqueous Solvation of Glycine, Alanine and Proline in Their Neutral and Zwitterionic Forms.

231. M. W. Wong, K. B. Wiberg, and M. J. Frisch, *J. Am. Chem. Soc.*, **114**, 523 (1992). Solvent Effects. 2. Medium Effect on the Structure, Energy, Charge Density, and Vibrational Frequencies of Sulfamic Acid.

232. S. Woodcock, D. V. S. Green, M. A. Vincent, I. H. Hillier, M. F. Guest, and P. Sherwood, *J. Chem. Soc., Perkin Trans. 2*, 2151 (1992). Tautomeric Equilibria in 3- and 5-Hydroxyisoxazole in the Gas Phase and in Aqueous Solution: A Test of Molecular Dynamics and Continuum Models of Solvation.

233. M. W. Wong, R. Leung-Toung, and C. Wentrup, *J. Am. Chem. Soc.*, 115, 2465 (1993). Tautomeric Equilibrium and Hydrogen Shifts of Tetrazole in the Gas Phase and in Solution.

234. J.-L. Rivail and B. Terryn, *J. Chim. Phys.*, 79, 1 (1982). Free Energy of an Electric Charge Distribution Separated from an Infinite Dielectric Medium by a 3-Axes Ellipsoidal Cavity—Application to the Study of Molecular Solvation.

235. D. Rinaldi, J.-L. Rivail, and N. Rguini, *J. Comput. Chem.*, 13, 675 (1992). Fast Geometry Optimization in Self-Consistent Reaction Field Computations on Solvated Molecules.

236. V. Dillet, D. Rinaldi, J. G. Ángyán, and J.-L. Rivail, *Chem. Phys. Lett.*, 202, 18 (1993). Reaction Field Factors for a Multipole Distribution in a Cavity Surrounded by a Continuum.

237. D. Rinaldi, M. F. Ruiz-López, and J.-L. Rivail, *J. Chem. Phys.* 78, 834 (1983). Ab Initio SCF Calculations on Electrostatically Solvated Molecules Using a Deformable 3-Axes Ellipsoidal Cavity.

238. D. Rinaldi and R. R. Pappalardo, to be submitted to QCPE, Bloomington, IN.

239. M. J. Frisch, in *Abstracts of Papers, 205th National Meeting of the American Chemical Society*, Denver, CO, American Chemical Society, Washington, DC, 1993. Paper COMP 3: A Reaction Field Model Which Includes an Ab Initio Definition of the Reaction Cavity and a Comparison of All Current Reaction Field Models.

240. R. R. Pappalardo, E. S. Marcos, M. F. Ruiz-López, D. Rinaldi, and J.-L. Rivail, *J. Am. Chem. Soc.*, 115, 3722 (1993). Solvent Effects on Molecular Geometries and Isomerization Processes: A Study of Push–Pull Ethylenes in Solution.

241. X. Assfeld, J. A. Sordo, J. González, M. F. Ruiz-López, and T. L. Sordo, *J. Mol. Struct. (THEOCHEM)*, in press. Electrostatic Solvent Effect on the Ketene–Imine Cycloaddition Reaction.

242. C. Cativiela, J. L. García, J. A. Mayoral, A. J. Royo, L. Salvatella, X. Assfeld, and M. F. Ruiz-López, *J. Phys. Org. Chem.*, 5, 230 (1992). Experimental and Theoretical Study of the Influence of the Solvent on Asymmetric Diels–Alder Reactions.

243. M. F. Ruiz-López, X. Assfeld, J. I. García, J. A. Mayoral, and L. Salvatella, *J. Am. Chem. Soc.*, 115, 8780 (1993). Electrostatic Solvent Effect on Asymmetric Diels–Alder Reactions.

244. M. J. Huron and P. Claverie, *J. Phys. Chem.*, 76, 2123 (1972). Calculations of Interaction of One Solvent Molecule with Its Whole Surrounding. 1. Method and Application to Pure Nonpolar Solvents.

245. A. J. Stone, *Chem. Phys. Lett.*, 83, 233 (1981). Distributed Multipole Analysis, or How to Describe a Molecular Charge Distribution.

246. F. Colonna, E. Evleth, and J. G. Ángyán, *J. Comput. Chem.*, 13, 1234 (1992). Critical Analysis of Electric Field Modeling: Formamide.

247. C. A. Coulson and H. C. Longuet-Higgins, *Proc. R. Soc. London A*, 191, 39 (1947). The Electronic Structure of Conjugated Systems. I. General Theory.

248. R. S. Mulliken, *J. Chem. Phys.*, 3, 564 (1935). Electronic Structures of Molecules. X. Aldehydes, Ketones, and Related Molecules.

249. R. S. Mulliken, *J. Chem. Phys.*, 23, 1833 (1955). Electronic Population Analysis on LCAO-MO Molecular Wave Functions. I.

250. F. L. Hirshfeld, *Theor. Chim. Acta*, 44, 129 (1977). Bonded Atom-Fragments for Describing Molecular Charge Densities.

251. I. Mayer, *Chem. Phys. Lett.*, 97, 270 (1983). Charge, Bond Order and Valence in the Ab Initio SCF Theory.

252. I. Mayer, *Chem. Phys. Lett.*, 110, 440 (1984). Comments on the Quantum Theory of Valence and Bonding: Choosing between Alternative Definitions.

253. R. F. W. Bader, *Acc. Chem. Res.*, 18, 9 (1985). Atoms in Molecules.

254. A. E. Reed, R. B. Weinstock, and F. Weinhold, *J. Chem. Phys.*, 83, 735 (1985). Natural Population Analysis.

255. A. E. Reed, L. A. Curtiss, and F. Weinhold, *Chem. Rev.*, 88, 899 (1988). Intermolecular Interactions from a Natural Bond Orbital Donor–Acceptor Viewpoint.

256. J. Cioslowski, *J. Am. Chem. Soc.*, 111, 8333 (1989). A New Population Analysis Based on Atomic Polar Tensors.

257. B. H. Besler, K. M. Merz Jr., and P. A. Kollman, *J. Comput. Chem.*, 11, 431 (1990). Atomic Charges Derived from Semiempirical Methods.

258. K. M. Merz Jr., *J. Comput. Chem.*, 13, 749 (1992). Analysis of a Large Data Base of Electrostatic Potential Derived Atomic Charges.

259. M. N. Ramos and B. de B. Neto, *Chem. Phys. Lett.* 199, 482 (1992). Comparative Study of Atomic Charges Derived from Infrared Intensities and from Electrostatic Potentials Using AM1 and MNDO Wavefunctions.

260. M. A. Spackman, *Chem. Rev.*, 92, 1769 (1992). Molecular Electric Moments from X-Ray Diffraction Data.

261. E. R. Davidson and S. Chakravorty, *Theor. Chim. Acta*, 83, 319 (1992). A Test of the Hirshfeld Definition of Atomic Charges and Moments.

262. G. Rauhut and T. Clark, *J. Comput. Chem.*, 14, 503 (1993). Multicenter Point Charge Model for High-Quality Molecular Electrostatic Potentials from AM1 Calculations.

263. C. Chipot, D. Rinaldi, and J.-L. Rivail, *Chem. Phys. Lett.*, 191, 287 (1992). Intramolecular Electron Correlation in the Self-Consistent Reaction Field Model of Solvation. A MP2/6-31G* Ab Initio Study of the NH_3-HCl Complex.

264. R. Bonaccorsi, P. Palla, and J. Tomasi, *J. Comput. Chem.*, 4, 567 (1983). Ab Initio Evaluation of Absorption and Emission Transitions for Molecular Solutes, Including Separate Evaluation of Orientational and Inductive Solvent Effects.

265. R. Bianco, S. Miertuš, M. Persico, and J. Tomasi, *Chem. Phys.*, 168, 281 (1992). Molecular Reactivity in Solution. Modelling of the Effect of the Solvent and of Its Stochastic Fluctuation on an S_N2 Reaction.

266. J. Tomasi, R. Bonaccorsi, R. Cammi, and F. J. Olivares del Valle, *J. Mol. Struct. (THEOCHEM)*, 234, 401 (1991). Theoretical Chemistry in Solution. Some Results and Perspectives of the Continuum Methods and in Particular of the Polarizable Continuum Model.

267. R. Bonaccorsi, R. Cammi, and J. Tomasi, *J. Comput. Chem.*, 12, 301 (1991). On the Ab Initio Geometry Optimization of Molecular Solutes.

268. M. Peterson and R. Poirer, MONSTERGAUSS, Department of Chemistry, University of Toronto, Ontario, Canada.

269. M. A. Aguilar and F. J. Olivares del Valle, *Chem. Phys.*, 129, 439 (1989). Solute–Solvent Interactions. A Simple Procedure for Constructing the Solvent Cavity for Retaining a Molecular Solute.

270. G. E. Chudinov and D. V. Napolov, *Chem. Phys. Lett.*, 201, 250 (1993). A New Method of Geometry Optimization for Molecules in Solution in the Framework of the Born–Kirkwood–Onsager Approach.

271. F. Floris and J. Tomasi, *J. Comput. Chem.*, **10**, 616 (1989). Evaluation of the Dispersion Contribution to the Solvation Energy. A Simple Computational Model in the Continuum Approximation.

272. F. M. Floris, J. Tomasi, and J. L. Pascual-Ahuir, *J. Comput. Chem.*, **12**, 784 (1991). Dispersion and Repulsion Contributions to the Solvation Energy: Refinements to a Simple Computational Model in the Continuum Approximation.

273. F. M. Floris, A. Tani, and J. Tomasi, *Chem. Phys.* **169**, 11 (1993). Evaluation of the Dispersion–Repulsion Contributions to the Solvation Energy. Calibration of the Uniform Approximation with the Aid of RISM Calculations.

274. F. J. Olivares del Valle and M. A. Aguilar, *J. Mol. Struct. (THEOCHEM)*, **280**, 25 (1993). Solute–Solvent Interactions. Part 5. An Extended Polarizable Continuum Model Including Electrostatic and Dispersion Terms and Electronic Correlation in the Solute.

275. F. J. Olivares del Valle and J. Tomasi, *Chem. Phys.*, **150**, 139 (1991). Electron Correlation and Solvation Effects. I. Basic Formulation and Preliminary Attempt to Include the Electron Correlation in the Quantum Mechanical Polarizable Continuum Model so as to Study Solvation Phenomena.

276. F. J. Olivares del Valle, M. A. Aguilar, and S. Tolosa, *J. Mol. Struct. (THEOCHEM)*, **279**, 223 (1993). Polarizable Continuum Model Calculation Including Electron Correlation in the Ab Initio Wavefunction.

277. M. A. Aguilar, F. J. Olivares del Valle, and J. Tomasi, *J. Chem. Phys.*, **98**, 7375 (1993). Nonequilibrium Solvation: An Ab Initio Quantum-Mechanical Method in the Continuum Cavity Model Approximation.

278. R. A. Pierotti, *J. Phys. Chem.*, **67**, 1840 (1963). Solubility of Gases in Liquids.

279. I. Tuñón, E. Silla, and J. Tomasi, *J. Phys. Chem.*, **96**, 9043 (1992). Methylamines Basicity Calculations. In Vacuo and in Solution Comparative Analysis.

280. G. Alagona, C. Ghio, J. Igual, and J. Tomasi, *J. Mol. Struct. (THEOCHEM)*, **204**, 253 (1990). An Appraisal of Solvation Effects on Chemical Function Groups: The Amidic and the Esteric Linkages.

281. R. Montagnani and J. Tomasi, *Int. Quantum Chem.*, **39**, 851 (1991). The Influence of the Solvent on the Conformational Energy Differences Due to the Anomeric Effect.

282. M. Aguilar, R. Bianco, S. Miertuš, M. Persico, and J. Tomasi, *Chem. Phys.*, **174**, 397 (1993). Chemical Reactions in Solution: Modeling of the Delay of Solvent Synchronicism (Dielectric Friction) Along the Reaction Path of an S_N2 Reaction.

283. R. Bonaccorsi, E. Scrocco, and J. Tomasi, *Proc. Int. Symp. Biomol. Struct. Interactions, Suppl. J. Biosci.*, **8**, 627 (1985). Simple Theoretical Models for Biochemical Systems, with Applications to DNA.

284. R. Bonaccorsi, E. Scrocco, and J. Tomasi, *Int. J. Quantum Chem.*, **29**, 717 (1986). Structural Deformations of the DNA Double Helix in the First Stages of DNA Transcription Studied with a Simple Model.

285. J. Tomasi, in *QSAR in Drug Design and Toxicology*, D. Hadži and B. Jerman-Blažič, Eds., Elsevier, Amsterdam, 1987, p. 269. Effective and Practical Ways of Introducing the Effect of the Solvent in the Theoretical Evaluation of Conformational Properties of Biomolecules.

286. R. Bonaccorsi, E. Ojalvo, and J. Tomasi, *Collect. Czech. Chem. Commun.*, **53**, 2320 (1988). A Preliminary Report on a Quantum-Mechanical Model for the Energetics of a Solute at the Surface Separating Two Immiscible Liquid Phases.

287. R. Bonaccorsi, F. Floris, and J. Tomasi, *J. Mol. Liq.*, **47**, 25 (1990). A Computational Ab-Initio Model for the Evaluation of Thermodynamic Functions for Solvent Transfer Processes.

288. R. Bonaccorsi, E. Ojalvo, P. Palla, and J. Tomasi, *Chem. Phys.*, **143**, 245 (1990). Influence of a Liquid–Liquid Phase Boundary on the Energetics of a Molecular Solute.

289. R. Bonaccorsi, F. Floris, P. Palla, and J. Tomasi, *Thermochim. Acta*, **162**, 213 (1990). Theoretical Determination of the Gibbs Energy of Solution and Transfer Between Immiscible Solvents, with Comments on the Dynamics of Phase Transfer.

290. M. Solà, A. Lledós, M. Duran, J. Bertrán, and J.-L. M. Abboud, *J. Am. Chem. Soc.*,113, 2873 (1991). Analysis of Solvent Effects on the Menschutkin Reaction.

291. R. Montagnani and J. Tomasi, *J. Mol. Struct. (THEOCHEM)*, 279, 131 (1993). On the Use of Potential Derived (PD) Atomic Changes for the Evaluation of Solvation Free Energy.

292. J. J. P. Stewart, in *Reviews in Computational Chemistry*, Vol. 1, K. B. Lipkowitz and D. B. Boyd, Eds., VCH Publishers, New York, 1990, pp. 45–81. Semiempirical Molecular Orbital Methods.

293. M. C. Zerner, in *Reviews in Computational Chemistry*, Vol. 2, K. B. Lipkowitz and D. B. Boyd, Eds., VCH Publishers, New York, 1991, pp. 313–365. Semiempirical Molecular Orbital Methods.

294. J. A. Pople and D. L. Beveridge, *Approximate Molecular Orbital Theory*, McGraw-Hill, New York, 1970.

295. M. J. S. Dewar and W. Thiel, *J. Am. Chem. Soc.*, 99, 4899 (1977). Ground States of Molecules. 38. The MNDO Method. Approximations and Parameters.

296. M. J. S. Dewar, E. G. Zoebisch, E. F. Healy, and J. J. P. Stewart, *J. Am. Chem. Soc.*, 107, 3902 (1985). AM1: A New General Purpose Quantum Mechanical Molecular Model.

297. J. J. P. Stewart, *J. Comput. Chem.*, 10, 209 (1989). Optimization of Parameters for Semiempirical Methods. 1. Method.

298. J. J. P. Stewart, *J. Comput. Chem.*, 10, 221 (1989). Optimization of Parameters for Semiempirical Methods. 2. Applications.

299. AMPAC—version 4.0. Semichem, Shawnee, KS. See Appendix 2, this volume.

300. J. J. P. Stewart, MOPAC-93 (program no. 455 of the Quantum Chemistry Program Exchange, Indiana University, Bloomington, IN), *QCPE Bull.*, 13, 40 (1993).

301. D. Rinaldi, P. E. Hoggan, and A. Cartier, GEOMOS (program no. 584 of the Quantum Chemistry Program Exchange, Indiana University, Bloomington, IN), *QCPE Bull.*, 9, 128 (1989).

302. G. Rauhaut, A. Alex, J. Chandrasekhar, and T. Clark, VAMP 4.5, Oxford Molecular Ltd., Oxford, U.K., 1993.

303. R. L. Longo and L. C. G. Freitas, *Int. J. Quantum Chem., Quantum Biol. Symp.*, 17, 35 (1990). Adenine–Thymine Proton Relay—Electric Field and Environment Effects on Point Mutation of DNA.

304. M. M. Karelson, T. Tamm, A. R. Katritzky, S. J. Cato, and M. C. Zerner, *Tetrahedron Comput. Methodol.*, 2, 295 (1989). Molecular Orbital Calculations Applicable to Condensed Phases: The Combination of Self-Consistent Reaction Field Theory with Semiempirical Quantum Chemical Models.

305. J. A. Pople and G. A. Segal, *J. Chem. Phys.*, 43, S136 (1965). Approximate Self-Consistent Molecular Orbital Theory. II. Calculations with Complete Neglect of Differential Overlap.

306. O. Tapia, F. Sussman, and E. Poulain, *J. Theor. Biol.*, 71, 49 (1978). Environmental Effects on H-Bond Potentials: A SCRF MO CNDO/2 Study of Some Model Systems.

307. J. A. Pople, D. L. Beveridge, and P. A. Dobosh, *J. Chem. Phys.*, 47, 2026 (1967). Approximate Self-Consistent Molecular Orbital Theory. V. Intermediate Neglect of Differential Overlap.

308. O. Tapia, *Theor. Chim. Acta*, 47, 157 (1978). Some Remarks on the SCRF Theory of Solvent Effects and the Calculation of Proton Potentials.

309. J. E. Ridley and M. C. Zerner, *Theor. Chim. Acta*, 32, 111 (1973). An Intermediate Neglect of Differential Overlap Technique for Spectroscopy: Pyrrole and the Azines.

310. T. Fox and N. Rösch, *J. Mol. Struct. (THEOCHEM)*, 276, 279 (1992). On the Cavity Model for Solvent Shifts of Excited States—A Critical Appraisal.

311. M. Karelson and M. C. Zerner, *J. Am. Chem. Soc.*, 112, 9405 (1990). On the $n \rightarrow \pi^*$ Blue Shift Accompanying Solvation.

312. T. Fox and N. Rösch, *Chem. Phys. Lett.*, 191, 33 (1992). The Calculation of Solvatochromic Shifts: The n-π^* Transition of Acetone.

313. A. R. Katritzky, *Handbook of Heterocyclic Chemistry,* Pergamon Press, Oxford, 1985, pp. 121–123.

314. P. Beak, *Acc. Chem. Res.,* **10,** 186 (1977). Energies and Alkylations of Tautomeric Heterocyclic Compounds—Old Problems New Solutions.

315. M. Karelson, T. Tamm, A. R. Katritzky, M. Szafran, and M. C. Zerner, *Int. J. Quantum Chem.,* **37,** 1 (1990). Reaction Field Effects on the Electronic Centers of Carbon Radical and Ionic Centers.

316. B. Terryn, J.-L. Rivail, and D. Rinaldi, *J. Chem. Res.,* 141 (1981). Electrostatic Solvent Effect and Basicity of Amines in Aqueous Solution.

317. J. Bertrán, A. Olive, D. Rinaldi, and J.-L. Rivail, *Nouv. J. Chim.,* **4,** 209 (1980). Investigations on the Role of Electrostatic Interactions on Frontier Orbitals and Chemical Reactivity in the Liquid State.

318. G. P. Ford and B. Wang, *J. Comput. Chem.,* **13,** 229 (1992). The Optimized Ellipsoidal Cavity and Its Application to the Self-Consistent Reaction Field Calculation of Hydration Energies of Cations and Neutral Molecules.

319. T. Varnali, V. Aviyente, B. Terryn, and M. F. Ruiz-López, *J. Mol. Struct. (THEOCHEM),* **280,** 169 (1993). Conformational Equilibria of α-Substituted Carbonyl Compounds. Study of Solvent Effects.

320. M. Negre, M. Orozco, and F. J. Luque, *Chem. Phys. Lett.,* **196,** 27 (1992). A New Strategy for the Representation of Environment Effects in Semi-Empirical Calculations Based on Dewar's Hamiltonians.

321. B. Wang and G. P. Ford, *J. Chem. Phys.,* **97,** 4162 (1992). Molecular-Orbital Theory of a Solute in a Continuum with an Arbitrarily Shaped Boundary Represented by Finite Surface Elements.

322. B. Wang and G. P. Ford, *J. Am. Chem. Soc.,* **114,** 10563 (1992). Incorporation of Hydration Effects within the Semiempirical Molecular Orbital Framework. AM1 and MNDO Results for Neutral Molecules, Cations, Anions, and Reacting Systems.

323. T. Fox, N. Rösch, and R. J. Zauhar, *J. Comput. Chem.,* **14,** 253 (1993). Electrostatic Solvent Effects on the Electronic Structure of Ground and Excited States of Molecules: Applications of a Cavity Model Based upon a Finite Element Method.

324. G. Rauhut, T. Clark, and T. Steinke, *J. Am. Chem. Soc.,* **115,** 9174 (1993). A Numerical Self-Consistent Reaction Field (SCRF) Model for Ground and Excited States in NDDO-Based Methods.

325. A. Klamt and G. Schüürmann, *J. Chem. Soc., Perkin Trans. 2,* 799 (1993). COSMO: A New Approach to Dielectric Screening in Solvents with Explicit Expressions for the Screening Energy and Its Gradient.

326. S. Olivella, *QCPE Bull.,* **4,** 109 (1984).

327. H. Hoshi, M. Sakurai, Y. Inouye, and R. Chujo, *J. Chem. Phys.,* **87,** 1107 (1987). Medium Effects on the Molecular Electronic Structure. 1. The Formulation of a Theory for the Estimation of a Molecular Electronic Structure Surrounded by an Anisotropic Medium.

328. S. Miertuš, V. Frecer, and M. Majekova, *J. Mol. Struct. (THEOCHEM),* **179,** 353 (1988). The Extended Polarizable Continuum Model for Calculation for Solvent Effects.

329. G. E. Chudinov, D. V. Napolov, and M. V. Basilevsky, *Chem. Phys.,* **160,** 41 (1990). Quantum Chemical Calculations of the Hydration Energies of Organic Cations and Anions in the Framework of a Continuum Solvent Approximation.

330. G. E. Chudinov and D. V. Napolov, *Chem. Phys. Lett.,* **201,** 250 (1993). A New Method of Geometry Optimization for Molecules in Solution in the Framework of the Born–Kirkwood–Onsager Approach.

331. A. Klamt, Bayer AG, Leverkusen, Germany, personal communication. COSMO (AM1) Hydration Energies.

332. B. Wang and G. P. Ford, personal communication.

333. D. R. Armstrong, P. G. Perkins, and J. J. P. Stewart, *J. Chem. Soc., Dalton Trans.,* 838 (1973). Bond Indices and Valency.

334. J. Hine and P. K. Mookerjee, *J. Org. Chem.*, 40, 287 (1975). The Intrinsic Hydrophilic Character of Organic Compounds. Correlations in Terms of Structural Contributions.

335. S. Cabani, P. Gianni, V. Mollica, and L. Lepori, *J. Solution Chem.*, 10, 563 (1981). Group Contributions to the Thermodynamic Properties of Non-Ionic Organic Solutes in Dilute Aqueous Solution.

336. R. G. Pearson, *J. Am. Chem. Soc.*, 108, 6109 (1986). Ionization Potentials and Electron Affinities in Aqueous Solution.

337. L. F. Kuyper, R. N. Hunter, D. Ashton, K. M. Merz Jr., and P. A. Kollman, *J. Phys. Chem.*, 95, 6661 (1991). Free Energy Calculations on the Relative Solvation Free Energies of Benzene, Anisole, and 1,2,3-Trimethoxybenzene: Theoretical and Experimental Analysis of Aromatic Methoxy Solvation.

338. D. J. Giesen, J. W. Storer, C. J. Cramer, and D. G. Truhlar, *J. Am. Chem. Soc.*, 117, 1057 (1995). A General Semiempirical Quantum Mechanical Solvation Model for Nonpolar Solvation Free Energies. *n*-Hexadecane.

339. C. J. Cramer, G. C. Lynch, G. Hawkins, D. G. Truhlar, and D. A. Liotard, AMSOL—version 4.0 (program no. 606 of the Quantum Chemistry Program Exchange, Indiana University, Bloomington, IN), *QCPE Bull.*, 13, 78 (1993).

340. SPARTAN version 3.0, Wavefunction, Inc., Irvine, CA. See Appendix 2, this volume.

341. R. Wolfenden, *Biochemistry*, 17, 201 (1978). Interaction of a Peptide Bond with Solvent Water—Vapor Phase Analysis.

342. G. P. Ford and B. Wang, *J. Comput. Chem.*, 14, 1101 (1993). New Approach to the Rapid Semiempirical Calculation of Molecular Electrostatic Potential Based on the AM1 Wave Function: Comparison with Ab Initio HF/6-31G* Results.

343. C. J. Cramer and D. G. Truhlar, *Chem. Phys. Lett.*, 198, 74 (1992); 202, 567 (Erratum) (1993). Polarization of the Nucleic Acid Bases in Aqueous Solution.

344. C. J. Cramer and D. G. Truhlar, *J. Am. Chem. Soc.*, 113, 8552 (1991). Molecular Orbital Theory Calculations of Aqueous Solvation Effects on Chemical Equilibria.

345. I. R. Gould and I. H. Hillier, *J. Chem. Soc., Perkin Trans. 2*, 1771 (1993). Modelling of Tautomeric Equilibria of 5-Hydroxyisoxazole in Aqueous Solution.

346. C. J. Cramer and D. G. Truhlar, *J. Chem. Soc.*, 115, 8810 (1993). Solvation Effects on Heterocyclic Equilibria in Aqueous Solution.

347. S. J. Weiner, P. A. Kollman, D. T. Nguyen, and D. A. Case, *J. Comput. Chem.*, 7, 230 (1986). An All-Atom Force Field for Simulations of Proteins and Nucleic Acids.

348. R. K. Hill, in *Asymmetric Synthesis*, Vol. 3, J. D. Morrison, Ed., Academic Press, Orlando, FL, 1984, p. 503. Stereodifferentiating Addition Reactions.

349. M. J. S. Dewar and E. F. Healy, *J. Am. Chem. Soc.*, 106, 7127 (1984). MNDO Study of the Claisen Rearrangement.

350. R. M. Coates, B. Rogers, S. J. Hobbs, D. R. Peck, and D. P. Curran, *J. Am. Chem. Soc.*, 109, 1160 (1987). Synthesis and Claisen Rearrangement of Alkoxyallyl Enol Ethers. Evidence for a Dipolar Transition State.

351. J. J. Gajewski, J. Jurayj, D. R. Kimbrough, M. E. Gande, B. Banem, and B. K. Carpenter, *J. Am. Chem. Soc.*, 109, 1170 (1987). On the Mechanism of Rearrangement of Chorismic Acid and Related Compounds.

352. R. L. Vance, N. G. Rondan, K. N. Houk, F. Jensen, W. T. Borden, A. Komornicki, and E. Wimmer, *J. Am. Chem. Soc.*, 110, 2314 (1988). Transition Structures for the Claisen Rearrangement.

353. M. J. S. Dewar and C. Jie, *J. Am. Chem. Soc.*, 111, 511 (1989). Mechanism of the Claisen Rearrangement of Allyl Vinyl Ethers.

354. P. A. Grieco, *Aldrichimica Acta*, 24, 59 (1991). Organic Chemistry in Unconventional Solvents.

355. D. L. Severance and W. L. Jorgensen, *J. Am. Chem. Soc.*, 114, 10966 (1992). Effect of Hydration on the Claisen Rearrangement of Allyl Vinyl Ether from Computer Simulations.

356. C. J. Cramer and D. G. Truhar, *J. Am. Chem. Soc.*, 114, 8794 (1992). What Causes Aqueous Acceleration of the Claisen Reaction?

357. J. J. Urban, C. J. Cramer, and G. R. Famini, *J. Am. Chem. Soc.*, 114, 8226 (1992). A Computational Study of Solvent Effects on the Conformation of Dopamine.

358. C. J. Cramer and D. G. Truhlar, *J. Am. Chem. Soc.*, 115, 5745 (1993). Quantum Chemical Conformational Analysis of Glucose in Aqueous Solution.

359. B. P. van Eijck, L. M. J. Kroon-Batenburg, and J. Kroon, *J. Mol. Struct.*, 237, 315 (1990). Hydrogen-Bond Geometry Around Sugar Molecules: Comparison of Crystal Statistics with Simulated Aqueous Solutions.

360. L. M. J. Kroon-Batenburg and J. Kroon, *Biopolymers*, 29, 1243 (1990). Solvent Effect on the Conformation of the Hydroxymethyl Group Established by Molecular Dynamics Simulations of Methyl-β-D-Glucoside in Water.

361. S. Ha, J. Gao, B. Tidor, J. W. Brady, and M. Karplus, *J. Am. Chem. Soc.*, 113, 1553 (1991). Solvent Effect on the Anomeric Equilibrium in D-Glucose: A Free Energy Simulation Analysis.

362. P. L. Polavarapu and C. S. Ewig, *J. Comput. Chem.*, 13, 1255 (1992). Ab Initio Computed Molecular Structures and Energies of the Conformers of Glucose.

363. E. Juaristi and G. Cuevas, *Tetrahedron*, 48, 5019 (1992). Recent Studies of the Anomeric Effect.

364. P. Bash, U. C. Singh, R. Langridge, and P. A. Kollman, *Science*, 236, 564 (1987). Free Energy Calculations by Computer Simulation.

365. L. Nilsson and M. Karplus, *J. Comput. Chem.*, 7, 59 (1986). Empirical Energy Functions for Energy Minimization and Dynamics of Nucleic Acids.

366. J. Pranata, S. G. Wierschke, and W. L. Jorgensen, *J. Am. Chem. Soc.*, 113, 2810 (1991). OPLS Potential Functions for Nucleotide Bases—Relative Association Constants of Hydrogen-Bonded Base Pairs in Chloroform.

367. D. W. Urry, *Angew. Chem., Int. Ed. Engl.*, 32, 819 (1993). Molecular Machines: How Motion and Other Functions of Living Organisms Can Result from Reversible Chemical Changes.

368. We have begun to implement a new solvation model called SM4. This model is based on more accurate partial atomic charges obtained by the new AM1-CM1A or PM3-CM1P charge model.[369] Version 5.0 of AMSOL[370] contains general SM4 parameters[338,371] for organic solutes in any alkane solvent and specific SM4 parameters[372,373] for hydrocarbons, ethers, aldehydes, alcohols, and sugars in water. The latter were used to reexamine solvation effects on the Claisen rearrangement.[372]

369 J. W. Storer, D. J. Giesen, C. J. Cramer, and D. G. Truhlar, *J. Comput.-Aided Mol. Design*, in press. Class IV Charge Models: A New Semiempirical Approach in Quantum Chemistry.

370. C. J. Cramer, G. D. Hawkins, G. C. Lynch, D. J. Giesen, I. Rossi, J. W. Storer, D. G. Truhlar, and D. A. Liotard, AMSOL (version 5.0), Program 606, QCPE, Bloomington, IN, to be published.

371. D. J. Giesen, C. J. Cramer, and D. G. Truhlar, *J. Phys. Chem.*, submitted for publication. A Semiempirical Quantum Mechanical Solvation Model for Solvation Free Energies in All Alkane Solvents.

372. J. W. Storer, D. J. Giesen, G. D. Hawkins, G. C. Lynch, C. J. Cramer, D. G. Truhlar, and D. A. Liotard, in *Structure and Reactivity in Aqueous Solutions*, C. J. Cramer and D. G. Truhlar, Eds., American Chemical Society, Washington, DC, 1994, pp. 24–49. Solvation Modeling in Aqueous and Nonaqueous Solvents: New Techniques and a Reexamination of the Claisen Rearrangement.

373. S. E. Barrows, F. J. Dulles, C. J. Cramer, D. G. Truhlar, and A. D. French, *Carbohydrate Res.*, submitted for publication. Relative Stability of Alternative Chair Forms and Hydroxymethyl Conformations of D-Glucopyranose.